

University of South Wales



2053131

A SPECTROSCOPIC STUDY OF HALOGENATED AND NITRILE SUBSTITUTED
HYDROCARBONS IN LOW TEMPERATURE INERT MATRICES AND OTHER PHASES.

by

Edgar Neil Lewis B.Sc.(Hons), GRSC

A thesis submitted during October 1984 in part fulfilment of the requirements for the award of Ph.D degree by the CNAA, describing work carried out in the Department of Science at the sponsoring establishment:

The Polytechnic of Wales.

Collaborating Establishment:
BP Chemicals PLC

ACKNOWLEDGEMENTS

This work was funded jointly by the Science and Engineering Research Council and BP Chemicals Ltd. Sunbury in collaboration with the Polytechnic of Wales and the support of each of these establishments is gratefully acknowledged.

On a personal note I would firstly like to thank Dr. W.O. George (POW) for giving me the opportunity to start this project and for his constant interest and guidance to complete it. Thanks is also expressed to Dr. W.F. Maddams (BP Sunbury) for his many interesting and helpful discussions.

I would also like to thank all the staff at the Polytechnic of Wales both academic and technical who have given me advice and help throughout the last three years. A special word of thanks is due however to all the staff in the Science Dept. for their companionship especially Brian Minty for his additional technical support.

Finally I would like to thank Alun Williams with whom I jointly undertook some of the work described in chapter IV and with whom I have had many and varied discussions both of an academic and non-academic nature.

A SPECTROSCOPIC STUDY OF HALOGENATED AND NITRILE SUBSTITUTED
HYDROCARBONS IN LOW TEMPERATURE INERT MATRICES AND OTHER PHASES.

by

Edgar Neil Lewis

ABSTRACT

Infrared and Raman spectra of halogenated and nitrile substituted hydrocarbons have been studied in various phases including temperatures as low as 8 K by isolation in matrices of solid argon or krypton.

In the compounds :-



where $n = 0, 1, 2$ and $\text{X} = \text{CH}_3, \text{Cl}, \text{Br}$ and $\text{C}\equiv\text{N}$

comparisons are made between the spectra in the gas and matrix isolated phases. The alkene out-of-plane vibrations are sensitive to rotation, aggregation and conformational change. The twist and wag modes show consistent differences between the gas and matrix phases which are discussed in terms of different anharmonicities.

Using a specially constructed temperature control unit evidence was obtained for rotation of ethene and ethene- d_1 in the matrix.

The spectra of the larger molecules in the gas phase were measured (using Fourier Transform methods in some cases) leading to the calculation of rotational constants which corresponded with those calculated for particular structures.

Discrimination between various matrix effects is achieved by comparing the rate of conversion from high to low energy forms under careful temperature control. In acrylonitrile the low energy form is the result of an intermolecular effect leading to polymeric aggregate, in chloroprene this is an intramolecular effect. Rate constants are reported in each case at 500:1 and 5000:1 dilution in argon and vibrational assignments are made to various high and low energy forms in matrices.

Finally a series of dichloro and dibromohexanes and octanes have been prepared and purified and their Raman and infrared spectra recorded in the liquid state. A modified manipulative method has been developed for introducing these compounds of relatively low volatility into inert gas matrices and recording their infrared spectra. Assignments of bands are made within a limited range in relation to their conformational preference as model compounds for head to head PVC and PVBr.

CONTENTS

	<u>PAGE</u>
<u>CHAPTER I</u>	
<u>Introduction</u>	1
1. Scope of work	2
2. List of compounds studied	3
3. Matrix isolation	6
 <u>CHAPTER II</u>	
<u>Experimental Procedures</u>	21
1. Infrared spectra	22
2. Raman spectra	23
3. Matrix isolation	23
4. Synthesis of model compounds for head to head PVC and PVBr	33
5. Synthesis of 4-cyanobut-1-ene	35
6. Purification of samples	36
 <u>CHAPTER III</u>	
<u>Comparison of matrix isolation spectra and gas spectra between 900-1000 cm^{-1}</u>	38
1. Introduction	39
2. General theory for a diatomic molecule	39
3. General theory for the out-of-plane vibrations of a vinyl group	43
4. Vinyl series	48
5. Allyl series	58
6. But-1-ene series	65
7. Rotation in matrices	70
8. Conclusions	80

CHAPTER IV

<u>Polymeric aggregation or multiple site effects as the cause of band splittings</u>	81
1. Introduction	82
2. Vinyl series	85
3. Allyl series	102
4. But-1-ene series	110
5. Conclusions	110

CHAPTER V

<u>Matrix effects in the infrared spectra of cyanoethene (acrylonitrile) and 2-chlorobuta-1,3-diene (chloroprene)</u>	112
1. Introduction	113
2. Matrix effects and comparison of intensity changes at different dilutions	115
3. Comparison of Time dependence of intensity changes at different dilutions	118
4. High and low energy forms	127

CHAPTER VI

<u>A spectroscopic study of head to head model compounds for head to head PVC and PVBr</u>	130
1. Introduction	131
2. Model compounds for head to head PVC	135
3. Model compounds for head to head PVBr	149
4. Conclusions	159

<u>REFERENCES</u>	161
-------------------	-----

CHAPTER 1.

INTRODUCTION

1. SCOPE OF WORK

2. COMPOUNDS STUDIED

- (I) UNSATURATED
- (II) SATURATED

3. MATRIX ISOLATION

- (I) APPLICATIONS OF THE TECHNIQUE
- (II) ADVANTAGES
- (III) DISADVANTAGES
- (IV) MATRIX PROPERTIES
 - (A) INERTNESS
 - (B) RIGIDITY
 - (C) VOLATILITY
 - (D) PURITY
 - (E) VIBRATIONAL SPECTRUM
 - (F) THE LATENT HEAT OF FUSION
 - (G) LATTICE ENERGY
 - (H) THERMAL CONDUCTIVITY
- (V) MATRIX DEPOSITION

CHAPTER 1.

INTRODUCTION

1. SCOPE OF WORK

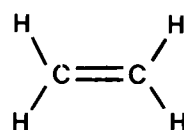
The work reported in this thesis has used various methods of vibrational spectroscopy, particularly infrared studies at very low temperatures and in the gaseous state. Also Raman measurements have been made when needed. Information is obtained on a series of saturated and unsaturated substituted hydrocarbons from these comparative studies by vibrational spectroscopy. The saturated molecules, which act as model compounds for head to head PVC and PVBr, have been studied using dispersive infrared and Raman spectroscopy in various phases, namely, matrix isolation, liquid and gas. The unsaturated compounds have been studied using both dispersive and Fourier transform infrared techniques, particularly in the gas and matrix phases, and a detailed study is undertaken on the comparison of spectra in both these phases. The matrix isolation technique has also been studied in some detail in relation to the multiplicity of bands arising from certain vibrational modes in terms of the causes of such splittings, and a means of distinguishing between them. Thus comparisons are made over a wide range of phase boundaries including gas and low temperature matrix isolation in which intermolecular interactions are minimised. Selected modes are expected to be very sensitive probes of structural factors under these conditions.

2. COMPOUNDS STUDIED

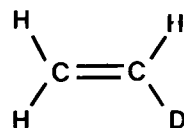
The following comprises of a list of the compounds studied during this piece of work, the trivial names are used in some instances with the IUPAC names in brackets where necessary.

(1) UNSATURATED

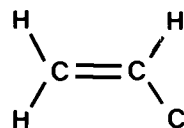
Ethene



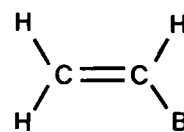
Ethene-d₁



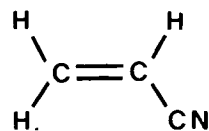
Vinyl Chloride (Chloroethene)



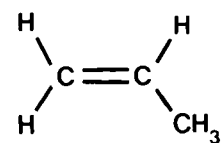
Vinyl Bromide (Bromoethene)



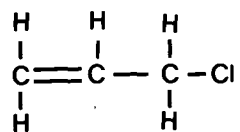
Acrylonitrile (2-Propenenitrile)



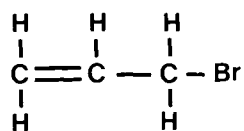
Propene



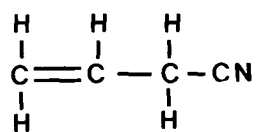
Allyl Chloride (3-Chloroprop-1-ene)



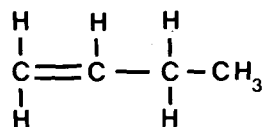
Allyl Bromide (3-Bromoprop-1-ene)



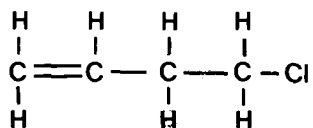
Allyl Cyanide (3-Butenenitrile)



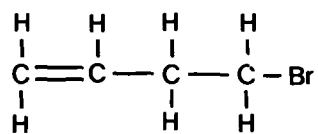
But-1-ene



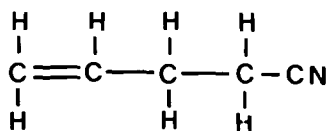
4-Chlorobut-1-ene



4-Bromobut-1-ene

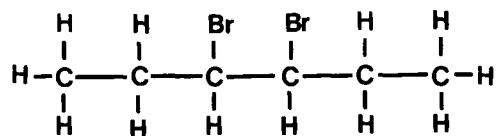


4-Pentenitrile

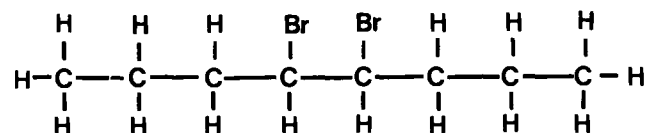


$$\begin{array}{ccccccc} \text{H} & & \text{H} & & \text{H} & & \text{H} \\ | & & | & & | & & | \\ \text{C} & = & \text{C} & - & \text{C} & - & \text{C} - \text{CH}_3 \\ | & & & & | & & | \\ \text{H} & & & & \text{H} & & \text{H} \end{array}$$
$$\begin{array}{ccccccc} \text{H} & & \text{H} & & & & \text{H} \\ | & & | & & & & | \\ \text{C} & = & \text{C} & - & \text{C} & = & \text{C} \\ | & & & & | & & | \\ \text{H} & & & & \text{Cl} & & \text{H} \end{array}$$
$$\begin{array}{ccccccc} \text{H} & \text{Cl} & \text{Cl} & \text{H} & \text{H} & \text{H} \\ | & | & | & | & | & | \\ \text{H}-\text{C}-\text{C}-\text{C}-\text{C}-\text{C}-\text{C}-\text{H} \\ | & | & | & | & | & | \\ \text{H} & \text{H} & \text{H} & \text{H} & \text{H} & \text{H} \end{array}$$
$$\begin{array}{ccccccccc} & \text{H} & & \text{H} & & \text{Cl} & & \text{Cl} & & \text{H} & & \text{H} \\ & | & & | & & | & & | & & | & & | \\ \text{H} & - \text{C} & - & \text{C} & - & \text{C} & - & \text{C} & - & \text{C} & - & \text{C} & - \text{H} \\ & | & & | & & | & & | & & | & & | \\ & \text{H} & & \text{H} & & \text{H} & & \text{H} & & \text{H} & & \text{H} \end{array}$$
$$\begin{array}{ccccccccc} & \text{H} & & \text{H} & & \text{Cl} & & \text{H} & & \text{H} & & \text{H} \\ & | & & | & & | & & | & & | & & | \\ \text{H} & - \text{C} & - & \text{C} & - & \text{C} & - & \text{C} & - & \text{C} & - & \text{C} & - \text{H} \\ & | & & | & & | & & | & & | & & | \\ & \text{H} & & \text{H} & & \text{H} & & \text{Cl} & & \text{H} & & \text{H} \end{array}$$
[illegible]
$$\begin{array}{ccccccc} \text{H} & \text{Br} & \text{Br} & \text{H} & \text{H} & \text{H} \\ | & | & | & | & | & | \\ \text{H}-\text{C}- & \text{C}- & \text{C}- & \text{C}- & \text{C}- & \text{C}-\text{H} \\ | & | & | & | & | & | \\ \text{H} & \text{H} & \text{H} & \text{H} & \text{H} & \text{H} \end{array}$$

meso-3,4-dibromohexane



Meso-4,5-dibromoöctane



3. MATRIX ISOLATION.

Matrix isolation is a technique for trapping chemical species as isolated entities in an excess of an inert host matrix, usually argon or krypton, by condensation of the gases at very low temperatures, typically 8K, in order to investigate their chemical and physical properties usually by spectroscopic means.

The technique has been used in conjunction with a variety of spectroscopic techniques i.e. ultraviolet, visible, infrared, electron spin resonance, nuclear magnetic resonance etc. (1) and has been used to solve problems relating to free radicals, unstable molecules, molecular rotation, molecular association, vibrational analysis etc. High matrix:sample ratios M/S , typically 1000:1, must be used in order that the sample molecules are isolated, under which conditions, ideally, the species under study is only subject to matrix sample interactions and only spectral features relating to the isolated molecule will be apparent.

The technique was first applied in the 1940's for the production and trapping of free radicals at low temperatures (2). The matrix isolation technique as it is known today, however, was proposed independently by Norman and Porter (3) and Whittle Dows and Pimentel

(4). However it was Pimentel who first introduced the term "matrix isolation", pioneered its use with infrared spectroscopy (5) and pointed out its potential for studying H-bonded species. The development of the technique to the present day therefore owes much to Pimentel.

(1) APPLICATIONS OF THE TECHNIQUE

The technique has been applied as a means of tackling many different types of chemical problems, and various review articles have dealt with the general results and applications of the technique, (6-17) as well as some specifically aimed at the application of the technique coupled with infrared spectroscopy (10,11,17-21). As previously stated the technique was originally developed as a means of studying free radicals since under these conditions of low temperature and isolation the lifetime of the species in question is considerably enhanced. Collisions with other radicals is severely restricted by the lattice and reactions with activation energies greater than several kilojoules are prevented by the cryogenic temperatures. Many different transient species have therefore been effectively studied using this technique (1,10,12).

A further application of the technique lies in its ability to obtain spectra of isolated molecules of metal halides and oxides (22). This is done by creating a molecular beam of the material from a Knudsen furnace using very high temperatures and then trapping the vapour normally in an excess of an inert gas on the cold window. The spectra obtained are an improvement over those for conventional techniques for studying such species.

The technique has also been employed in a quantitative role in the analysis of gas mixtures. Rochkind carried out quantitative analyses of both gas mixtures and mixtures of volatile stable molecules by this method. The success of the technique in this sphere of work however depends on whether the Beer-Lambert law is applicable under matrix conditions. Early workers (23-24) studied the applicability of Beer's law and found it was obeyed to within $\pm 0.5\%$. Rochkind(25,64) later carried out further quantitative tests for the law and concluded it was obeyed to within an accuracy of 5%.

Another application of this technique is its use for studying conformational isomerism. The narrow band widths associated with the matrix environment allow bands separated by only a wavenumber or so to be resolved hence bands arising from different conformers of very little energy difference may be identified and a wide variety of molecules which display conformational isomerism have been studied by this technique (26). Barnes and Hallam (27) have studied the vibrational spectrum of ethanol and have made vibrational assignments for the *trans* and *gauche* conformers on the basis of the small splittings observed when this molecule is examined under matrix isolation conditions. Huber et al (28) have also applied the technique for conformational analysis and obtained a value for the energy difference between the conformers of 1,2-dichloroethane by trapping the gas phase equilibria at different temperatures.

The technique has also become invaluable in the vibrational assignment of stable molecules (1). In general the vibrational spectrum obtained for a species in the matrix phase is simpler than in other phases the narrow band widths allow the resolution of bands close in frequency. As such the technique has been used extensively to study the

vibrational assignment of HCl (29-34) and many other molecules both of an organic and inorganic nature. Barnes and Hallam (35) revised the vibrational assignment of methanol given by Van Thiel (36) using this technique.

(11) ADVANTAGES

The coupling of the technique with vibrational and rotational spectroscopy gives rise to a powerful analytical tool with many advantages over conventional systems. The main advantage lies in the fact that due to the isolation of each molecule from its nearest neighbour in an inert cage intermolecular interactions are greatly reduced and as stated previously there is a considerable sharpening of solute absorption when compared to other phases. This degree of sharpening of absorption bands however becomes less prominent as the size and complexity of the guest molecule increases. This may finally result in spectra containing little or no extra information than can be obtained from the liquid phase.

A further advantage is that with very few exceptions notably hydrogen halides and other small molecules such as water ammonia etc. (30,37-48) rotation does not occur in matrices and therefore much narrower bands than are produced in the vapour phase are obtained by this technique. Band width may be as little as one fifth or less than those of similar concentrations in the liquid phase resulting in the resolution of spectral features separated by as little as 1 cm^{-1} . Similar advantages can be seen to apply to matrix trapped multimeric species, broad bands using normal spectroscopic techniques exhibit resolution into bands due to isolated specific homogeneous or

heterogeneous multimeric species such as dimers, trimers etc. yielding the further advantage that information may be then obtained with regard to their geometry. Furthermore the association process may be controlled by careful temperature variation, typically 8-35K for argon, such that the rigidity of the matrix is decreased and solute molecules are allowed to diffuse through the medium encountering their previously trapped counterparts (5). This process may then be monitored spectroscopically, yielding far more information than similar studies in other phases.

Molecular rotation in matrices may also be studied by similar temperature cycling, and bands due to specific rotational levels may be seen to increase or decrease in intensity in favour of other specific higher rotational levels. At these very low temperatures only the lowest rotational levels are significantly populated and for small diatomics bands associated with specific rotational levels such as R(1), R(0) and P(1) have been identified. An interesting observation here however is that rotation only seems to occur in matrices with symmetrical trapping sites, such as the noble gases. The important point about features due to rotation in matrices is that they are easily distinguished from other matrix effects by their temperature reversibility. A further advantage of matrix isolating a sample is in the ability of the technique to obtain information on hydrogen bonding between like and unlike species within the matrix and much information has been obtained with regard to the nature and structure of the complexes obtained.

(III) DISADVANTAGES

Apart from the obvious advantages of the matrix isolation technique there are certain drawbacks both as a result of the practical requirements and as a direct result of the nature of the technique itself.

Due to the sensitivity of the technique to temperature variation or instability, and/or atmospheric contamination of either the sample or cryotip, rigorous experimental procedures and techniques have to be observed in order that meaningful results can be obtained. The highly sensitive nature of the technique and complexity of the system in terms of stringent vacuum and temperature requirements makes the method both expensive and time consuming. Some techniques take months/years to get a spectrum.

Disadvantages as a direct result of the nature of the technique itself are many-fold, it is assumed that molecular energy levels of the trapped species are not significantly perturbed by the matrix environment. Perturbations however, do occur and are reflected in a wavenumber shift of absorptions when comparing gas and matrix frequencies. This is analogous to the solvent shift, except that the rigidity of the matrix cage means that forces of repulsion become important as well as the forces pertaining to the solvent shift so that the matrix shift is given (49) by :-

$$\begin{aligned}\Delta\nu &= \nu_{matrix} - \nu_{gas} \\ &= \Delta\nu_{dis} + \Delta\nu_{ind} + \Delta\nu_{elec} + \Delta\nu_{rep} + \Delta\nu_{dyn}\end{aligned}$$

The term $\Delta\nu_{dis}$ in the above equation is the dispersive interaction

between the host lattice and the guest molecules, and is due to a net attractive force as a result of their instantaneous electronic configurations. The second term arises as a result of the inductive effect of the charge distribution of one molecule induced in another. The electrostatic term arises from the interaction of the permanent charge distribution of the guest species with that of the host lattice. This is zero for the noble gases but not the case for other matrix materials. The repulsive term arises from the short-range valence force interactions between molecules as a result of the small intermolecular distances obtained in the condensed phase. Finally the dynamic contribution results from the constrained translational motion of the guest molecule.

Various expressions have been proposed for the evaluation of these above terms on the basis of idealised models. The semi-empirical Lennard-Jones potential (29,50-55) is usually employed to evaluate the dispersive and repulsive terms while Friedman and Kimel (56) gave an expression for the dynamic contribution to the frequency shift. It has been noted that generally high frequency stretching modes shift to lower frequency, whereas low frequency bending modes shift to higher frequency, particularly in matrices with unsymmetrical trapping sites.

Another feature of the possible interactions with the host lattice is that the degeneracy of certain vibrational modes may be lifted and inactive vibrations may be induced. For example, an induced 'Q' branch in the spectrum of HCl in argon as a result of nitrogen contamination. In noble gas matrices, however, the interactions and shifts are usually relatively small.

Finally it is generally assumed that the condensation process freezes out the room temperature or vapour phase equilibrium mixture so

that spectra recorded prior to annealing consist of bands due to room temperature molecular species and not species which would be present if the system were to equilibrate at liquid helium temperatures. This however is by no means certain.

Another disadvantage lies in the difficulty in making accurate quantitative intensity measurements. The reason for this is that although accurate sample concentrations can be obtained and known amounts sprayed onto the low temperature window there is uncertainty as to how much actually adheres and ends up in the spectrometer beam. Gas mixture may be just pumped away or condense on another part of the system not in the beam. A further point is that the solute and solvent will probably have different freezing points and hence there may be preferential "sticking" of one of the components to the window thereby producing a different M/S ratio than was originally intended.

A further limitation of the standard technique is that the sample must be in the gas phase before deposition, and hence, only samples of relatively high vapour pressures at room temperatures can be used. As previously stated specialised techniques have however been developed to overcome these problems such as high temperature injection systems (22).

A major drawback of the technique and the cause of many multiple bands arising from a single vibrational mode are what are termed as "site effects". The rapid condensation of the sample at these temperatures is unlikely to result in an ideal crystalline solid and as a result different sample molecules may become trapped in sites of differing symmetry, resulting in non-uniform perturbations of frequencies. Multiplet bands due to site effects have been observed in

many spectra such as the hydrogen halides in N_2 , CO_2 and CO (57). Many of these site effects however, may be minimised by the use of the noble gases since they have symmetrical trapping sites as a result of their hexagonal close packed structure in the solid state. However, three separate trapping sites may be distinguished namely, an interstitial site, a substitutional site and a screw or edge dislocation boundary site. The smaller diatomics such as HCl can occupy an interstitial site which has an octahedral hole with a diameter of approximately 2Å in argon. Larger molecules however must occupy the two latter sites, or indeed a partial or total combination of all three, so that bands arising from molecules trapped in sites of different symmetry pose difficult problems in terms of assignments of vibrational modes. The distinctive feature of site effect bands is that their relative intensities usually remain unchanged by varying the solute concentration, whereas their intensities can be altered by annealing the sample, or by varying the deposition conditions. The solute absorption bands of molecules trapped in noble gas matrices are, however, usually very sharp, implying the trapping sites must be fairly well defined.

The phenomenon probably responsible for the most common cause of band multiplicity in matrix isolation spectroscopy and hence providing one of the main disadvantages the technique has, is unwanted molecular association or aggregation which thwarts the entire "isolation" principle. Isolation is effectively achieved at M/S ratios of 1000:1 or greater and unless true isolation is achieved as far as possible frequency shifts of varying degrees may occur as a result of solute interactions or complex formation of hydrogen bonding species. Molecular association may be distinguished from site effects by varying

the concentration of the solute, the result of which is that bands due to molecular complexes may be seen to increase or decrease in intensity, whereas site effects bands will remain unchanged.

The problems related to the technique are constant ones and are only overcome with careful regard to the experimental requirements and limitations of the technique.

(IV) MATRIX PROPERTIES

Materials available as potential matrix supports are many. The suitability of many of these materials for particular experiments requires they have certain properties (1,5) if their use is to be successful. The properties must be carefully considered in relation to the piece of work to be carried out, and the following attributes must therefore apply to the majority of useful matrix materials.

(A) INERTNESS

The matrix support must not react with the solute. This is an obvious requirement for the vast majority of experiments likely to be carried out, since solute solvent interactions must be kept to a minimum if the vibrational spectrum of the guest molecules is to be as representative of the "isolated" species. The construction of a matrix such that it reacts with the guest molecules is another facet of the technique and constitutes special types of experiments. For most purposes therefore the noble gases are ideal matrix materials since they can be considered chemically inert for all solutes.

(B) RIGIDITY

Rigidity of the matrix is of prime importance since the ultimate goal of the technique is to isolate the sample molecules. If this prerequisite is not fulfilled diffusion may be able to take place through the medium leading to the ultimate breakdown of the technique by the formation of aggregated species.

The rigidity of the matrix is of prime importance and is then highly dependent on the melting point of the materials to be used. Various workers (58-59) have given a guide to the minimum value for the melting point of the matrix material as approximately twice the temperature at which the temperature of the experiment is to be performed. This leads to what has become known as Tammann's rule, which relates the temperature at which diffusion through the medium becomes appreciable to the melting point of the matrix material.

$$T_d = 0.57 T_m$$

Where T_d is the temperature ~~diffusion occurs~~ and T_m is the melting point of the matrix material. This is obviously only a rough guide, since diffusion increases gradually as the temperature rises and does not suddenly occur at any one specific temperature. These temperature requirements therefore limit the number of materials usable by different types of cryostat.

(C) VOLATILITY

The matrix material and solute are mixed in the gas phase and then deposited onto the cold window, this means therefore that the host material as well as the sample must have a reasonably high vapour pressure at ambient temperatures to allow it to be easily handled. On

the other hand once deposited the sample mixture must have a sufficiently low vapour pressure at the base temperature so that the vacuum may be maintained (5). This therefore, in theory, gives an upper limit as well as a lower limit to the volatility of the matrix support, although in practice the limitations are rigidity rather than vapour pressure.

(D) PURITY

It is essential that the matrix material should be of high purity since several non-reproducible spectral features have been attributed to the presence of impurities introduced into the lattice (60-61) either as a result of poor vacuum technique or contaminated matrix gas.

(E) VIBRATIONAL SPECTRUM

With the high M/S ratios necessary for isolation fairly thick films have to be deposited to achieve solute bands of sufficient intensity. Therefore any solvent absorption bands in the region of the solute absorptions will ultimately mask the bands of interest and even weak modes may interfere greatly. It then becomes a very important feature of matrix support materials that they are transparent in the spectral region in which the experimental studies are to be carried out. The thick films also cause a high degree of scattering of the spectrometer beam and as a result sets an upper limit to the M/S ratio achievable. High ratios require the deposition of thicker layers producing matrices with low transmittance qualities. Ultimately the more "transparent" the matrix the greater will be the throughput of the energy from the spectrometer beam resulting in the production of superior spectra as a consequence of enhanced signal to noise ratio.

(F) THE LATENT HEAT OF FUSION

This is a measure of the amount of heat to be removed from the cryotip on condensation of the mixture to form a matrix and must ideally be as low as possible. The amount of heat dissipated on condensation also depends on the rate of deposition and must not exceed the cooling capacity of the cryostat otherwise the temperature of the sample area may rise and permit diffusion to occur.

(G) LATTICE ENERGY

This is a measure of the energy needed to form a lattice at 0K and is therefore related to the energy needed to remove a molecule from its place in the lattice, i.e. diffuse. For the most commonly used matrices (noble gases) the lattice energies are small and hence the interactions between the matrix and solute molecules isolated in the matrix is small.

(H) THERMAL CONDUCTIVITY

This is of considerable importance in the choice of a matrix material. Gas impinges on the cold window at room temperature and so during initial condensation the heat is removed through the window and finally the cold tip. However, as the layer of deposited sample begins to grow the heat from the sample now being deposited must be removed initially through the lattice itself. If the thermal conductivity of the matrix material is poor, some degree of local heating may occur with detrimental effects on the quality of the lattice formed. Secondly, local heating may cause some degree of surface diffusion to occur enabling sample molecules to aggregate with the ultimate loss of isolation. Good thermal conductivity of the matrix material is therefore an essential quality, although it will be intrinsically

linked to the deposition rate and the cooling capacity of the cryostat. Deposition rates which require a cooling capacity the cryostat is unable to meet will inevitably cause some degree of local heating and hence surface diffusion regardless of the thermal conductivity of the material in question.

(v) MATRIX DEPOSITION

Several factors play an important role in the attainment of the optimum conditions for good matrix isolation technique.

Matrix ratio is a very important factor, the degree of isolation is very much determined by this factor alone. Low ratios will inevitably lead to some degree of association as two species become trapped in contact with each other simply as a function of the probability of this event occurring. High ratios are therefore desirable usually 1000:1 or greater (62) although the actual M:I ratio for complete isolation will depend on the type of sample being used.

The deposition rate and/or technique are other factors. As previously described the rate of deposition must not be such that it imposes a load on the cryostat's cooling capacity it cannot possibly meet so that local heating will occur. Deposition rate is therefore usually a compromise between minimising local heating and minimising contamination possibilities both of which are opposing factors. Two methods have been devised to deposit the sample, namely, slow spray-on (SSO) and pulsed matrix isolation (PMI) developed by Rochkind (63-64). In the SSO method the sample is deposited as a slow continuous stream of gas using a needle valve, whereas the PMI technique uses a series of discrete pulses of sample applied over a period of several minutes,

allowing each sample to condense before the next is applied. Both techniques have their advantages and disadvantages. Perutz and Turner (65) advocated deposition of the sample by pulsing (PMI) and stated that this method resulted in less association than SSO coupled with fewer contamination possibilities as a result of the speed of deposition. More recent work however, on acrylonitrile (66) has shown that aggregation features are decreased and indeed may be entirely removed by SSO of dilute samples providing good experimental conditions are maintained.

The third parameter is the deposition temperature. This must ideally be as low as possible so that the solid film is quickly formed, rigid, and not highly scattering. As a general rule the deposition temperature should be well below half the melting point of the matrix material (11). The temperatures usually employed fall between 4 and 20K depending on the type of cryostat used.

CHAPTER 11

EXPERIMENTAL PROCEDURES

1. INFRARED SPECTRA

2. RAMAN SPECTRA

3. MATRIX ISOLATION

- (i) CRYOSTAT
- (ii) SERVICE TROLLEY
- (iii) THE HIGH VACUUM LINE
- (iv) SAMPLE PREPARATION AND DEPOSITION

4. THE SYNTHESIS OF MODEL COMPOUNDS FOR HEAD TO HEAD PVC AND PVBr

5. THE SYNTHESIS OF 4-CYANOBUT-1-ENE

6. PURIFICATION OF SAMPLES

CHAPTER II

EXPERIMENTAL PROCEDURES

1. INFRARED SPECTRA

All matrix spectra were recorded on a Perkin-Elmer 580B ratio-recording spectrophotometer occasionally attached to a Perkin-Elmer Data Station which allowed for computer enhancement of poor quality spectra from samples of low volatility. Liquid spectra of the model compounds for head to head PVC and PVBr were recorded on a Perkin-Elmer ratio-recording 457 spectrophotometer (B.P. Sunbury) while the gas spectra were either recorded on a Perkin-Elmer 580B spectrophotometer or a Nicolet 7199B Fourier transform infrared spectrophotometer (B.P. Sunbury).

Liquid spectra were recorded as thin films using NaCl plates whereas gas spectra were obtained at various pressures using a 10 cm gas cell with KBr windows. The gas cells were filled using vacuum handling techniques on a vacuum line described later. Gas spectra recorded using the Fourier transform instrument gave far superior resolution and hence more accurate frequency measurements. This was a necessary prerequisite for calculations of rotational constants from rotational fine structure which agrees with those constants derived from molecular parameters. Calibration of the two dispersive infrared

instruments was carried out periodically using standard procedures recommended by IUPAC Commission on Molecular Structure and Spectroscopy (67). The resolution available using the 457 was approximately 2 cm^{-1} , and using the 580B 0.5cm^{-1} . The accuracy of these instruments was believed to be $\pm(2-6)\text{ cm}^{-1}$ and $\pm(0.5-1.0)\text{ cm}^{-1}$ respectively.

2. RAMAN SPECTRA

All Raman spectra were recorded in the liquid phase at room temperature in sealed sample bottles using an Anaspec Model 33 Raman spectrometer (B.P. Sunbury) with an Argon Ion Laser. Laser lines at 514.5 nm and 457.9 nm giving between 20 and 100 mW power were used to obtain spectra recorded between $3200-2700\text{ cm}^{-1}$ and $1700-100\text{ cm}^{-1}$ at a scan speed of 100 cm min^{-1} .

3. MATRIX ISOLATION

All the compounds studied in the present work have had infrared spectra recorded using the matrix isolation technique. The apparatus needed to produce suitable matrices for study using this technique consists fundamentally of three distinct parts, the cryostat, the service trolley and the high vacuum line.

(1) CRYOSTAT

There have been several different types of cryostat on the market using different methods of obtaining the very low temperatures required. Early systems used single-Dewar cryostats which were replaced by double-Dewar cryostats (68-69). Later systems used the Joule-Thomson effect and employed open-cycle cryostats (70-72). These cryostats were not only expensive to use since large amounts of

hydrogen were consumed for each experiment but also suffered from other drawbacks. Firstly hydrogen gas is potentially explosive and hence rigorous safety precautions have to be observed during its use. Secondly the minimum temperature available using these systems is only 20 K.

Later cryostats and the cryostat used throughout this work are known as closed-cycle cryostats and operate by the Stirling refrigeration cycle (73). Closed-cycle cryostats are extremely efficient and able to run for prolonged periods with little or no maintenance. They are much lower in running costs than their open-cycle forerunners since there is no continued expenditure for refrigerant gas, the reservoir needs only occasional topping up. They are also far safer since they employ helium gas instead of hydrogen and also have greater refrigerating power, the base temperature is approximately 8 K. High purity helium is always used with the system because trace impurities in the refrigerating gas will solidify at these low temperatures causing a blockage and the ultimate failure of the displacer.

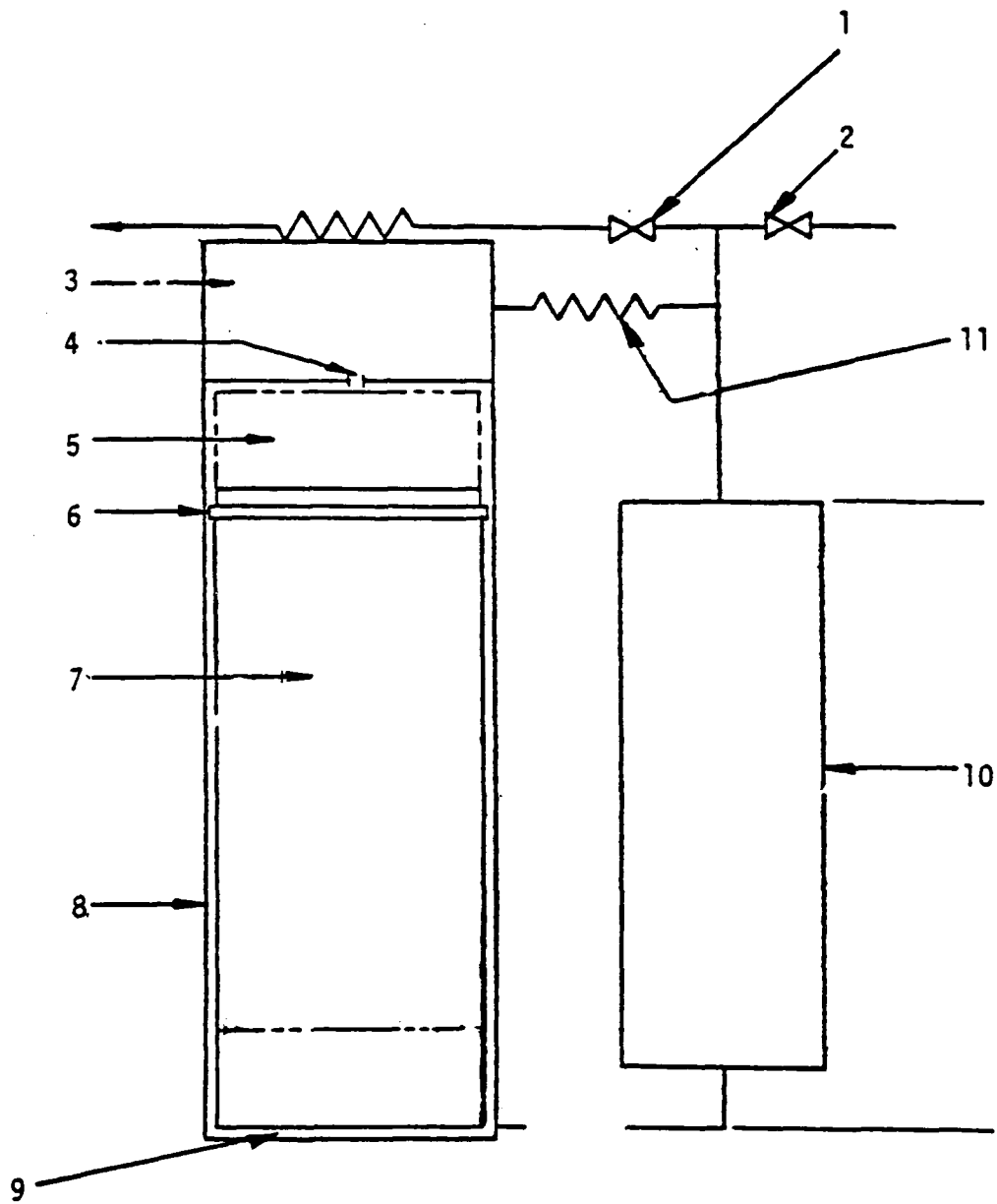
The system used during this work was the Air-Products CS-202 displacer. An idea of the mode of operation of the closed cycle system can be obtained by a step-by-step description of one complete cycle since the process is repeated in both stages.

The gas is first of all compressed and then the high pressure gas flows through the regenerator where it is cooled to the refrigeration temperature. The displacer then moves towards the warm end as gas bleeds out of the orifice into the surge volume (Fig.1). Before it reaches the warm end the inlet valve is opened and the expanding gas

Fig.1.

Air Products CS-202
liquid helium cryostat

- | | |
|-----------------------------|-----------------------------|
| 1. Exhaust Valve | 6 Seal |
| 2 Inlet Valve | 7. Displacer |
| 3 Surge Volume | 8 Displacer Cylinder |
| 4 Orifice | 9 Cold End Displaced Volume |
| 5 Warm End Displaced Volume | 10 Regenerator |
| | 11 Pressure Control Tube |



in the cold volume leaves at a lower temperature than the entering temperature hence refrigerating and cooling the regenerator matrix as it flows out. During this phase of the cycle, the warm volume pressure drops and the displacer moves toward the cold end as gas begins to flow back through the orifice from the surge volume.

The displacer moves toward the cold end at constant velocity as gas continues to bleed through the orifice from the surge volume and the cold gas flows out through the regenerator. The exhaust valve is shut before the displacer hits bottom, thus achieving a partial recompression and also decelerating the displacer. The displacer remains at the cold end for a brief period while the gas pressure in the warm volume increases. The cycle is then repeated. Work energy which is dissipated to heat by throttling in the orifice is removed by heat exchange with the exhaust gas as it leaves the unit.

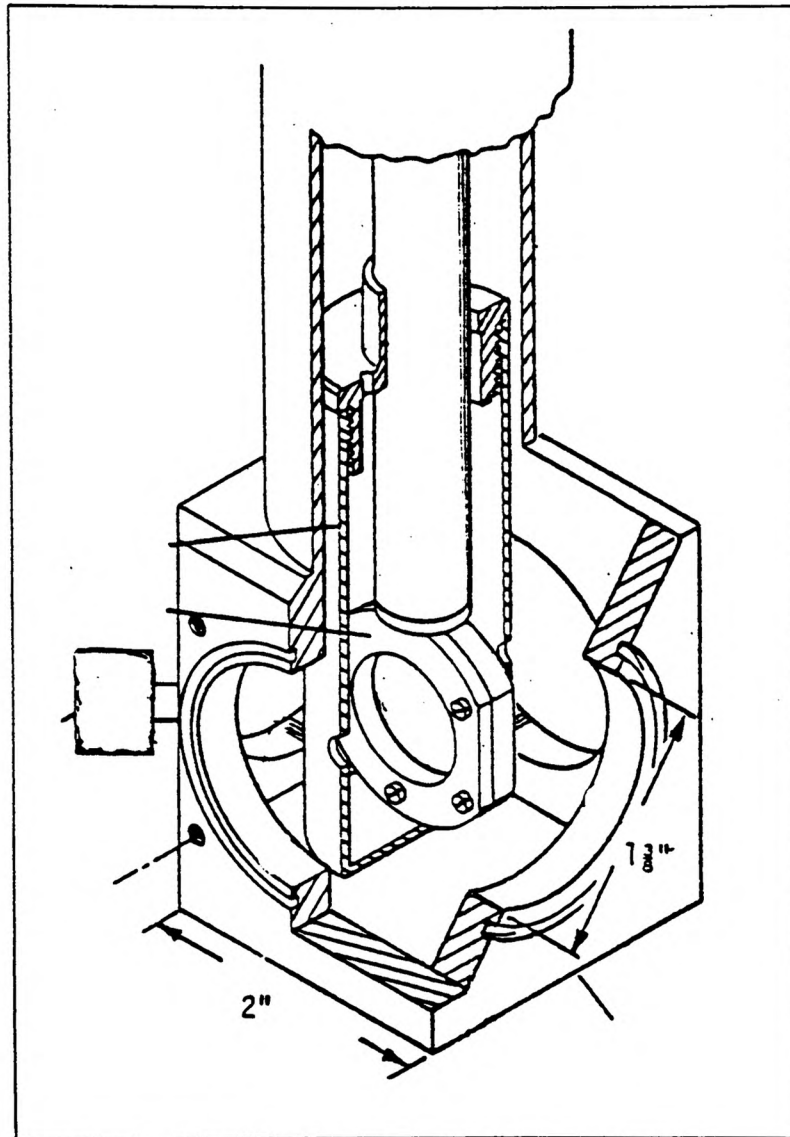
(11) THE SERVICE TROLLEY

The service trolley acts as a unit for mounting the matrix isolation cryotip and also carries all the necessary equipment for evacuating the cryotip shroud and delivering the sample to the cold window.

The cryotip itself is constructed of stainless steel and together with the sample holder is surrounded by a vacuum shroud and a radiation shield (Fig.2). The shroud is fitted with two KBr windows and a stainless steel capillary tube through which the sample passes prior to deposition on the cold window. The sample holder contains the cold window (CsI or Si), which is approximately 25mm X 3mm. This is the surface onto which the samples are actually deposited. Indium gaskets

Fig.2.

Cold end of cryotip assembly
with CsI window

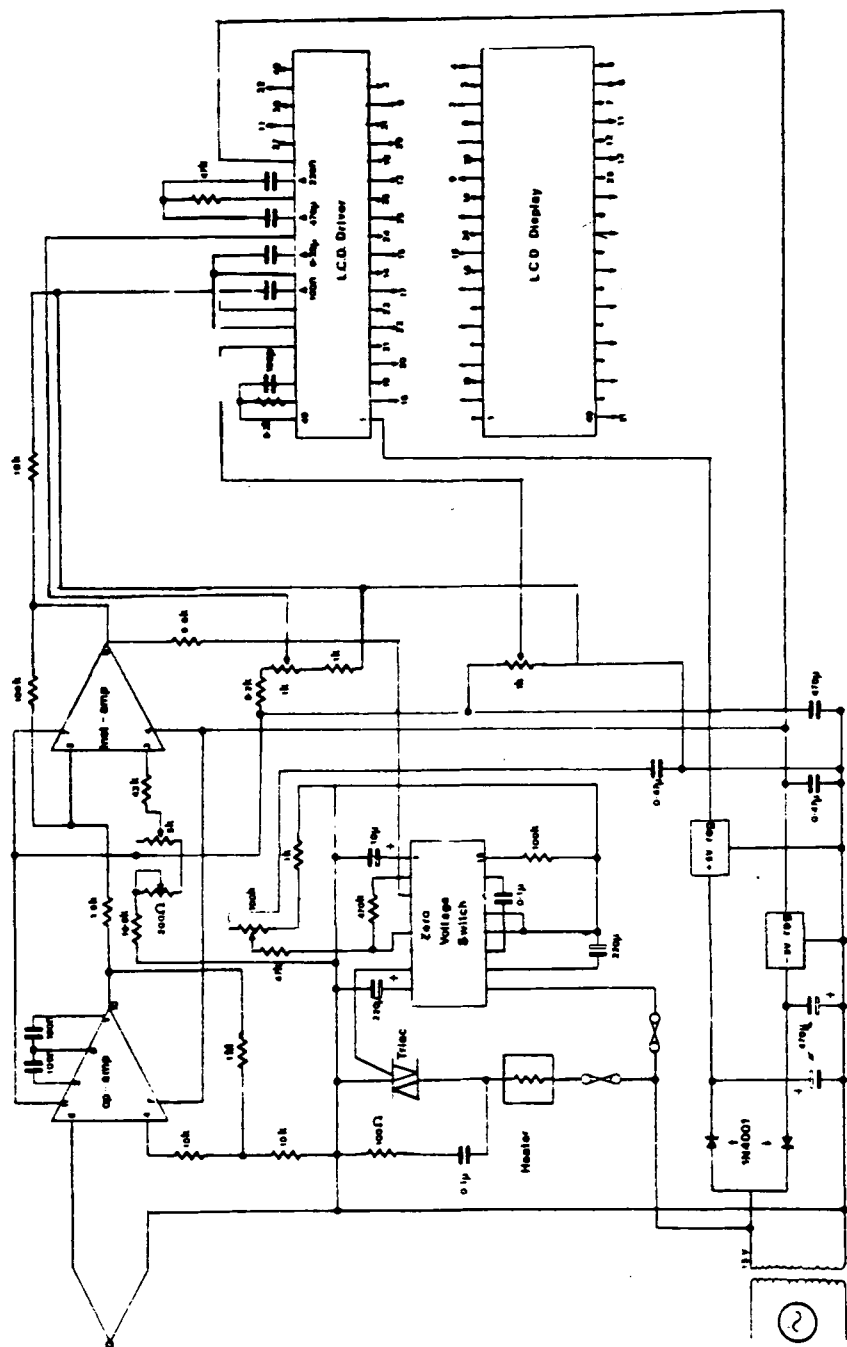


are used to both embed the window in the holder and embed the sample holder into the cold tip itself. The use of Indium gaskets ensures good thermal contact between the window and cold tip and hence maintains the sample at the lowest possible temperatures. The temperature is monitored and controlled by two iron doped vs chromel thermocouples and a heating element on the cold tip which are attached to an external purpose built temperature control unit (Fig.3) constructed at the Polytechnic of Wales. Temperature control between 8K and 50K can be maintained to within ± 0.5 K.

The stainless steel shroud is evacuated to low pressures by a combination of Edwards rotary and oil diffusion pumps coupled with a liquid nitrogen cold trap. Pressures are monitored using Pirani and Penning gauges, and pressures lower than 10^{-6} Torr are attained within the vicinity of the cold tip. The air external to the cryotip and in the spectrometer beam is purged of water by the use of a second shroud so constructed to totally encapsulate the cryotip and isolate it from the surroundings. Air inside the shroud is dried by circulating it through a molecular sieve.

The sample deposition system (Fig.4) consists of a 3 litre bulb of mixture mounted directly over the cryotip via an evacuable manifold, a 10 cm^3 pulsing bulb, a needle valve separated by suitable taps and a length of thin stainless steel tubing. This terminates within the cryotip as a fine capillary tube perpendicular to the CsI window approximately 1 cm from the centre. The capillary tube was positioned to allow spectra to be recorded during sample deposition and to cause minimum cut-off to the spectrometer beam. This arrangement permitted the same sample to be deposited on the window by either SSO or by PMI

	Temperature	Control	Unit
1	70	On	F
2	80	Off	F
3	90	On	F
4	100	Off	F
5	110	On	F
6	120	Off	F
7	130	On	F
8	140	Off	F
9	150	On	F
10	160	Off	F
11	170	On	F
12	180	Off	F
13	190	On	F
14	200	Off	F
15	210	On	F
16	220	Off	F
17	230	On	F
18	240	Off	F
19	250	On	F
20	260	Off	F
21	270	On	F
22	280	Off	F
23	290	On	F
24	300	Off	F
25	310	On	F
26	320	Off	F
27	330	On	F
28	340	Off	F
29	350	On	F
30	360	Off	F
31	370	On	F
32	380	Off	F
33	390	On	F
34	400	Off	F
35	410	On	F
36	420	Off	F
37	430	On	F
38	440	Off	F
39	450	On	F
40	460	Off	F
41	470	On	F
42	480	Off	F
43	490	On	F
44	500	Off	F
45	510	On	F
46	520	Off	F
47	530	On	F
48	540	Off	F
49	550	On	F
50	560	Off	F
51	570	On	F
52	580	Off	F
53	590	On	F
54	600	Off	F
55	610	On	F
56	620	Off	F
57	630	On	F
58	640	Off	F
59	650	On	F
60	660	Off	F
61	670	On	F
62	680	Off	F
63	690	On	F
64	700	Off	F
65	710	On	F
66	720	Off	F
67	730	On	F
68	740	Off	F
69	750	On	F
70	760	Off	F
71	770	On	F
72	780	Off	F
73	790	On	F
74	800	Off	F
75	810	On	F
76	820	Off	F
77	830	On	F
78	840	Off	F
79	850	On	F
80	860	Off	F
81	870	On	F
82	880	Off	F
83	890	On	F
84	900	Off	F
85	910	On	F
86	920	Off	F
87	930	On	F
88	940	Off	F
89	950	On	F
90	960	Off	F
91	970	On	F
92	980	Off	F
93	990	On	F
94	1000	Off	F
95	1010	On	F
96	1020	Off	F
97	1030	On	F
98	1040	Off	F
99	1050	On	F
100	1060	Off	F
101	1070	On	F
102	1080	Off	F
103	1090	On	F
104	1100	Off	F
105	1110	On	F
106	1120	Off	F
107	1130	On	F
108	1140	Off	F
109	1150	On	F
110	1160	Off	F
111	1170	On	F
112	1180	Off	F
113	1190	On	F
114	1200	Off	F
115	1210	On	F
116	1220	Off	F
117	1230	On	F
118	1240	Off	F
119	1250	On	F
120	1260	Off	F
121	1270	On	F
122	1280	Off	F
123	1290	On	F
124	1300	Off	F
125	1310	On	F
1			

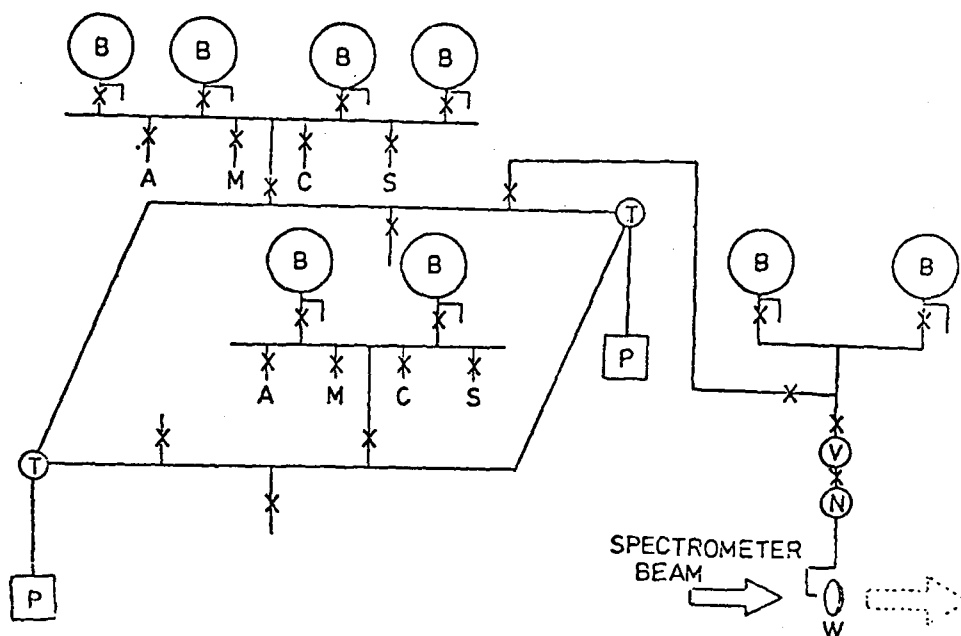


by only changing tap or needle valve positions.

(III) THE HIGH VACUUM LINE

The gas handling line is a multi purpose system for evacuating and filling infrared gas cells evacuating and mixing matrix isolation samples in sample bulbs and evacuating the sample deposition system (Fig.4). The line is constructed in Pyrex in a cyclic arrangement evacuated by two identical pumping stations consisting again of Edwards rotary and oil diffusion pumps coupled to liquid nitrogen cold traps. The cyclic arrangement enables continued use of the vacuum line even in the event of failure or breakage of any part of the system. The taps on the vacuum line are mostly greaseless high vacuum taps with inert Teflon seals. Greased taps proved unreliable due to the nature of the samples used, the sample vapours dissolved the vacuum grease and caused the system to leak. High purity inert gas, argon or krypton, (99.999%) is always used and introduced into the line from a cylinder via a pressure regulator and finally a needle valve. Pressure measurements on the vacuum line are carried out using a mercury manometer with the surface of the mercury covered by a layer of diffusion pump oil to prevent the possible contamination of samples by mercury vapour. All peripheral equipment such as the manometer and the gas cylinders are connected to the vacuum line via stainless steel high vacuum flexible lines with glass-metal interfaces connected by Edwards high vacuum coupling flanges using Viton 'O' rings.

Fig.4. Equipment for recording infrared spectra by matrix isolation



- | | |
|--|------------------------------|
| P - Pumping Stations; Cold trap, Penning, Pirani, Diffusion, Rotary Pump | T - Two-way trap |
| A - Inert Gas Supply | V - Pulsing volume |
| M - Manometer or transducer | N - Needle Valve |
| C - Cylinder - Sample Gas | W - Window-CsI (in Cryostat) |
| S - Sample- Liquid | |
| B - Bulb Detachable | |

(IV) SAMPLE PREPARATION AND DEPOSITION

The technique for sample preparation is devised so as to yield a sample which excludes extraneous material as far as possible. Samples are redistilled and dried using a suitable drying agent usually CaSO_4 . The vacuum handling line and sample bulb (Fig.4) are evacuated to high vacuum ($< 10^{-5}$ torr) using the pumping arrangement described previously. The use of a mercury manometer and simple pressure/volume calculations allows the trapping of known amounts of sample in a bulb using liquid nitrogen and the subsequent dilution with a large excess of inert gas, this results in the production of accurate samples of any concentration, the upper limit of which is determined only by spectrometer transmission requirements. That is, high dilution factors require the deposition of more sample in order to produce adequate band intensity, simultaneously producing a matrix with poor transmission qualities. However, quality spectra have been produced to date with diluent sample ratios of up to 10000:1 with an average diluent sample ratio of 1000:1.

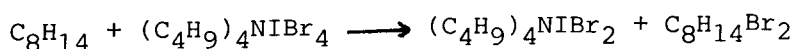
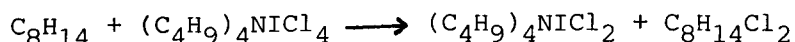
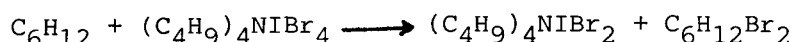
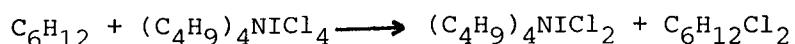
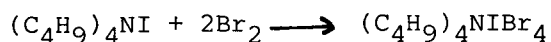
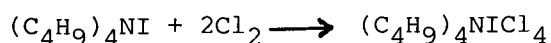
The cryotip is also highly evacuated (10^{-6} torr) and the window cooled to 8-10 K as measured by two thermocouples at either end of the window. The cryotip must also be highly evacuated the reasons for which are two-fold, firstly to prevent contamination of the sample by atmospheric condensation and secondly to prevent heat leaks by conduction losses through the air inside the shroud both of which must be kept to an absolute minimum. The prepared sample can then be transferred to the sample deposition system (Fig.4) and the space between the sample and the cryotip also highly evacuated. Using the needle valve to control flow, SSO spectra can be obtained over a period of up to 24 hrs. at a rate of as little as 1 m Mole/hr. Using the pulsing

bulb with the needle valve open, a number of discrete pulses of the sample (10 cm^3 at 450 torr) can be applied. Annealing can be carried out by slowly warming up the matrix whilst rapidly scanning a selected region. As soon as some change is observed (typically 35-40K), the matrix is re-cooled to 8-10 K and the spectrum re-recorded. The temperature control unit described earlier also allows for the indefinite maintenance of any temperature between 8 K and 50 K accurately so that reversible temperature dependent spectral features can be examined at leisure.

4. THE SYNTHESIS OF MODEL COMPOUNDS FOR HEAD TO HEAD

PVC AND PVBr

The synthesis of model compounds for head to head PVC and PVBr, notably meso-2,3-dichlorohexane, meso and d,l-3,4-dichlorohexane, meso-4,5-dichlorooctane and the corresponding brominated species, is carried out by the addition of either chlorine or bromine across the double bond of an appropriate olefin using a halogenating agent namely tetrabutyl ammonium iodotetrachloride synthesised from tetrabutyl ammonium iodide (74).



- (1) trans-2-hexene \longrightarrow meso-2,3-dichlorohexane/dibromohexane
- (2) Trans-3-hexene \longrightarrow meso-3,4-dichlorohexane/dibromohexane
- (3) cis-3-hexene \longrightarrow d,l-3,4-dichlorohexane/dibromohexane
- (4) trans-4-octene \longrightarrow meso-4,5-dichlorooctane/dibromooctane

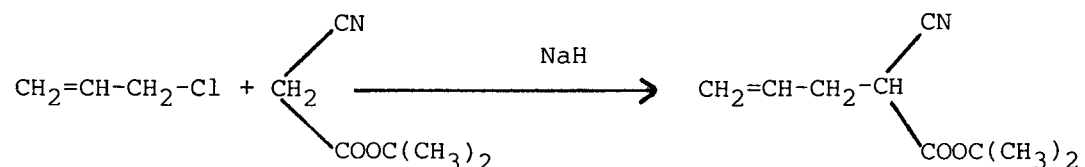
METHOD

To a flask containing a mechanical stirrer tetrabutyl ammonium iodide (70 g.) is dissolved in chloroform (500 ml.). Chlorine gas is then passed slowly through the solution (2 hrs.) with the formation of a yellow precipitate tetrabutyl ammonium iodotetrachloride. A similar arrangement using liquid bromine dissolved in chloroform and added dropwise yielded the bromo analogue. Both compounds are extracted and dried. Elemental analysis on both products concurred with the expected empirical formulae.

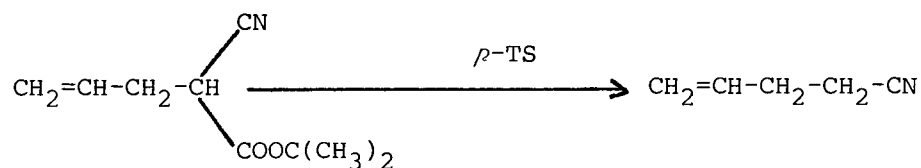
The halogenating agents (20 g.) are then dissolved in dichloromethane (30 ml.) and added to the various olefins (2 g. in 10 ml DCM). The resulting mixtures are then allowed to react in the dark for 3 days (light decomposes the halogenating agents). The solvent is then evaporated and the remainder extracted with diethyl ether (3 x 50 ml.). After evaporation the product is distilled under reduced pressure. Analysis of all products by GLC showed between 94% and 99% stereospecific purity in all cases.

5. THE SYNTHESIS OF 4-CYANOBUT-1-ENE

The synthesis of 4-cyanobut-1-ene (75) is carried out in two distinct stages. Firstly t-butyl cyanoacetate and allyl chloride are condensed in the presence of sodium hydride to form t-butyl allylcyanoacetate.



The t-butyl allylcyanoacetate is then cleaved in the presence of *p*-toluene-sulphonic acid yielding the required product.



METHOD

To a 2 litre three necked flask, fitted with a mechanical stirrer, a reflux condenser and a dropping funnel is added sodium hydride (9.0 g.) covered with redistilled 1,4-dioxane (750 ml.). To this is added dropwise t-butyl cyanoacetate (42.3 g.) over a period of five minutes. after the sodium hydride is consumed allyl chloride (23 g.) is added over a period of several minutes and the mixture refluxed for three hours with the stirring continued for a further thirty hours. The dioxane is then removed and the remainder poured into water (200 ml.),

the water is then extracted with ether (3 x 100 ml.). The combined ether extracts are then dried over sodium sulphate. Fractionation gives the main product with bp. 55-56°C/0.15 mm Hg. Into a distillation flask is placed t-butyl allylcynoacetate (18.1g.) with *p*-toluene-sulphonic acid (0.1 g.) and heated to 170°C. During the decomposition the product distilled, bp. 138-139°C/760 mm Hg.

6. PURIFICATION OF SAMPLES

The following is a list containing the sources and means of purification of those samples used, but not prepared, throughout this piece of work. They were either obtained on a commercial basis or supplied courtesy of B.P. Chemicals Ltd.

Argon :- BOC Ltd. (99.999%)

Krypton :- BOC Ltd. (99.999%)

Acrylonitrile :- Aldrich Chemical Co. (99%)

Vinyl Bromide :- Aldrich Chemical Co. (98%)

Allyl Bromide :- Aldrich Chemical Co. (98%)

Allyl Cyanide :- Aldrich Chemical Co. (98%)

4-bromobut-1-ene :- Aldrich Chemical Co. (99%)

Pent-1-ene :- Aldrich Chemical Co. (99%)

Ethene :- BDH Chemicals (99.8%)

Propene :- BDH Chemicals (99%)

But-1-ene :- BDH Chemicals (99%)

Allyl Chloride :- BDH Chemicals (99%)

4-chlorobut-1-ene :- ICN Pharmaceuticals Inc. (99%)

Ethene-d₁ :- MSD Isotopes (99%)

Chloroprene :- BP Chemicals Ltd. (50/50 with xylene)

Vinyl Chloride :- BP Chemicals Ltd.

All Samples were purified on the vacuum line by repeated trap to trap distillation and dried over CaSO_4 . Samples which had a tendency to polymerise while on the vacuum line were stored in darkened tubes.

CHAPTER III

COMPARISON OF MATRIX ISOLATION SPECTRA AND GAS SPECTRA BETWEEN 900-1000 cm^{-1}

1. INTRODUCTION

2. GENERAL THEORY FOR A DIATOMIC MOLECULE

3. GENERAL THEORY FOR THE OUT-OF PLANE

VIBRATIONS OF A VINYL GROUP

4. VINYL SERIES

5. ALLYL SERIES

6. BUT-1-ENE SERIES

7. ROTATION IN MATRICES

(i) ETHENE

(ii) ETHENE- d_1

8. CONCLUSIONS

CHAPTER III

COMPARISON OF MATRIX ISOLATION AND GAS SPECTRA BETWEEN 900-1000cm⁻¹

1. INTRODUCTION

This section of the work will attempt to compare the matrix isolation spectra with the gas spectra for a series of terminally substituted alkenes. In order to do this, however, an understanding of the vibrational and or rotational transitions which can or do occur in both these phases is a necessary requirement.

The matrix isolation technique aims to simplify spectra by, amongst other things, restricting any rotation of the sample molecule by holding it in what may termed a pseudo gas phase. However, some molecules can freely rotate in certain matrices while others can exhibit partial or hindered rotation. HCl can freely rotate in an argon matrix (32,76) so that even completely isolated molecules show several ir bands due to rotational fine structure. In order to develop a firm basis for this work we have made comparisons with the diatomic system HCl.

2. GENERAL THEORY FOR A DIATOMIC MOLECULE

Matrix isolation studies of HCl have been carried out by various workers (1,32,76) and all have been able to identify bands arising from

vibration-rotation transitions occurring within the matrix as well as bands arising from various aggregates (dimer, trimer, tetramer). Bands due to aggregation may be successively removed by increasing the dilution of the matrix and/or extending the spray-on time (Fig.5), however bands arising from the free rotation of HCl in the matrix persist. To aid in the understanding and interpretation of these bands it is necessary to first consider the theory behind the vibration-rotation transitions of a simple diatomic molecule in the gas phase.

The band assigned to the fundamental stretching mode in a simple heteronuclear diatomic molecule in the gas phase shows fine structure. This structure is due to simultaneous changes in vibrational and rotational energy levels (Fig.5). The values of the energy levels associated with these transitions may be calculated on the basis of the Born-Oppenheimer approximation which expresses the vibration energy $E_{V,J}$ as the sum of the component vibrational and rotational energies E_V and E_J respectively i.e.

$$E_{V,J} = E_V + E_J$$

The energy level values from the solution of the Schrodinger wave equation, taking into account anharmonicity and centrifugal distortion, are as follows :-

$$\tilde{E}_{V,J} = \tilde{\nu}_e (V + \frac{1}{2}) - \tilde{\nu}_e x_e (V + \frac{1}{2})^2 + \tilde{B} J(J+1) - \tilde{D} J^2 (J+1)^2$$

$$\text{where } \tilde{B} = h/8\pi^2 I_B c$$

where $\tilde{\nu}_e$ is the equilibrium vibrational frequency, V is the vibrational quantum number, J is the rotational quantum number I_B is

the moment of inertia about an axis perpendicular to the principal axis and passing through the centre of gravity, χ_e is the anharmonicity constant, \tilde{B} is the rotational constant, \tilde{D} is the centrifugal distortion constant, h is Planck's constant, and c is the velocity of light, \sim indicates the units are cm^{-1} . These energy levels are shown in Fig.5. The selection rules $\Delta V = \pm 1$, $\Delta J = \pm 1$ govern the transitions which are shown as P, Q and R branches. If \tilde{D} is small and $\tilde{B}_0 = \tilde{B}_1 = \tilde{B}$ the wavenumber values of the R branches for transitions from energy levels J' are :-

$$\tilde{\nu}_R = \tilde{\nu}_e (1 - 2 \chi_e) + 2 \tilde{B} (J' + 1)$$

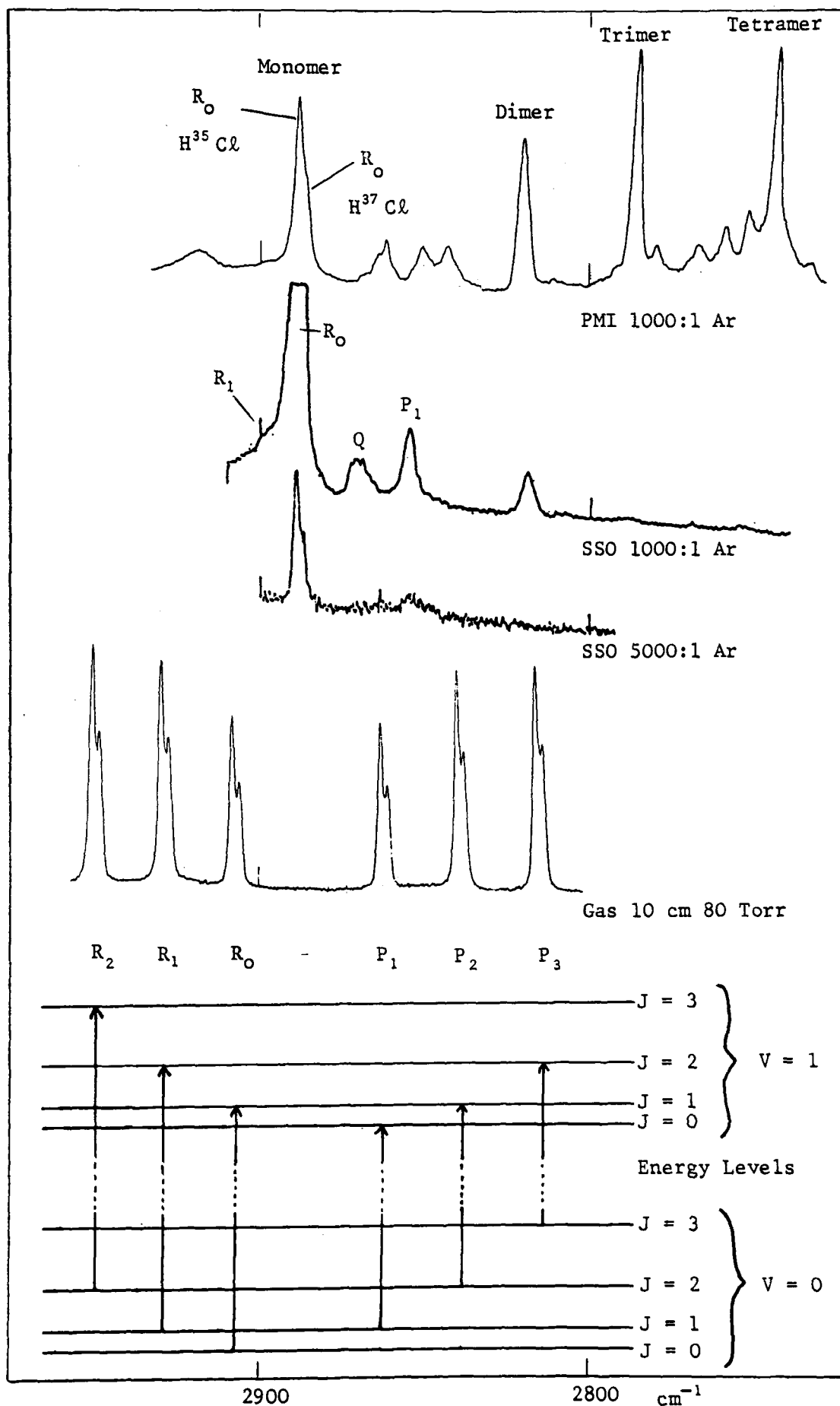
and P branches :-

$$\tilde{\nu}_P = \tilde{\nu}_e (1 - 2 \chi_e) - 2 \tilde{B} J'$$

So far we have assumed that vibration and rotation can proceed quite independently of each other. If the vibration is simple harmonic the mean bond length will be the same as the equilibrium bond length and will not vary with vibrational energy, but in the case of anharmonic vibrations an increase in vibrational energy will lead to an increase in the average bond length.

From the theory and general observation we establish that the Q branch ($\Delta V = +1, \Delta J = 0$) is a forbidden transition and is therefore inactive in the matrix phase. The main band occurring in the matrix spectra (2889cm^{-1}) is therefore not a pure vibrational transition but a vibration-rotation termed R(0) where the selection rules are $\Delta V = +1$, $\Delta J = +1$ (fig.5). Other vibration-rotation transitions have also been

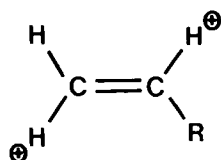
Fig.5 Vibration-rotation spectra of HCl and
corresponding energy levels



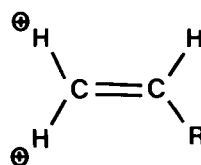
identified (1,7) such as R(1) and P(1) along with vibrational-rotational transitions associated with the enriched isotope (^{37}Cl). Higher rotational levels are highly improbable due to their collapse at the very low temperatures under which these measurements were made (8K). The occurrence of a band at 2865cm^{-1} associated with the "forbidden" Q branch has been shown to arise from the non-rotating molecule being perturbed by complex formation with a nitrogen impurity in the matrix (37,77).

3. GENERAL THEORY FOR THE OUT-OF-PLANE VIBRATIONS OF A VINYL GROUP

A vinyl group has three out-of-plane vibrations of which the twist and wag have been well characterised by empirical correlations (106) and normal coordinate calculations (108). In the simplest case of one alkyl substituent R the twist and wag have the following approximate forms and ranges :-



960 - 980



900 - 920 cm^{-1}

Substituted alkenes are asymmetric rotors and require an extension of the theory developed for diatomic molecules for the vibrational-rotational transitions allowed. For asymmetric rotors three types of band contours are recognised termed A,B and C depending on whether the dipole moment change is principally along the direction of one of the three axes (78,79). If the A and B axes are in the plane of the vinyl

group out-of-plane vibrations will involve a change in dipole moment along the C axis.

The separation between the maxima P,Q and R branch envelopes in the vibrational spectra will depend on the values of the three rotational constants which relate to the three moments of inertia about the respective principal axes in increasing order of magnitude I_A, I_B, I_C .

where:- $\tilde{A} = h/8\pi^2 I_A c$; $\tilde{B} = h/8\pi^2 I_B c$; $\tilde{C} = h/8\pi^2 I_C c$

The molecules considered here have values of rotational constants \tilde{A} , \tilde{B} and \tilde{C} which are different and are therefore termed asymmetric rotors. However, if two of these constants are approximately equal, the molecule may be classed as an accidental symmetric rotor and may be treated as such. There are two limiting cases, one in which $I_B = I_C$ (prolate symmetric top) and one in which $I_A = I_B$ (oblate symmetric top). All the molecules for which calculations have been carried out in this work in order to establish rotational constants have been treated as accidental prolate symmetric tops i.e

$$I_A < I_B = I_C$$

A measure of how closely the molecules studied throughout the context of this piece of work approximate to symmetric tops may be obtained by calculating kappa (κ) from the three rotational constants derived from the molecular geometry.

$$\kappa = \frac{2[\tilde{B} - \frac{1}{2}(\tilde{A} + \tilde{C})]}{\tilde{A} - \tilde{C}}$$

This is a useful term since it varies from -1 for a perfect

prolate symmetric top to +1 for the equivalent oblate symmetric top with values in between these two extremes for molecules with varying degrees of symmetry with respect to the above considerations.

Since we have two different rotational constants we need two quantum numbers to describe the degree of rotation, one for I_A and one for I_B or I_C . However, it turns out to be very convenient mathematically to have a quantum number to represent the total angular momentum of the molecule which is the sum of the separate angular momenta about the two different axes. This is usually chosen to be the quantum number J . It is then convention to use K to represent the component of this angular momentum along the unique axis of the molecule.

Both J and K must by the conditions of quantum mechanics be integral or zero. The total angular momentum governed by J can be as large as is possible, limited only by the theoretical possibility that a real molecule will be disrupted at very high rotational speeds. K is however rather more limited since it cannot take a value which is greater than J governed by the total angular momentum. If we take the case of a rigid symmetric top (ignoring centrifugal distortion), the Schrodinger equation may be solved to give the allowed levels for rotation as :-

$$\tilde{E}_{J,K} = \tilde{B}J(J+1) + (\tilde{A} - \tilde{B})K^2$$

The selection rules associated with transitions between these allowed energy levels depend on whether the transition is parallel or perpendicular to the top axis. The present work is concerned with the out-of-plane alkene vibration-rotation transitions of accidental prolate symmetric tops and hence the selection rules are

those which apply to perpendicular transitions :-

$$\text{i.e. } \Delta v = \pm 1, \quad \Delta J = 0, \pm 1, \quad \Delta K = \pm 1$$

$$\begin{array}{lll} \text{hence:- P branch lines} & \Delta J = +1 & \Delta K = \pm 1 \\ \text{Q branch lines} & \Delta J = 0 & \Delta K = \pm 1 \\ \text{R branch lines} & \Delta J = -1 & \Delta K = \pm 1 \end{array}$$

We see then that this type of vibration gives rise to many sets of P and R branch lines, since for each J value there are many allowed values of K. The wings of the spectrum will then be quite complicated and will not normally be resolvable into separate lines. The Q branch is also complex since it too will consist of a series of lines (Fig. 6) on both sides of ν_0 separated by $2(\tilde{A}-\tilde{B}) \text{ cm}^{-1}$. If $\tilde{A} \gg \tilde{B}$ the Q branch lines will be separated and will appear as a series of maxima above the P,R envelope. These lines are represented by :-

$$\tilde{\nu}_0^{\text{sub}} = \tilde{\nu}_0 + (\tilde{A}' - \tilde{B}') \pm 2(\tilde{A}' - \tilde{B}')K + [(\tilde{A}' - \tilde{B}') - (\tilde{A}'' - \tilde{B}'')]K^2$$

where \tilde{A}' and \tilde{B}' are the rotational constants in the ground vibrational state and \tilde{A}'' and \tilde{B}'' are the rotational constants in the excited state. It can be seen that by fitting Q branch frequencies to K values, (80) that values of $(\tilde{A}' - \tilde{B}')$ and $(\tilde{A}'' - \tilde{B}'')$ can be evaluated according to the equation using :-

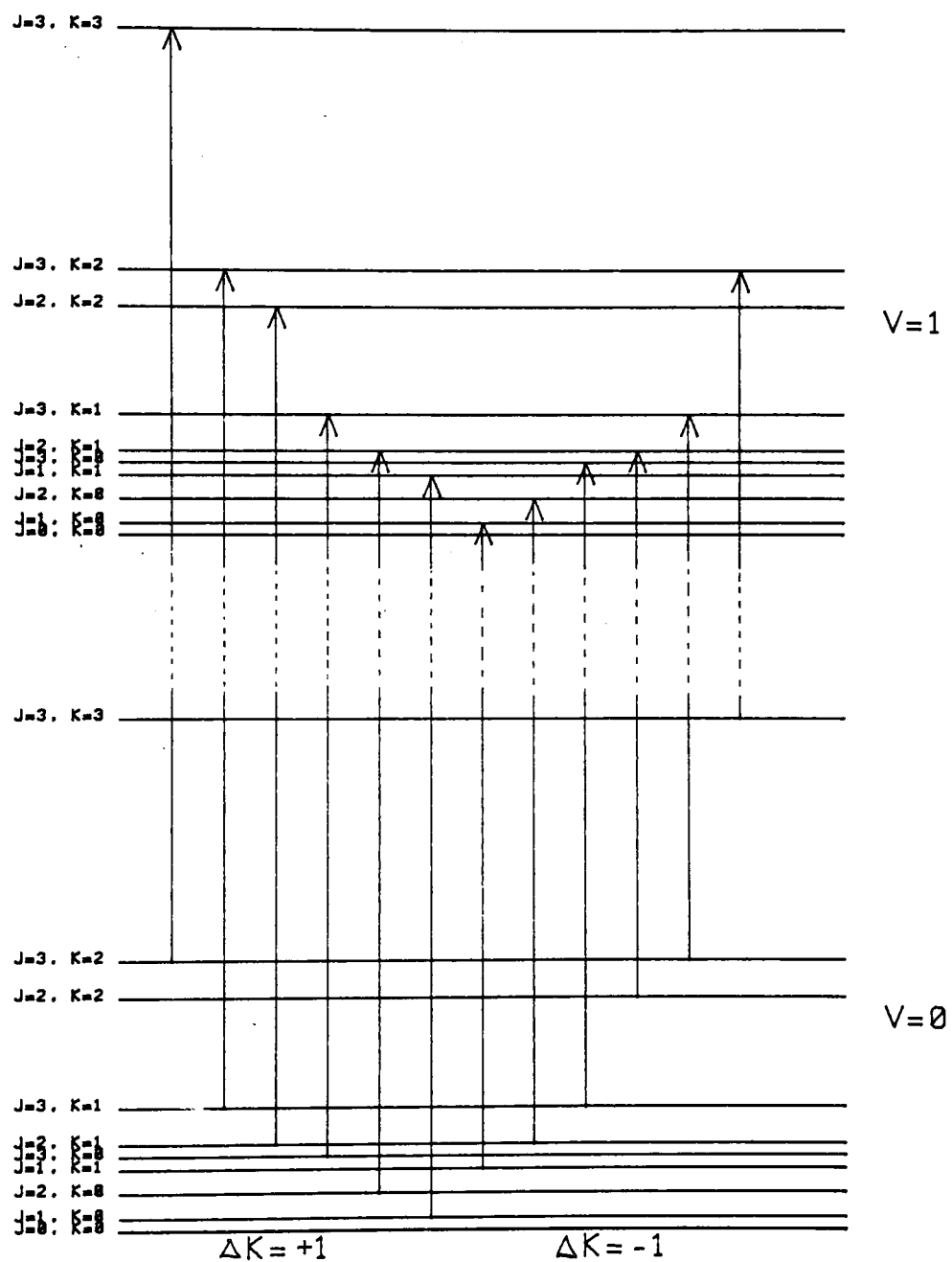
$$Q = a \pm bK - cK^2$$

$$\text{where } a = \tilde{\nu}_0 + (\tilde{A}' - \tilde{B}')$$

$$b = \pm 2(\tilde{A}' - \tilde{B}')$$

$$\text{and } c = [(\tilde{A}' - \tilde{B}') - (\tilde{A}'' - \tilde{B}'')]$$

Fig.6. Energy levels for the Q branch of a perpendicular transition in Vinyl Chloride ($2\text{ cm} = 3\text{ cm}^{-1}$)



a computer programme has been written which returns a, b and c for a series of values for Q and K. The values of ($\tilde{A}'-\tilde{B}'$) obtained by this method can then be directly compared to the values obtained from a computer program which returns the principal moments of inertia the rotational constants and hence kappa directly from the molecular geometry (CART PROGRAM).

The theory outlined here relating to accidental prolate symmetric top molecules and the subsequent values obtained from calculations linking proposed geometrical structures to those which fit experimental data can be applied in aiding comparisons between spectra obtained in both the gas and matrix phases for the following families of substituted olefins. The comparisons drawn may then also aid in the interpretation of some of the secondary features apparent when these species are studied in an argon matrix at very low temperatures.

4. VINYL SERIES

The vinyl compounds all show strong sharp bands in both the gas and matrix phase in this region corresponding to the twist (higher wavenumber) and the wag (lower wavenumber). The gas spectra show the characteristic patterns associated with perpendicular bands of symmetric tops and hence display rotational fine structure in all cases. The calculation of ($\tilde{A}'-\tilde{B}'$) from the spectra, assuming the prolate symmetric top model, appear to be in good agreement with ($\tilde{A}'-\tilde{B}'$) calculated from the geometry (Table 1) and those values calculated for vinyl chloride and vinyl bromide by other workers (80-82). The values derived for kappa vary from -0.98 to -0.94 and shows that these molecules do approximate very closely to prolate symmetric tops. It may be noted that the structure of the bands associated with propene are

TABLE 1

	<u>Cart</u> <u>program</u>	<u>$(\tilde{A} - (\tilde{B} + \tilde{C})/2)$</u>	<u>Spectra</u> <u>$(\tilde{A} - \tilde{B})$</u>	<u>kappa</u> <u>(κ)</u>
<u>Propene</u>	A= 1.497 B= 0.337 C= 0.289	1.184	1.203	-0.937
<u>Vinyl chloride</u>	A= 1.918 B= 0.215 C= 0.193	1.714	1.706	-0.976
<u>Vinyl bromide</u>	A= 1.880 B= 0.167 C= 0.154	1.719	1.691	-0.987
<u>Acrylonitrile</u>	A= 1.670 B= 0.165 C= 0.151	1.512	1.545	-0.980
<u>But-1-ene</u>	A= 0.780 B= 0.145 C= 0.130	0.642	0.625	-0.984
<u>Allyl chloride</u>	A= 0.753 B= 0.097 C= 0.095	0.657	0.640	-0.996
<u>Allyl bromide</u>	A= 0.698 B= 0.068 C= 0.067	0.630	0.677	-0.997
<u>Allyl cyanide</u>	A= 0.599 B= 0.126 C= 0.114	0.479	-	-0.950

not as symmetrical as the equivalent bands for the other members of the series (Fig.7-10). This is probably due to the presence of conformers as a result of the axis of rotation around the methyl group. The methyl group may be staggered or eclipsed with the plane of the molecule.

Comparison of rotational constants calculated for both these geometries with those derived from spectral data suggests that the lower energy staggered conformer is probably the predominant form at room temperature although the difference between the values obtained for both forms is very small.

For the comparison of the gas with the matrix spectra it may be noted that the pattern of band shift is the same in all cases. The bands arising from the two out-of-plane modes in the gas phase appear to be "inside" the matrix bands, hence, the wag is shifted to lower wavenumber and the twist to higher wavenumber in the matrix phase (Table 2). This means that $\Delta\nu$ is positive for the twisting mode and negative for the wagging mode in all cases where :-

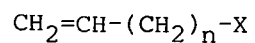
$$\Delta\nu = \nu_{matrix} - \nu_{gas}$$

The negative frequency shift obtained for the wagging mode in the vinyl series is unusual in that frequency shifts for bending vibrations are usually to higher wavenumber. This anomalous frequency shift may be a function of the anharmonicity of the vibration, it has been noted that wags produce overtone vibrations whereas twists do not (83). The perturbation between frequency values in the vapour and in a condensed phase such as that produced by matrix isolation is a complex phenomenon. This can be considered in terms of a range of interactions which can in turn influence the potential energy function which determines the frequency of the fundamental and its various harmonics.

The observation that $\Delta\nu$ is generally negative for stretching vibrations and positive for bending vibrations reflects the different potential functions for these modes and particular bending modes such as the twist and wag out-of-plane vinyl modes would therefore appear to have potential functions which relate to the gas and matrix isolated phases in different ways.

The anharmonicity constant measures the distortion from a simple harmonic function and is normally positive for stretching vibrations. A large number of values taken usually in inert solvent but also in the gas phase for the wag mode of various vinyl compounds (83) shows this is usually small or negative in these compounds. This constant measures the mechanical anharmonicity which derives from higher terms in the potential energy function. Another source of anharmonicity is electrical anharmonicity which derives from higher terms in the function describing the change in dipole moment with normal coordinate. This influences the intensity of the first overtone. Since these are typically strong for the vinyl wagging mode and are close to twice the fundamental frequency it may be that this mode is characterized by a large anharmonicity which is electrical rather than mechanical and the motion of the terminal vinyl hydrogens out of the plane of the molecule has some stretching character. The measurement of $\Delta\nu$ therefore for selected modes and molecules could be an important probe into this problem. Another feature which arises from this comparison is the appearance of a weak band several wavenumbers lower than the twist for all the vinyl compounds in the matrix phase. This weak band in the matrix approximately corresponds in wavenumber value to the band in the gas phase. The appearance of this feature, remarkable in its consistency, may be due to :-

TABLE 2



<u>X/n</u>	<u>n=0</u>			<u>n=1</u>			<u>n=2</u>		
	<u>matrix</u>	<u>gas</u>	<u>Δv</u>	<u>matrix</u>	<u>gas</u>	<u>Δv</u>	<u>matrix</u>	<u>gas</u>	<u>Δv</u>
<u>CH₃</u>									
twist	998	991	+7.0	999	994	+5.0	992.5	992	+0.5
wag	909	912.5	-3.5	910	912	-2.0	913	914	-1.0
<u>Cl</u>									
twist	950	942	+8.0	996	993	+3.0	998.5	989	-0.5
wag	893.5	896	-2.5	926.5	930	-3.5	922.5	922	+0.5
<u>Br</u>									
twist	948	941.5	+6.5	989.5	987.5	+2.0	996	988.5	+7.5
wag	899	902	-3.0	926.5	927.5	-1.0	922	922	0.0
<u>CN</u>									
twist	974	971	+3.0	987.5	986	+2.0	998	993.5	+4.5
wag	953	953.5	-0.5	927.5	931.5	-4.0	927	924.5	+2.5

1. Some degree of association within the lattice.
2. Some partial or hindered rotation of these compounds in a substitutional site in the matrix.
3. A matrix site effect which would appear to be a characteristic feature of this particular mode for these particular compounds.

If the feature is due to some degree of molecular association then these may be minimised by high dilution factors. The postulation that this feature is due to some form of rotation within the lattice is in some degree supported by a consideration of the theory for vibration-rotation transitions allowed in the gas phase for this particular mode. The strong central branch associated with the twisting mode in the gas phase corresponds to the transition $\Delta V=+1$, $\Delta J=0$, $\Delta K=+1$ and therefore arises from a change in both the vibrational and rotational energy of the molecule. If no rotation of this molecule is allowed in an argon cage the band associated with the matrix spectra would correspond to $\Delta V=+1$, $\Delta J=0$, $\Delta K=0$ and would be a pure vibration. This transition, forbidden in the gas phase, would occur at a lower frequency than the vibration-rotation (predicted from the theory). If some degree of hindered rotation can occur in the matrix it may then be argued that two bands, corresponding to those two modes discussed previously, may be seen in the matrix spectra with the stronger high wavenumber band corresponding to a vibration-rotation and the lower frequency weaker band corresponding to a pure vibration. Therefore the degeneracy of the $\Delta V=+1$, $\Delta J=0$, $\Delta K=0$ transition may be lifted by the matrix environment in

Fig.7 Infrared spectra of propene 900 - 1000 cm^{-1}

(a) Matrix Isolation in argon

M:I = 1000:1

(b) Gas 10cm path length 40 Torr

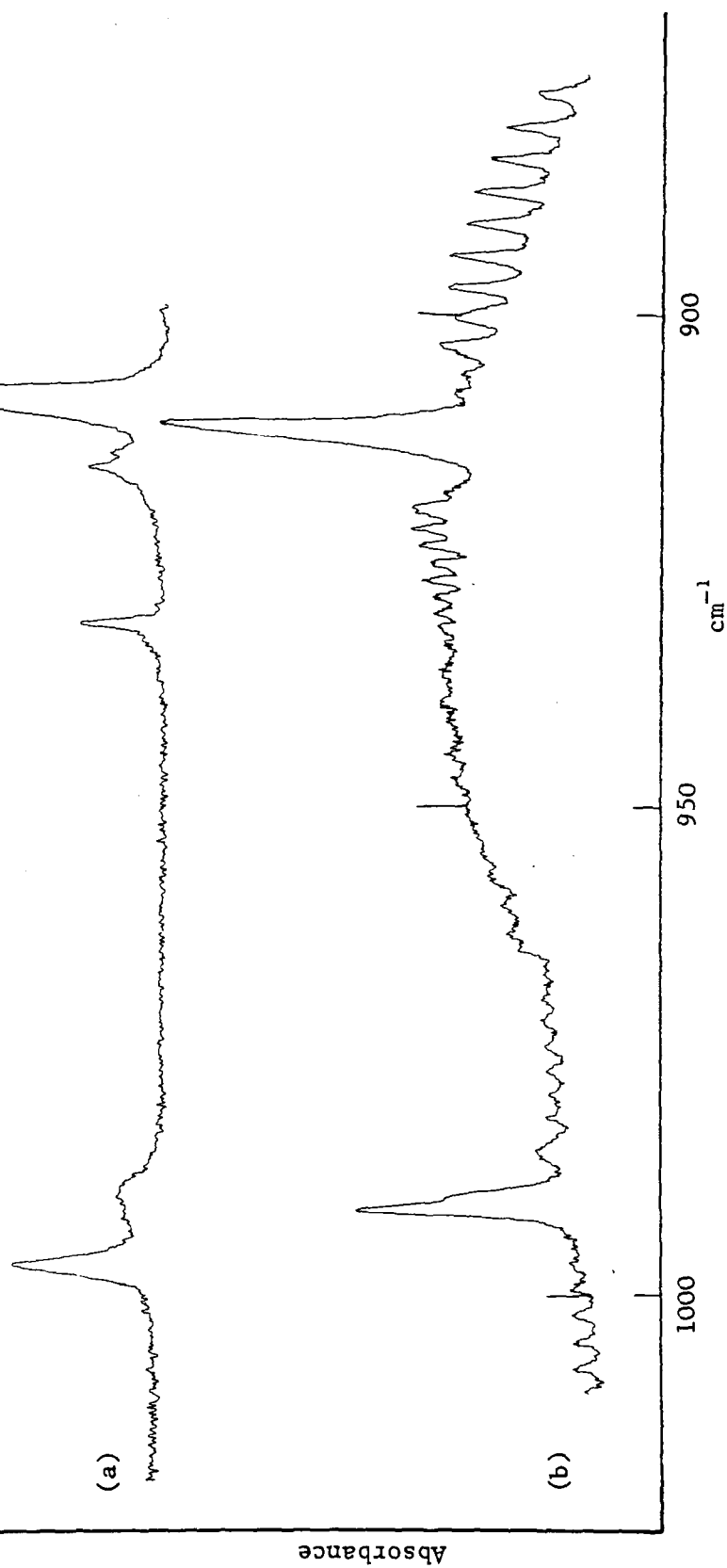


Fig.8. Infrared spectra of vinyl chloride 900 - 1000 cm^{-1}

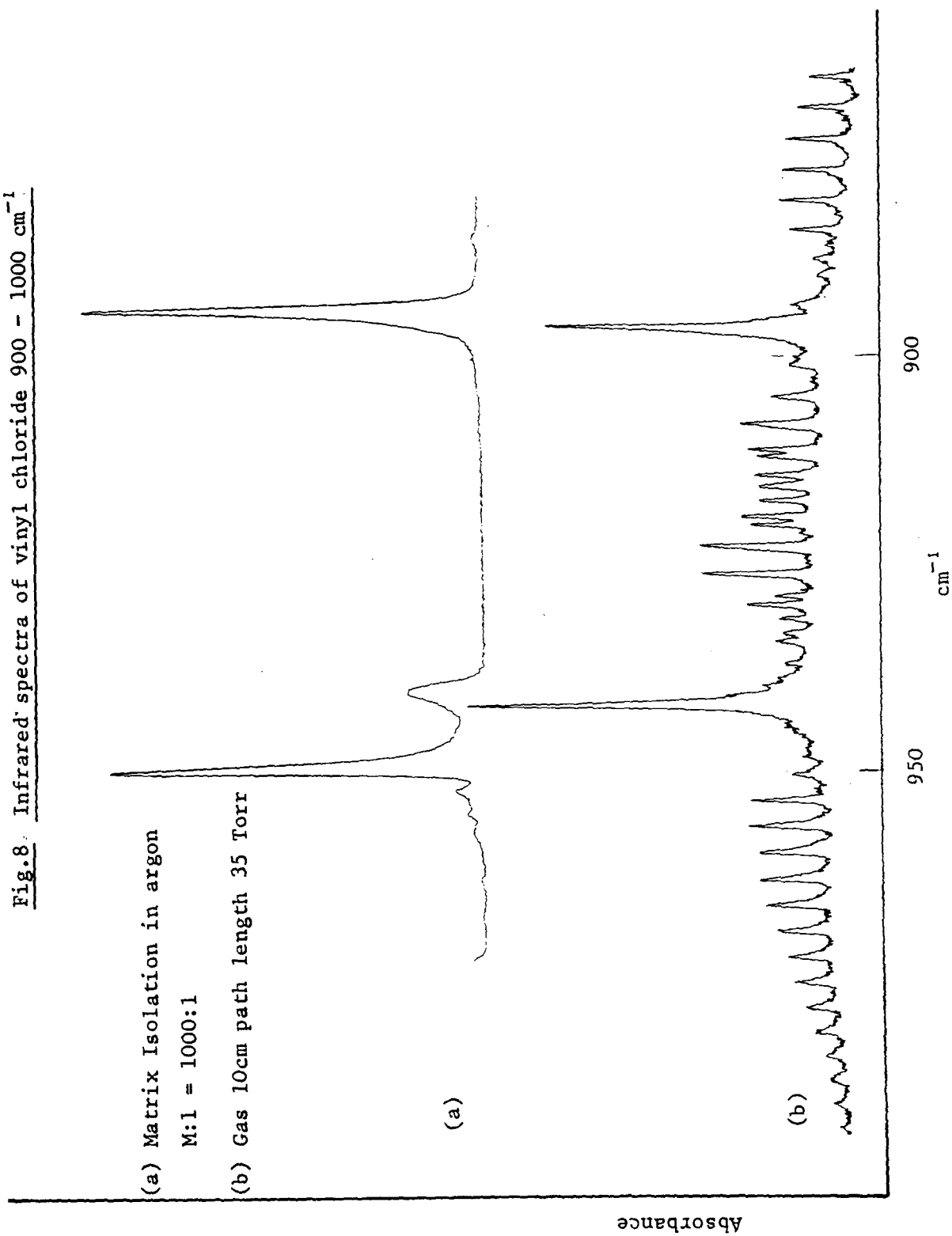


Fig.9 Infrared spectra of vinyl bromide 900 - 1000 cm^{-1}

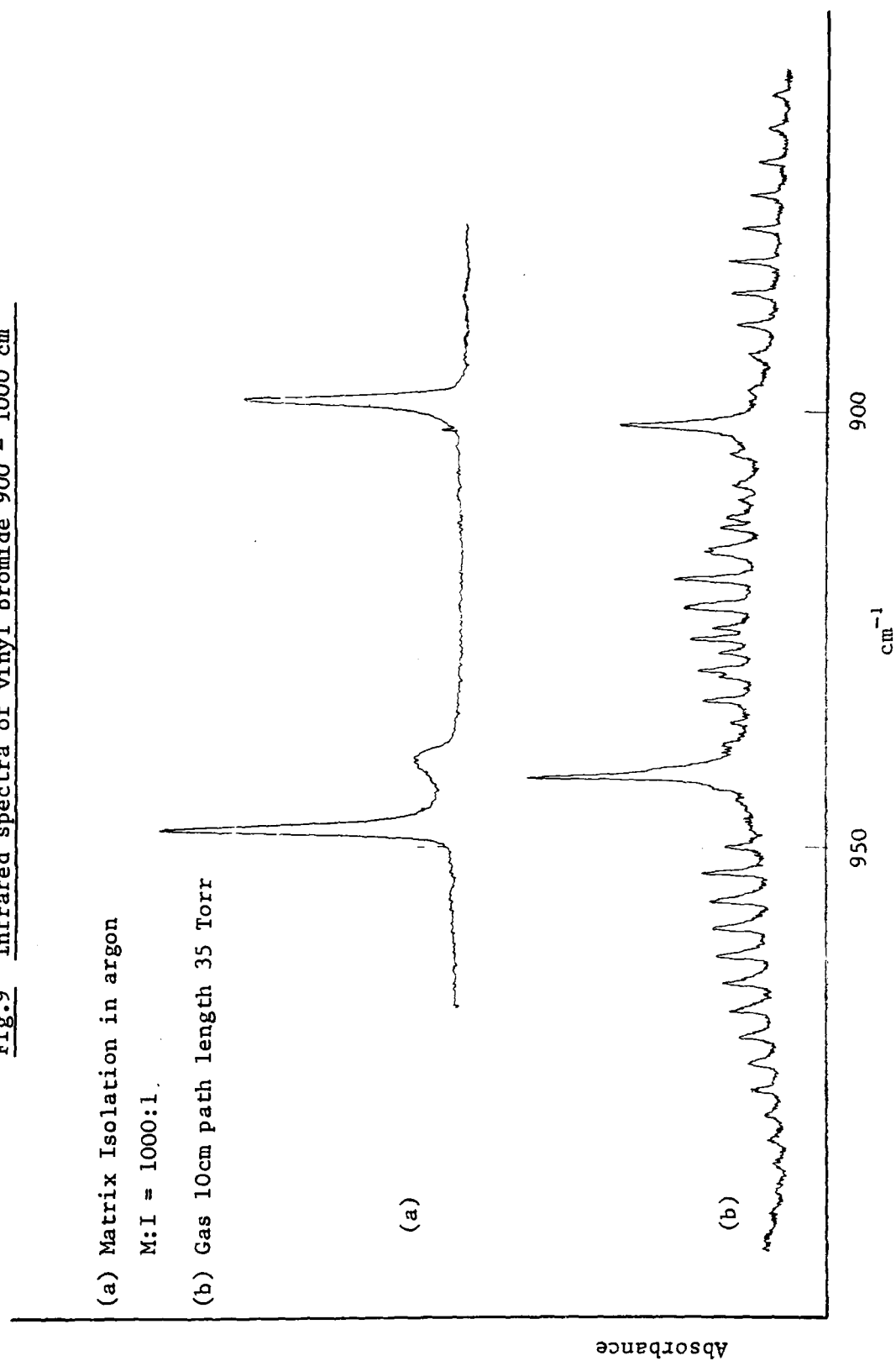
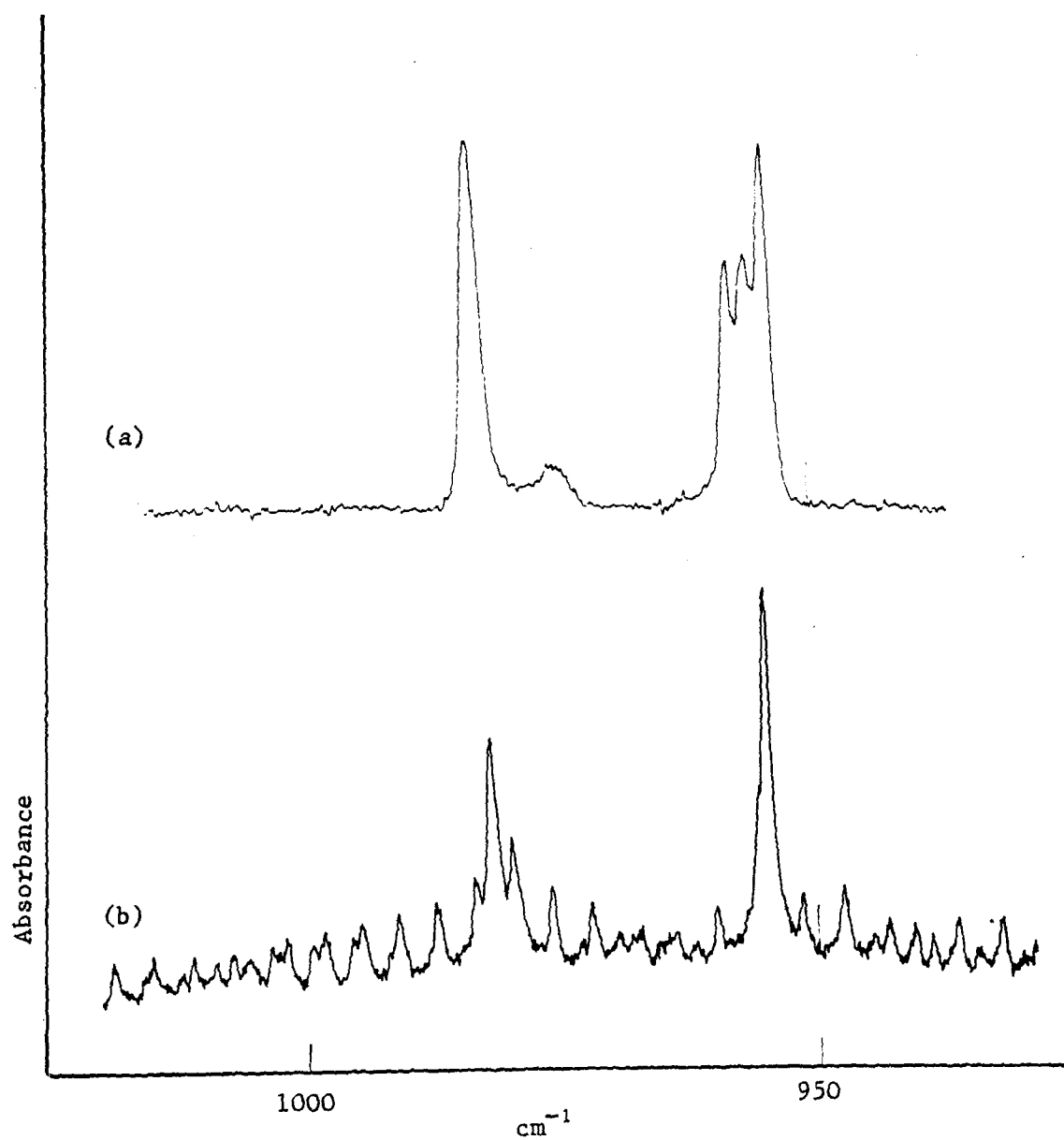


Fig.10 Infrared spectra of acrylonitrile 900 - 1000 cm^{-1}

(a) Matrix Isolation in argon

M:I = 1000:1

(b) Gas 10cm path length 40 Torr



a similar fashion to that seen in HCl.

An experimental test for rotational motion in a matrix is careful temperature variation. It may be assumed that the population of energy levels attain rapid equilibrium corresponding to the Maxwell-Boltzman distribution. Bands associated with vibration-rotation transitions should show a reversible intensity variation with temperature, corresponding to varying degrees of population of different rotational energy levels. By contrast distribution of molecules about various matrix sites is unlikely to show a systematic change with temperature or dilution.

The construction of an accurate temperature control and measurement system and the subsequent temperature cycling of these compounds did not suggest that any rotation was occurring in that no reversible temperature dependence could be easily detected. It may be speculated that in a prolate symmetric top the twist mode would be particularly sensitive to the kind of cavity within which the molecule exists. By elimination it may therefore be suggested that the bands were probably due to some well defined site effect related to this particular series of compounds.

5. ALLYL SERIES

The spectra of the allyl compounds (Figs. 11-14) proved far more difficult to understand in both phases since they are more complex molecules in terms of the possibility of different conformers being present in both the gas and matrix and the increased site effect possibilities in the matrix due to their larger size.

For the gas spectra some rotational fine structure was apparent for the out-of-plane modes in but-1-ene, allyl chloride and allyl

bromide however for allyl cyanide no rotational fine structure was observable at the limit of resolution available with the dispersive instrument.

These molecules have one or more axes of internal rotation but still approximate closely to prolate symmetric tops with κ varying from -0.99 to -0.95. Examination of the spectra of allyl chloride, and allyl bromide resulted in similar conclusions of those of other workers (84-86) in that the low energy *gauche* or *skew* form is the predominant conformer in the gas phase at room temperature. These assumptions are favoured by calculations involving the geometries of these assumed forms agreeing more closely with results derived from experimental data. Values of $(\tilde{A}'-\tilde{B}')$ obtained from the spectra for allyl chloride and allyl bromide were in good agreement with those values obtained for the *gauche* form from microwave data by Hirota and Niide et al (85-86). The values obtained using the Cart program were however not in such good agreement for reasons probably associated with software inadequacy in dealing with molecules of this type (Table 1). Previous studies of but-1-ene by various spectroscopic techniques (87-89) have differed over its conformational preference. A study by Woller et al using nmr (90) has stated that the *cis* form is the more stable. The present work however has revealed a better fit between spectral data and rotational constants calculated using molecular parameters associated with the *gauche* form. No similar analysis could be made for allyl cyanide since the gas spectra displayed no rotational fine structure, however, it may be assumed that the predominant form in the gas phase is the same as that for the other members of the series. The value of 0.504 calculated for $(\tilde{A}'-\tilde{B}')$ from the assumed geometry is however not in agreement with values calculated by other workers for

the *gauche* form (91-93). The error however appears to be almost totally due to the values determined for the rotational constant \tilde{A}' . More recent work carried out by Compton (94) suggests however that previous values determined for \tilde{A}' have only been done to a low degree of precision and as such the microwave spectra should probably be reexamined. The value of $(\tilde{A}' - \tilde{B}')$ calculated during this piece of work is much smaller than the value of 1.06 cm^{-1} previously determined for the *gauche* conformer and is the smallest for all the members of this series. This value therefore appears to more closely follow experimental data in that this was the only member of the series for which no rotational fine structure was observable in the gas phase.

The comparison of the spectra in gas and matrix phases revealed that the pattern of frequency shift established for the vinyl series was not obeyed so clearly here (Table 2). It must be emphasised however that this is by no means conclusive in that frequencies quoted for the different species may be open to question as a result of some degree of doubt in establishing the band centres in the gas phase and the "predominant" bands in the matrix phase, there is also some degree of overlap from a third fundamental in this region (84,95-96). However some evidence of assignment in the gas phase may be obtained by comparison with the matrix together with regard for the pattern of frequency shift established for the vinyl series.

As stated previously the matrix spectra are complicated by site effect bands together with aggregate bands and although the main form in the matrix is proposed to be the low energy *gauche* conformer some contribution occurs from the high energy *cis* form. The overall picture is therefore a complex one and any further conclusions drawn from the comparisons of spectra in both the gas and matrix phase for this series

Fig.11 Infrared spectra of but-1-ene 900 - 1000 cm^{-1}

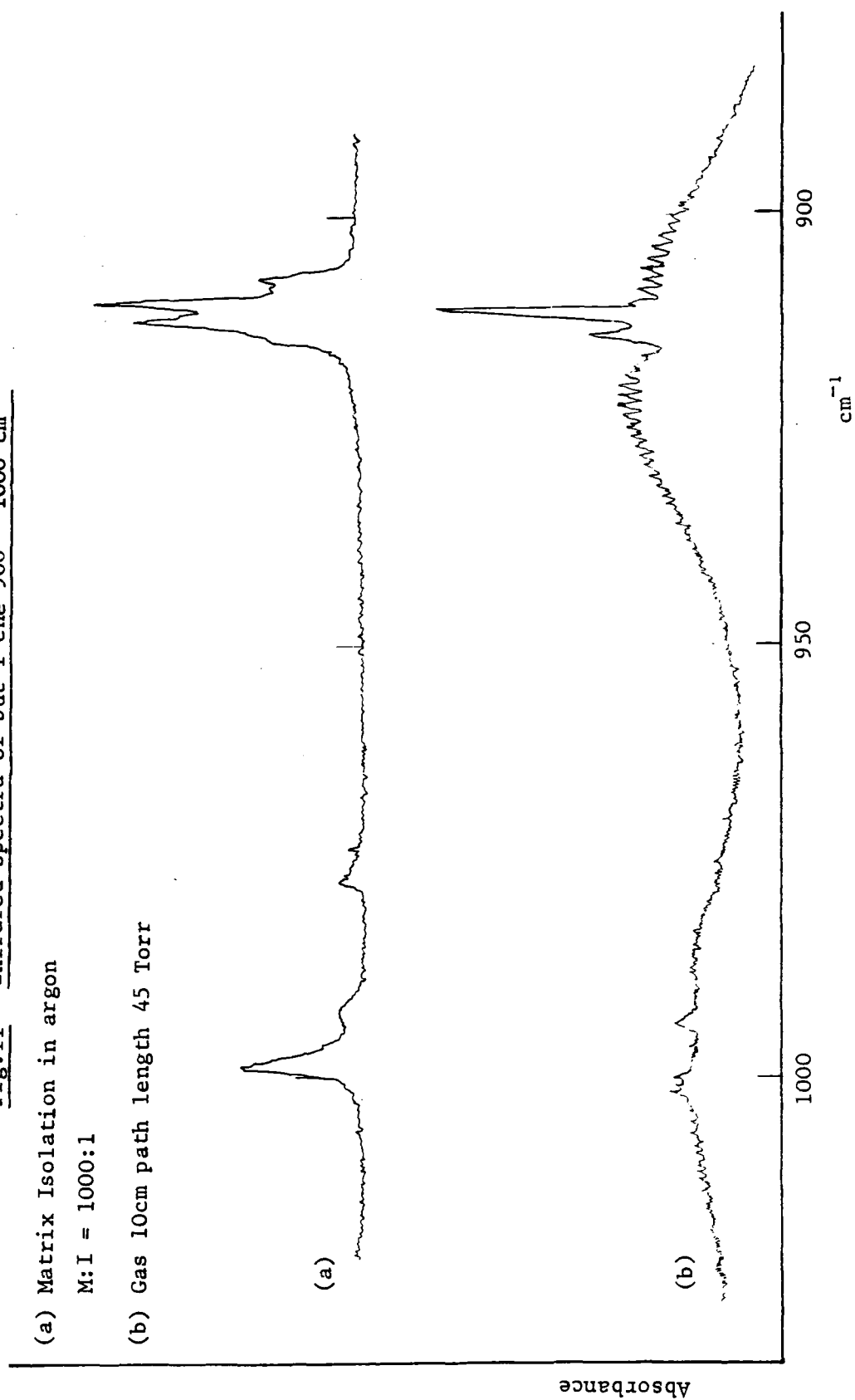


Fig.12 Infrared spectra of allyl chloride 900 - 1000 cm^{-1}

(a) Matrix Isolation in argon

M:I = 1000:1

(b) Gas 10cm path length 40 Torr

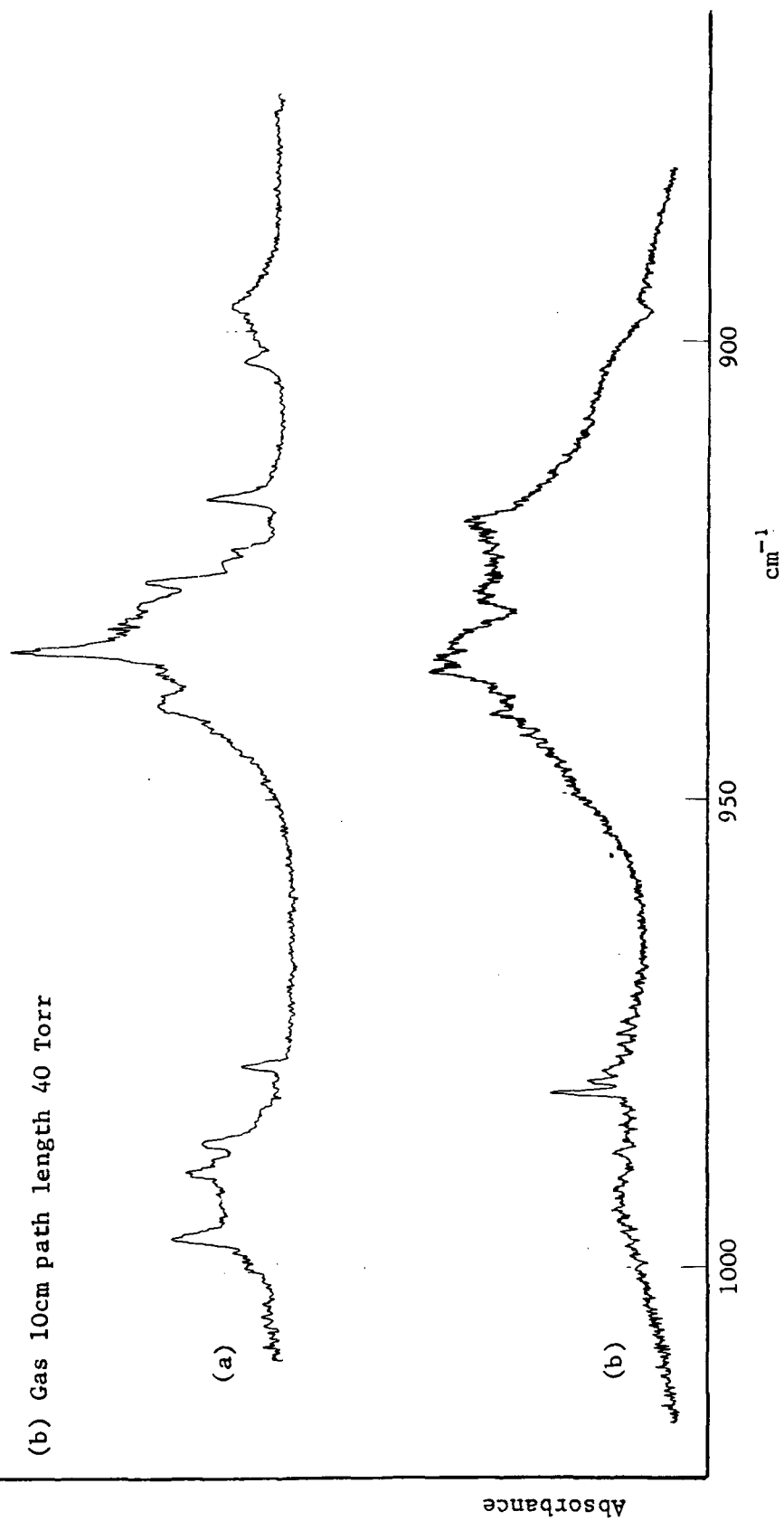


Fig.13 Infrared spectra of allyl bromide 900 - 1000 cm^{-1}

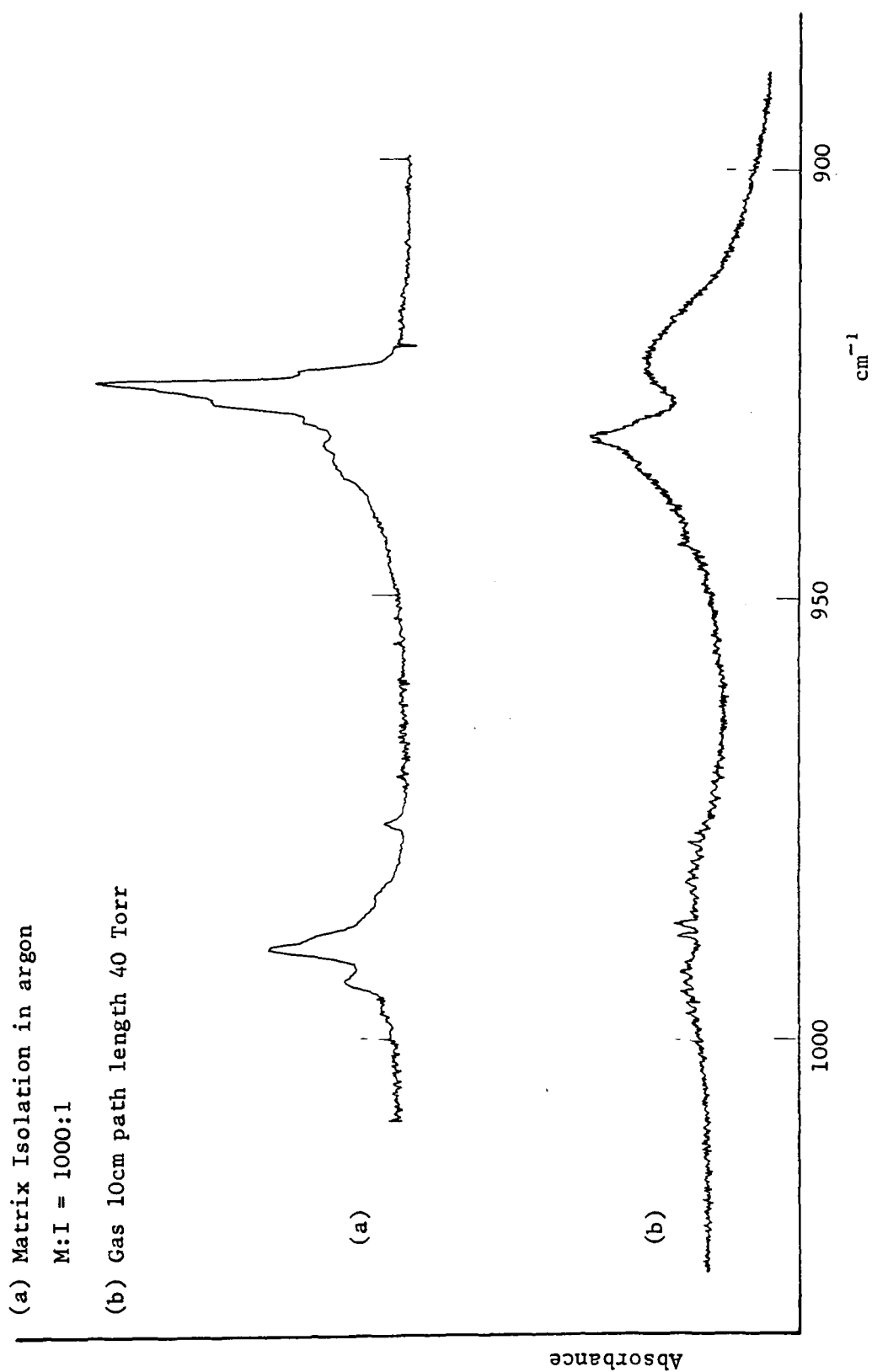
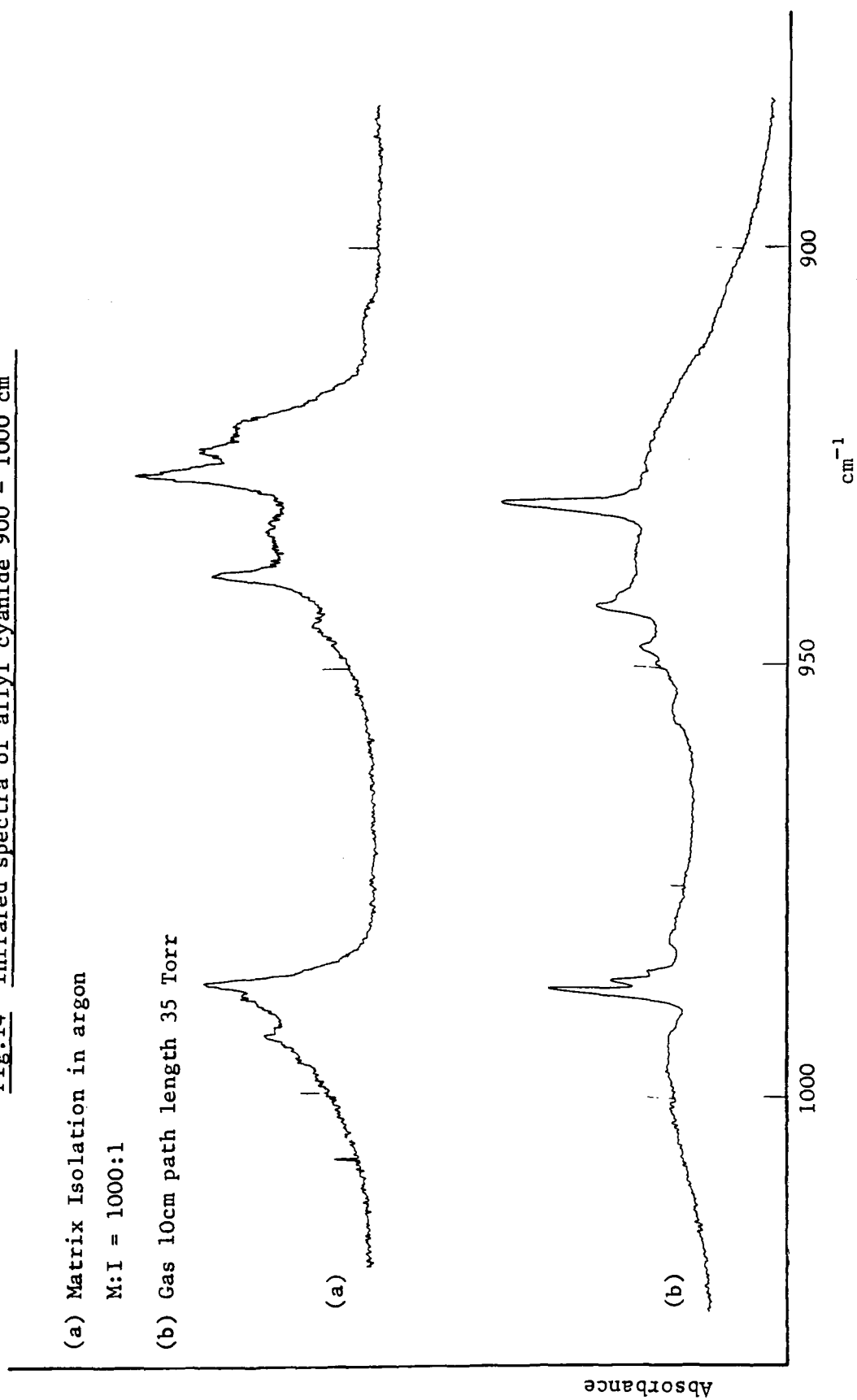


Fig.14 Infrared spectra of allyl cyanide 900 - 1000 cm^{-1}

(a) Matrix Isolation in argon

M:I = 1000:1

(b) Gas 10cm path length 35 Torr



of compounds must necessarily take these complications into consideration.

6. BUT-1-ENE SERIES

Examination of the spectra for this series (Figs. 15-18) did not appear to contribute much to the overall picture. The out-of-plane modes in the gas spectra gave rise to broad C-type bands displaying no rotational fine structure. The molecules have also deviated from the accidental prolate symmetric top model and as such the theory cannot be applied at all with any success. It was therefore considered inappropriate to carry out calculations to evaluate the rotational constants for this series of compounds since no comparisons of the results obtained could be made with those obtained from spectral data.

The increased complexity of the molecules has also given rise to increased spectral complexity in the matrix phase as a result of conformer and/or matrix site effect bands as well as aggregate bands. As with the gas spectra, the matrix spectra gave rise to a series of broad features which had only a marginal advantage in terms of resolution over spectra run in the liquid phase. The result of comparing the frequencies obtained for spectra of these molecules in both phases does not appear to show any clear pattern as was the case with the substituted vinyls (Table 2). In fact the advantage of applying the matrix isolation technique to molecules of this size or type at all appears to be debatable in that not much extra information is gained over that obtained from other phases.

Fig.15 Infrared spectra of pent-1-ene 900 - 1000 cm^{-1}

(a) Matrix Isolation in argon

M:I = 1000:1

(b) Gas 10cm path length 20 Torr

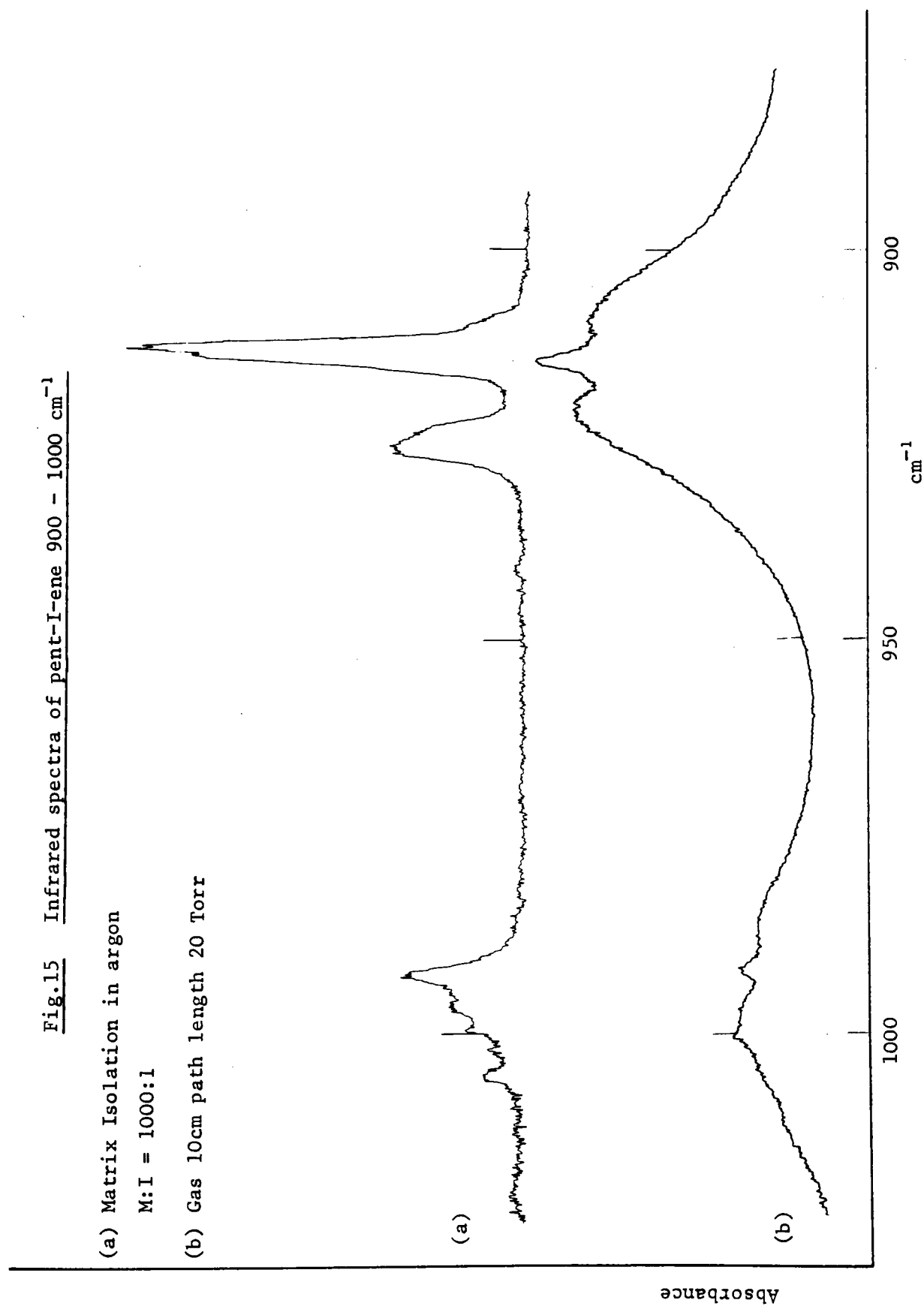


Fig.16 Infrared spectra of 4-chlorobut-1-ene 900 - 1000 cm^{-1}

(a) Matrix Isolation in argon

M:I = 1000:1

(b) Gas 10cm path length 12 Torr

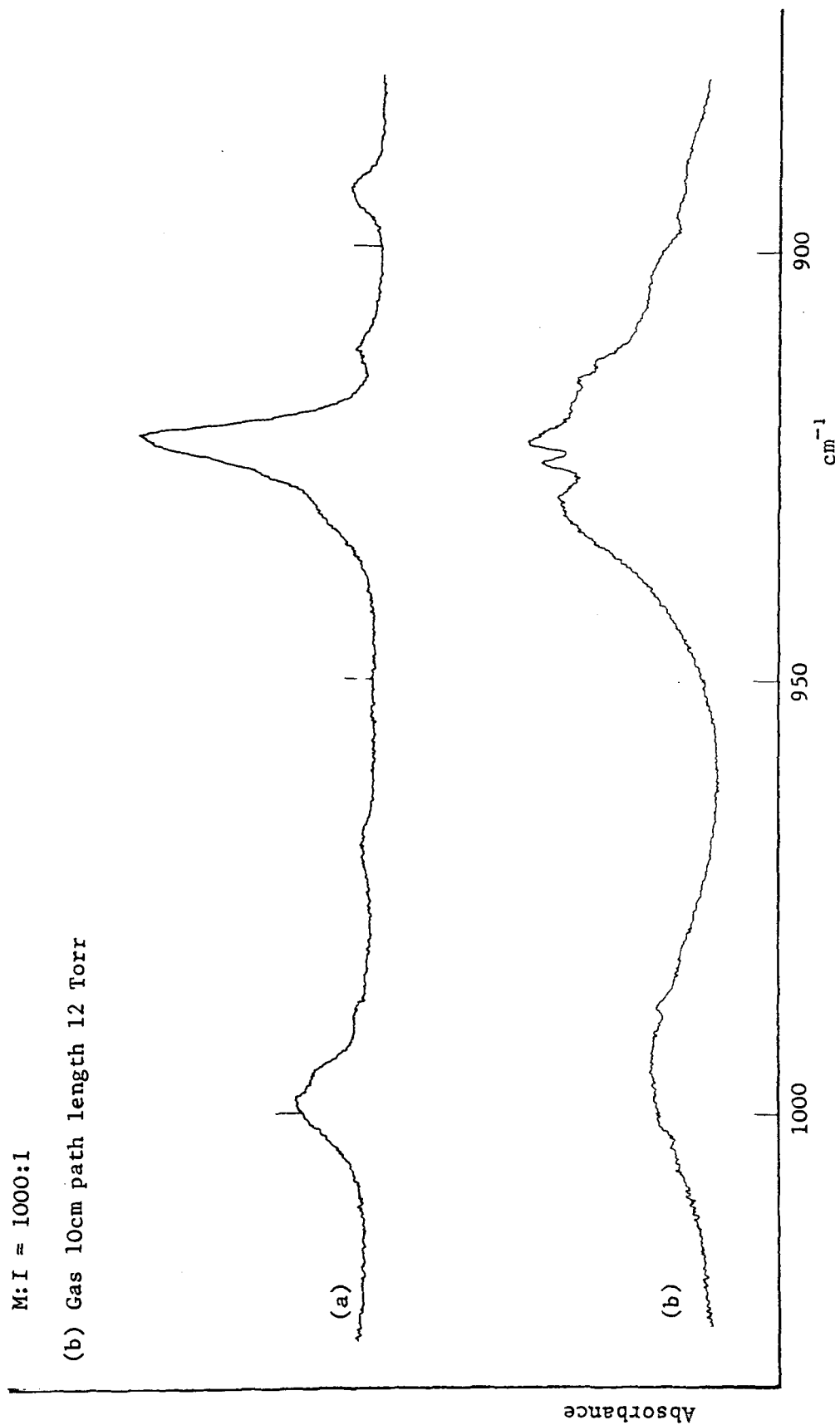


Fig.17 Infrared spectra of 4-bromobut-1-ene 900 - 1000 cm^{-1}

(a) Matrix Isolation in argon

M:I = 1000:1

(b) Gas 10cm path length 10 Torr

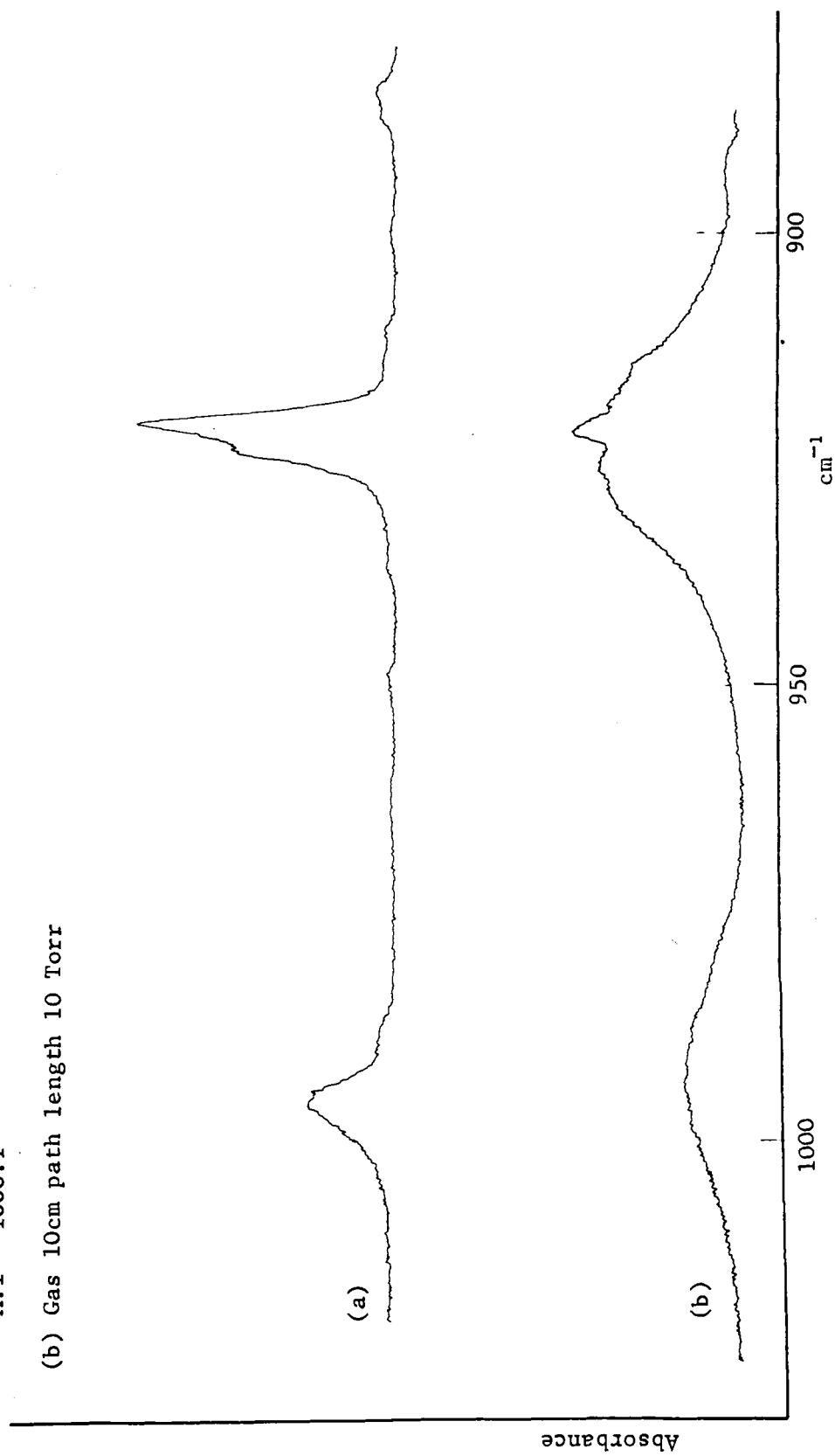
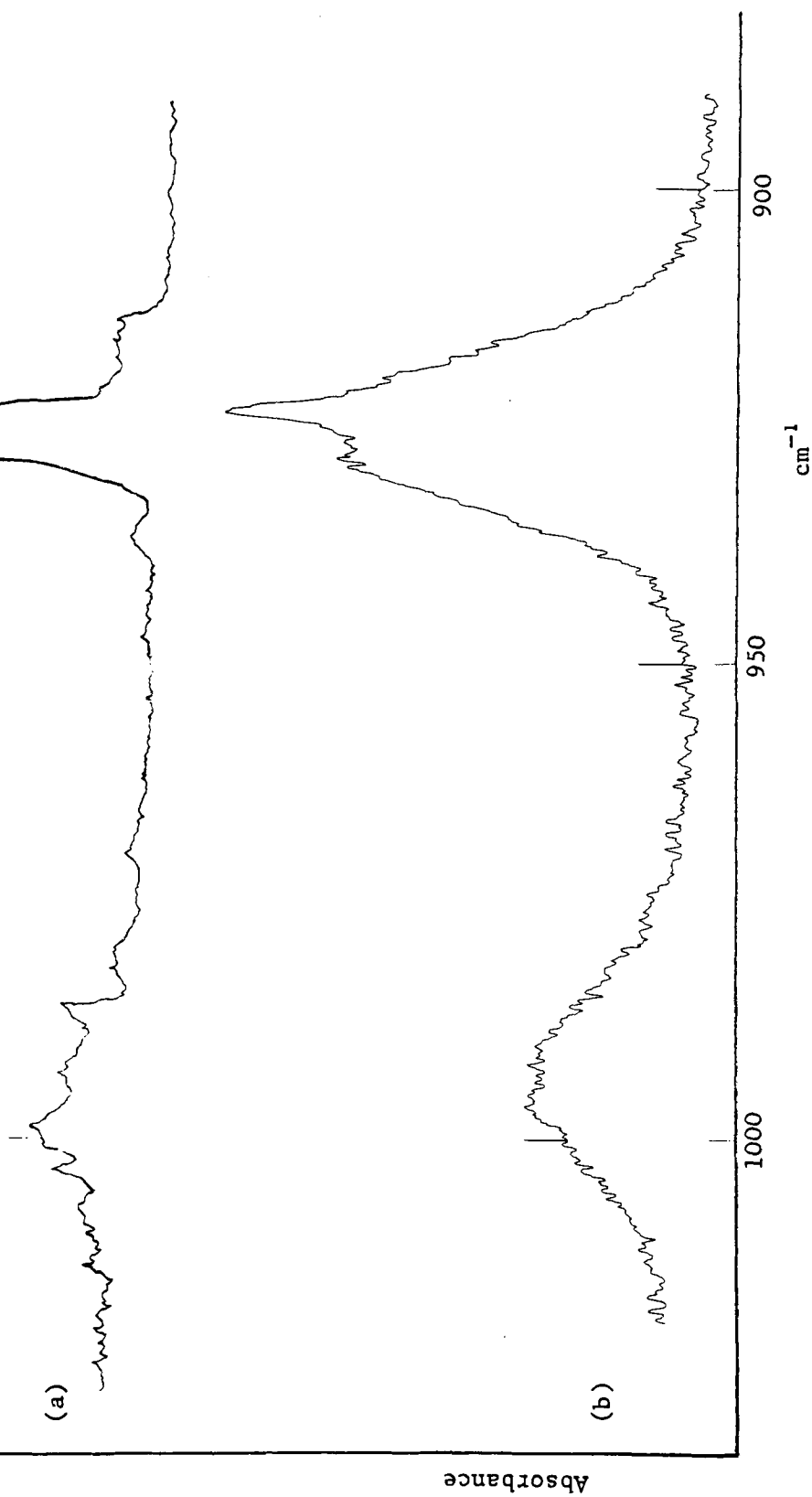


Fig.18 Infrared spectra of 4-cyanobut-1-ene 900 - 1000 cm^{-1}

(a) Matrix Isolation in argon

M:I = 1000:1

(b) heated gas cell 10cm
path length 70°C



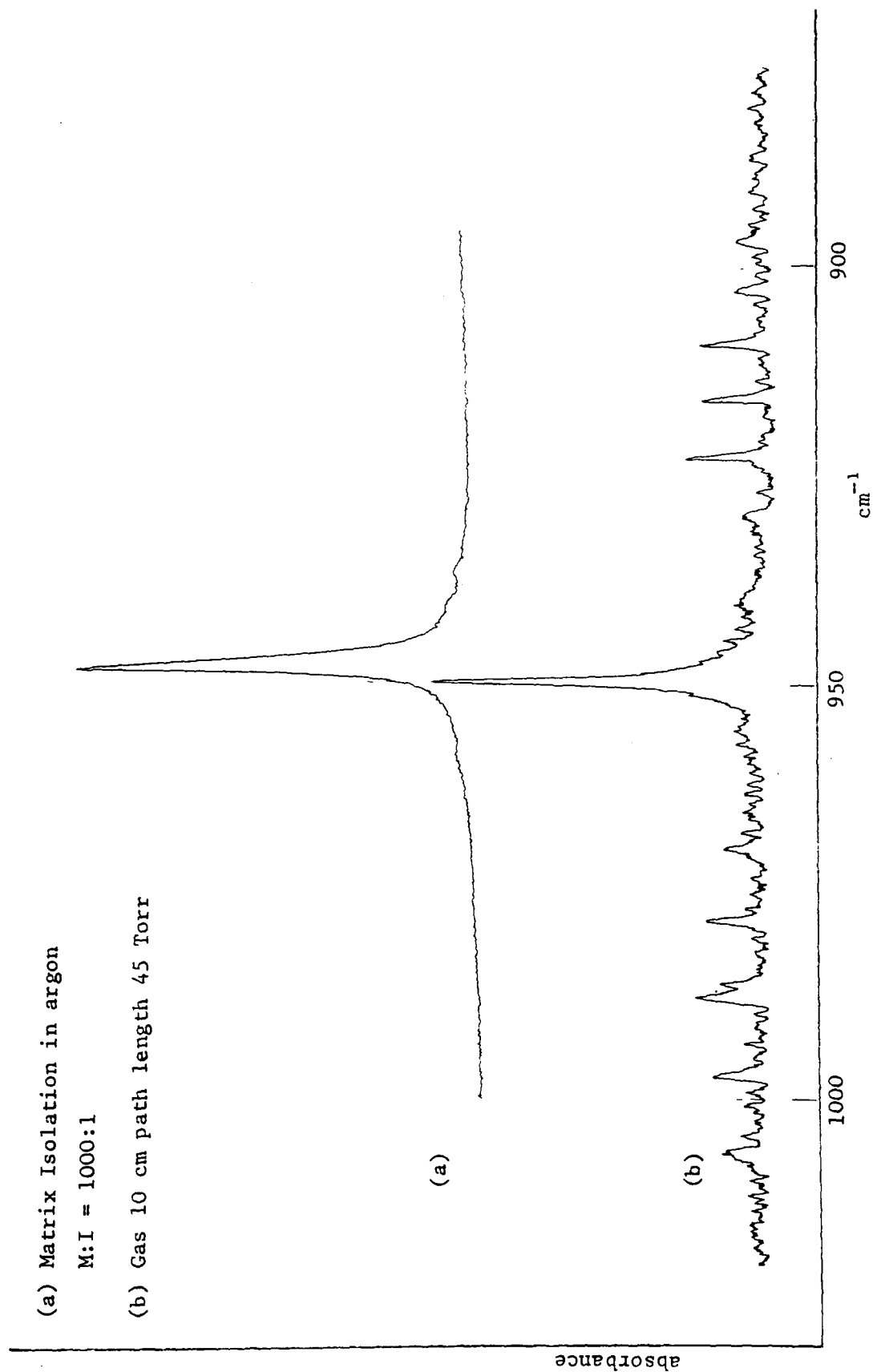
7. ROTATION IN MATRICES

As stated previously rotation of small molecules in matrices is well known, HCl rotates in argon matrices (32,76) and bands associated with specific rotational levels have been identified. In the gas phase many different rotational levels are populated but at the very low temperatures at which matrix isolation spectra are recorded only the lowest levels are significantly populated. The possibility of rotation was considered as an explanation for the weak feature several wavenumbers lower than the twist for the vinyl series. This postulation was discarded as a real possibility when these or any other spectral features appeared not to display any reversible temperature dependence. Molecular rotation for larger molecules such as substituted ethenes in solid argon may be feasible however if the substituent is sufficiently small i.e. H or D. These postulations led to the examination of ethene and ethene-d₁ in both the gas and matrix phases.

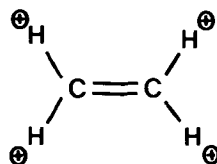
(1) ETHENE

The study of ethene, particularly for the out-of-plane vibrations, posed a different problem to those encountered for the substituted alkenes. Firstly the symmetry and hence modes of vibration differ, ethene belongs to the D_{2h} point group and has a centre of symmetry together with various planes and axes of symmetry whereas the monosubstituted ethenes belong to the C_s point group and have only a plane of symmetry. Secondly there is no distinct twist and wag but a single mode at 947.5 cm⁻¹ in the matrix and at 949.7 cm⁻¹ in the gas (Fig.19). There are three out-of-plane vibrations recognised for ethene (78) but only ν_7 is infrared active in the 1000-900 cm⁻¹

Fig.19 Infrared spectra of ethene 900 - 1000 cm^{-1}



region. This mode corresponds to that shown below where all four hydrogens move out of the plane together, and has the characteristic C-type structure of a perpendicular band.



This molecule has also been treated as an accidental prolate symmetric top and values obtained from the spectra for (\tilde{A}' - \tilde{B}') of 4.69 cm^{-1} reveals a good fit with those values calculated by Van Lerberghe et al and Harper et al (97-99) of 4.86 cm^{-1} .

A previous study on matrix isolated ethene (100) has shown the concentration dependence of bands due to monomer and dimer and has postulated a possible structure for the aggregated form. The present work on ethene has revealed a remarkable temperature reversible effect for the mode at 947.5 cm^{-1} . On raising the temperature from 8 K to 40 K the band steadily decreases in intensity, broadens and shifts to lower frequency by approximately 1 cm^{-1} . On cooling the matrix back to its base temperature it became apparent the effect was completely reversible (Fig.20). This is unlike any other effect found by similar studies carried out on the other systems. This series of events appears to be due to some form of rotation within the lattice, raising the temperature causes the highly populated lower rotational levels to become less populated and hence bands resulting from transitions within these levels will decrease in intensity. Bands due to higher rotational levels at either side of the band centre will become more highly populated and hence cause an apparent broadening if the spacings are

such that resolution between them is unobtainable. The broad feature at 40K is likely to consist of several bands arising from different rotational levels all separated by an interval of less than 1 cm^{-1} . Reduced separations when compared to the corresponding free molecular transitions in the gas phase implies a barrier to rotation imposed by the physical environment in the lattice. This can be compared with a similar effect in the rotation of HCl in an argon matrix. The apparent shift to lower frequency also implies a redistribution of the population of rotational energy levels. The rotational levels both sides of the band centre will become equally populated as the temperature is raised corresponding to Q branches where $\Delta K = +1$ and $\Delta K = -1$, however, for this class of molecule the vibration-rotation theory predicts a convergence for the Q branches towards shorter wavelengths hence the spacing between levels is larger at lower frequency and an overall apparent frequency shift to lower wavenumber may be predicted as these higher levels become appreciably populated.

(11) ETHENE- d_1

This molecule was studied primarily as an intermediate between the substituted vinyl series and ethene. The substitution of a deuterium atom for a hydrogen atom served two purposes. Firstly it altered the symmetry back to that of the vinyl series thereby behaving similarly in terms of vibrational and rotational modes but at the same time kept the molecule small enough to allow the possibility of some degree of hindered rotation.

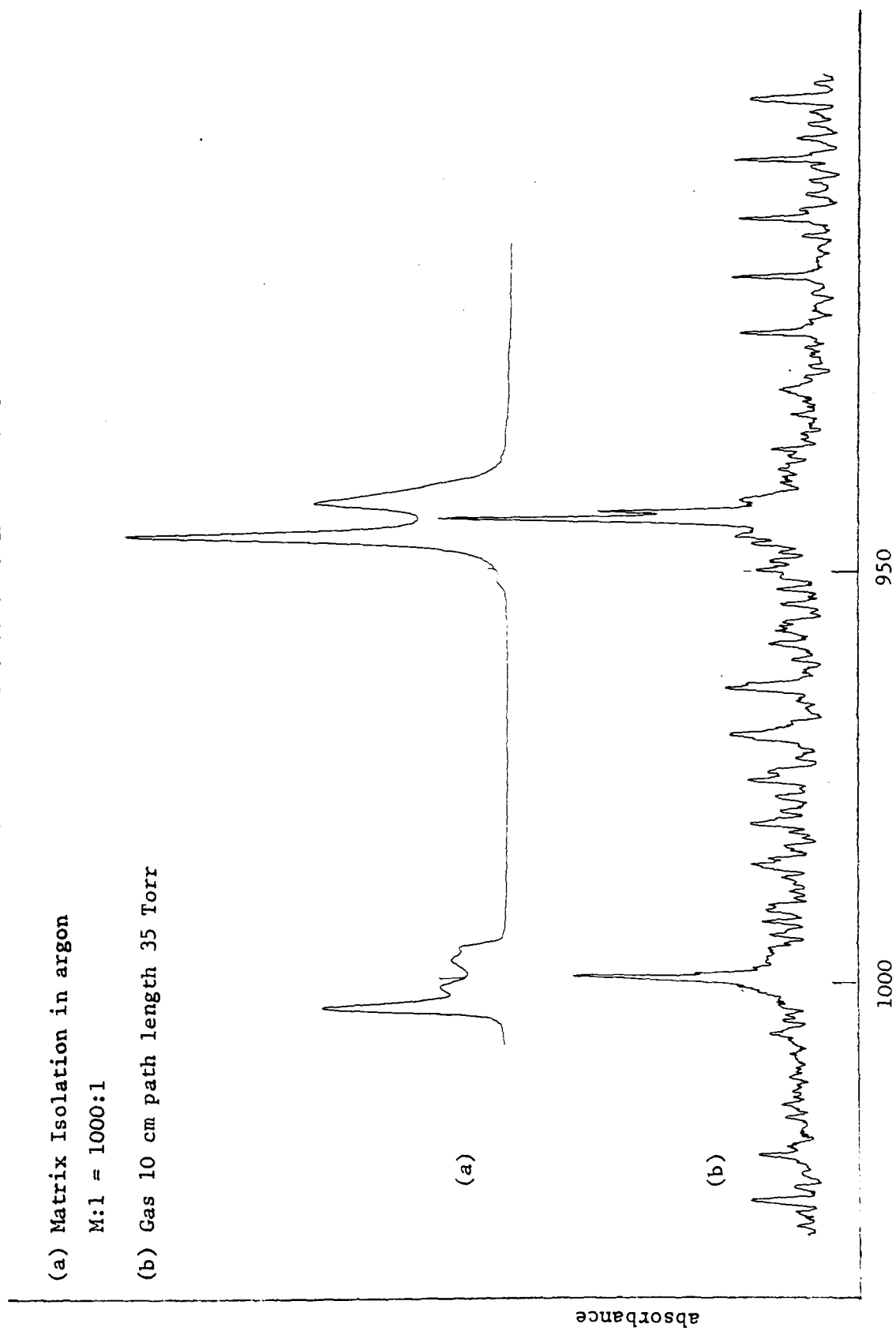
This molecule has three out-of-plane modes assigned (101) at 1000, 943.5 and 807.5 cm^{-1} with characteristic C-type structure. The band at 1000 cm^{-1} corresponding to the twist and at 943.5 cm^{-1}

Fig.21 Infrared spectra of ethene-d₁, 900 - 1000 cm⁻¹

(a) Matrix Isolation in argon

M:1 = 1000:1

(b) Gas 10 cm path length 35 Torr

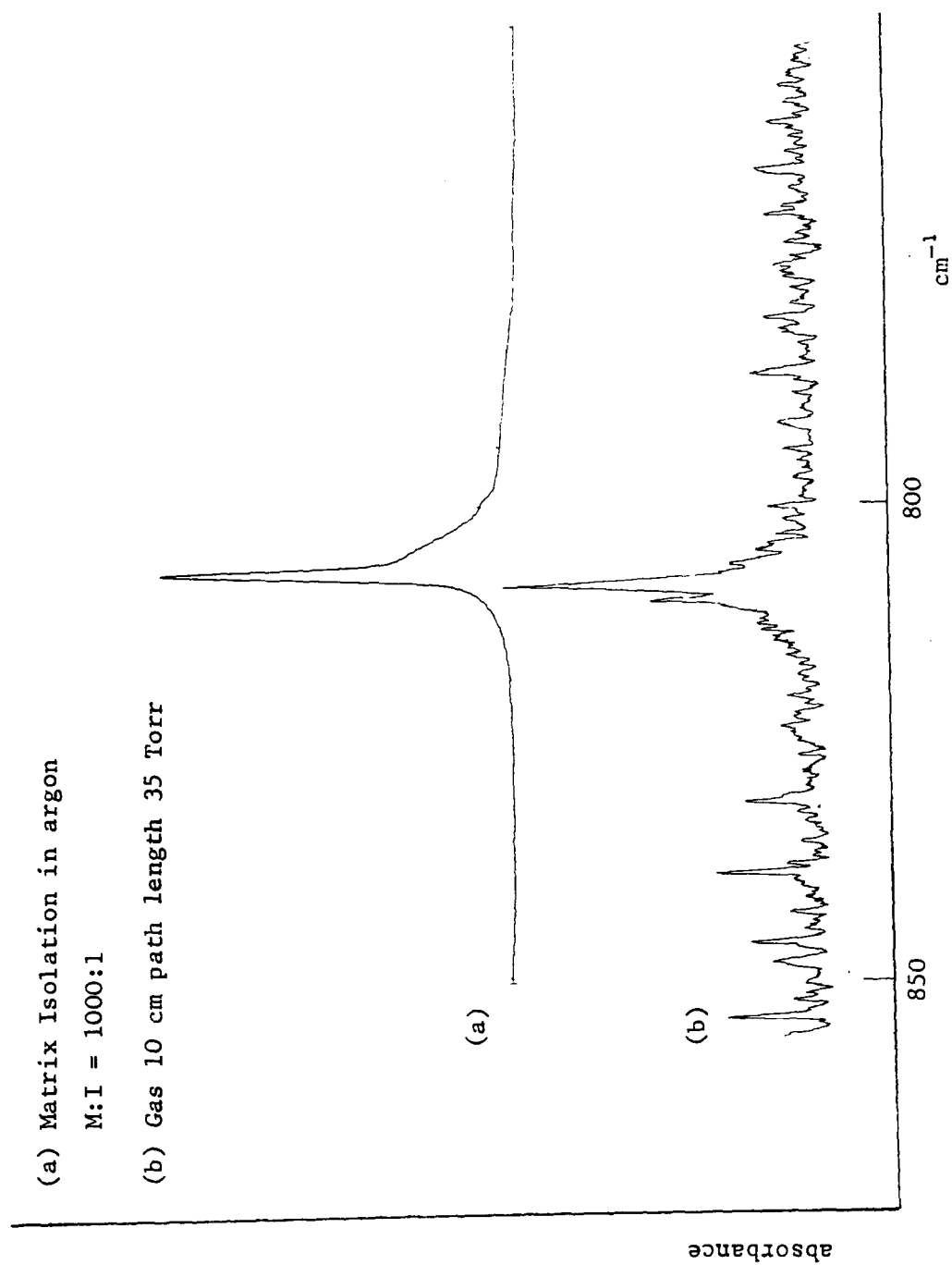


corresponding to the wag (Fig.21). As before this molecule also approximates to a prolate symmetric top and using this model so that the rotational spacings in the gas phase are $2(\tilde{A}' - \tilde{B}')$ a value for $(\tilde{A}' - \tilde{B}')$ of 3.79 cm^{-1} obtained from the spectra is in quite good agreement with those values given by other workers (101-103) of 4.00 cm^{-1} .

The matrix spectra showed two main bands at 1003.5 cm^{-1} and 946 cm^{-1} again corresponding to the twist and wag respectively. The pattern of frequency shift noted for the other members of this series, that is the gas bands being "inside" the matrix bands, is difficult to establish here in that although the main band corresponding to the twist is shifted to higher frequency in the matrix the wag consists of a doublet in both phases with the matrix bands straddling the frequency of the gas bands, the lower frequency component in the matrix phase is at 942 cm^{-1} (Fig.21).

The twist also displayed fine structure under high resolution with three low intensity shoulders at 1001 , 998 and 996.5 cm^{-1} . The relative intensities of these sub-bands remained unchanged when samples were either deposited by SSO or PMI indicating they were probably not bands arising from molecular association but site effects. Careful temperature cycling was carried out on all out-of-plane modes. No changes were detected for the two highest modes. Careful frequency measurements, however, of the third out-of-plane vibration at 807.5 cm^{-1} (Fig.22), which has a similar mode to that studied for ethene, indicates a weak but significant temperature reversible effect. Close examination indicates some band asymmetry at base temperature which disappears as the sample is warmed reappearing as it is cooled.

Fig.22 Infrared spectra of ethene-d₁ 750 - 880 cm⁻¹

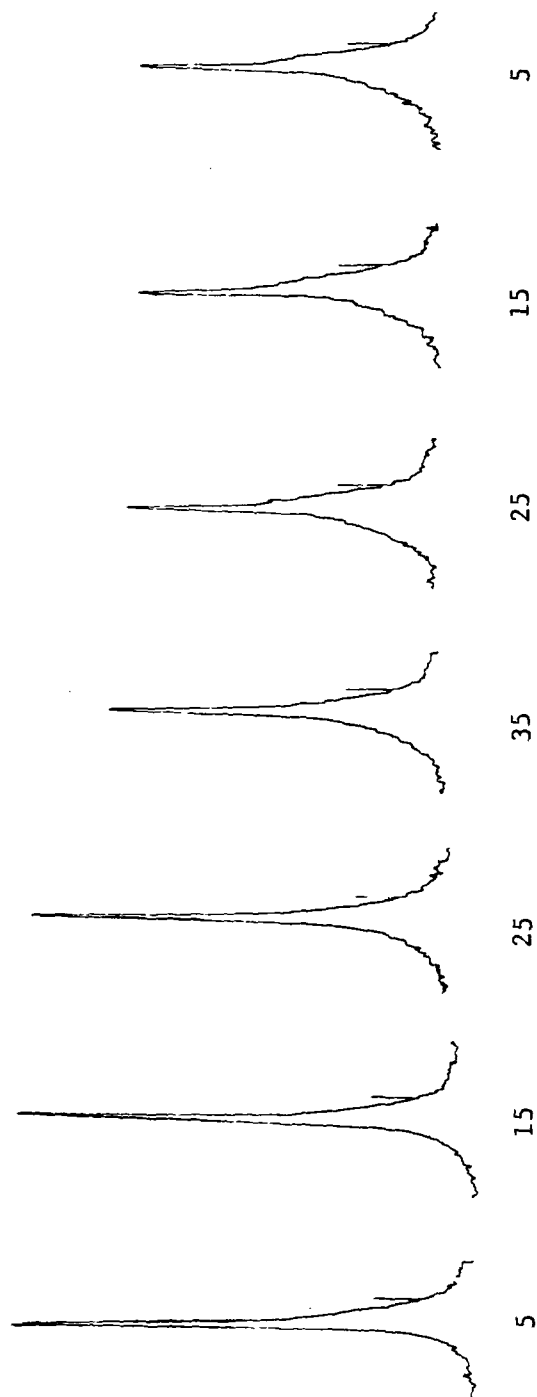


Secondly a small frequency shift of about 1 cm^{-1} is also be detected. Although the temperature reversibility of this mode appears to be conclusive the small frequency shift is difficult to establish for the following reasons.

Firstly, measurement of frequency shifts of this order of magnitude for this particular instrument (Perkin-Elmer 580B) are somewhat doubtful as the spectrometer is performing at the limits of its resolution capabilities. Secondly, unlike ethene the effect does not appear to be completely reversible in that the sharp bands associated with the sample before warming give way to broad bands after warming (Fig.23). This may not preclude rotation however but indicate that the effects of such rotation may be difficult to detect or masked by other features.

Fig.23 $\text{CH}_2=\text{CHD}$ 807.5 cm^{-1} Band SSO 1000:1 Ar

at different temperatures K



8. CONCLUSIONS

The arguments put forward for both ethene and ethene-d₁ may then also be applied to the other members of the vinyl series. Firstly the effects of rotation may be masked by features due to molecular association (66,94) which necessarily occurs as the matrix is softened. Unlike HCl, frequencies of bands due to rotation and aggregation may overlap. Secondly a marked decrease is predicted for the separation of the Q branch lines as the size of the substituent increases. If the spacing between the rotational lines is barely resolvable for ethene then for the other members of the series where the substituent is far larger they will be even less so.

The important difference to remember, however, when comparing the hindered rotation of HCl in argon matrices with the postulated rotation for ethene and possibly some other members of the vinyl series in argon matrices is that features due to the rotational motion of HCl are apparent at temperatures where the host lattice is rigid (8 K) whereas features due to the rotational motion of ethene only become apparent when the matrix is softened by heating. This observation therefore complicates the issue in that it is difficult to establish whether raising the temperature of the matrix simply causes a redistribution of the population of the rotational energy levels or just softens the matrix sufficiently to allow otherwise restricted rotation. Conclusions drawn from observations and theoretical considerations would seem to indicate it is probably a combination of both these factors.

CHAPTER IV

POLYMERIC AGGREGATION OR MULTIPLE SITE EFFECTS AS THE CAUSE OF BAND SPLITTINGS

1. INTRODUCTION
2. VINYL SERIES
3. ALLYL SERIES
4. BUT-1-ENE SERIES
5. CONCLUSIONS

CHAPTER IV

POLYMERIC AGGREGATION OR MULTIPLE SITE EFFECTS AS THE CAUSE OF BAND SPLITTINGS

1. INTRODUCTION

It is well known that the matrix isolation technique coupled with infrared analysis is a powerful tool for obtaining information on molecular symmetry changes, rotational effects (gross or internal), isotope effects or molecular interaction. (26) However this information may be bedevilled by band multiplicities arising from self-aggregation to polymers, conformational equilibria or from trapping of samples in differing sites. There appears to be an urgent need for a better experimental and theoretical grasp of these phenomena.

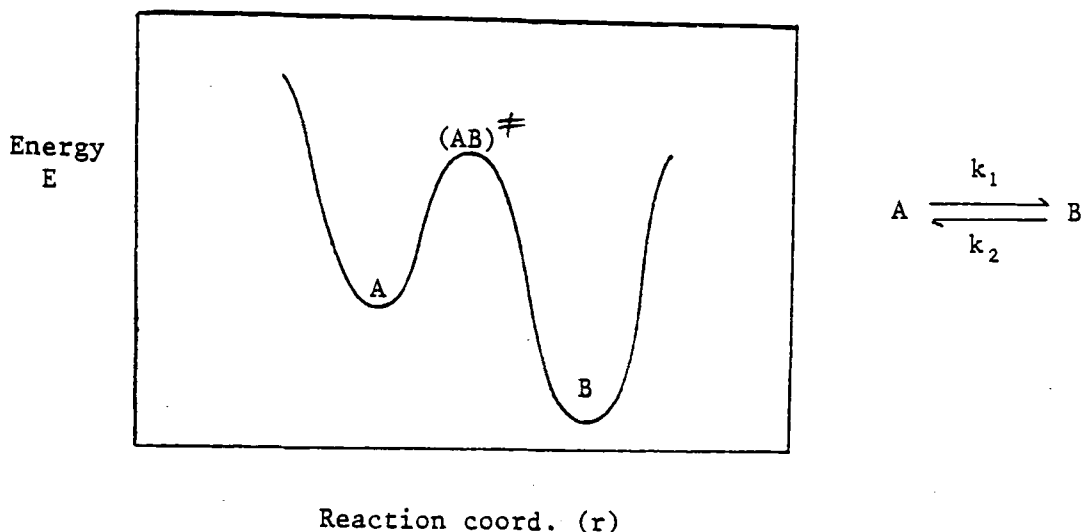
Polymer formation in matrices is well characterised in HCl(32) and methanol(35) but occurs less predictably in various compounds which lack well defined hydrogen bonded complexes at room temperature.

Recently Knozinger and Leutloff (104) interpreted the infrared spectrum below 150 cm^{-1} of acetonitrile isolated by SSO in noble gases in terms of monomers and dimers. The latter are favoured by dilutions of less than 1000:1 and by annealing, and are believed to comprise pairs of acetonitrile molecules that are antiparallel rather than linear.

Work described previously (25) showed that aggregation occurred under certain circumstances and was almost entirely dependent on the deposition conditions. Slow spray-on (SSO) produced less sample aggregation than did pulsing (PMI), an observation which led to contrary conclusions to that of Perutz and Turner(65).

Work on chloroprene (105) has demonstrated it has a similar behaviour pattern to acrylonitrile in the vinyl region under matrix isolation conditions but has not attributed this to polymer formation. This work will attempt to draw a distinction between the behaviour of various substituted olefins in matrices in terms of the different types of species present as a result of annealing and/or the application of different deposition conditions. The band splittings obtained as a result of the aforementioned criteria are interpreted by assignment to high and low energy forms either as a result of inter or intramolecular interactions. The distinction between various causes of matrix splittings is not necessarily subjected to easy experimental test. Annealing is expected to convert a system from a high energy form (A) to a low energy form (B) in which B may correspond to either a polymeric aggregate, or a monomeric form in a more energetically favoured site and/or in a more favoured conformation. A generalized diagram of change in energy (ΔE) with reaction coordinate (r) is shown (Fig 24).

Fig.24



$$\begin{aligned}
 A &\longrightarrow B & \text{Rate} &= k_1 C_A & k_1 &= A_1 e^{-E_1^\ddagger/RT} \\
 B &\longrightarrow A & \text{Rate} &= k_2 C_B & k_2 &= A_2 e^{-E_2^\ddagger/RT} \\
 E_1^\ddagger &= E(AB)^\ddagger - E_A \\
 E_2^\ddagger &= E(AB)^\ddagger - E_B \\
 \Delta E &= E_B - E_A
 \end{aligned}$$

AT EQUILIBRIUM

$$k_1 C_A = k_2 C_B$$

$$K = k_1/k_2 = C_B/C_A$$

$$\Delta G^\circ = -RT \ln K = \Delta H^\circ - T \Delta S^\circ$$

UNDER NON-EQUILIBRIUM CONDITIONS

E_2^\ddagger and E_1^\ddagger are large. Thus a molecule in state A (such as are isolated in a particular site of an inert matrix cage) cannot overcome the energy barrier to obtain a more favourable energy state B unless k_1 is large (A_1 is large and/or T is high). Normal criteria for experimental test of origin of matrix effects are listed in Table 3 (1-4).

TABLE 3

<u>Experimental test</u>	<u>Intermolecular effect</u>	<u>Intramolecular effect</u>
by comparison of infrared spectra of :-	B a polymeric aggregate.	B a monomeric form in low energy conformer and/or low energy site.
1. Matrices at different concentration, e.g. 500:1 and 5000:1.	Bands assigned to B diminish totally or partially according to strength of interaction at low concentrations.	Little change.
2. Matrices before and after annealing.	Bands assigned to A diminish totally and bands assigned to B enhanced.	Bands assigned to A diminish totally or partially and bands assigned to B become more prominent.
3. Different matrices e.g. Ar or Kr.	Little change.	Possible significant change.
4. Different deposition conditions e.g. SSO or PMI.	Contradictory information B favoured by SSO (ref.66) B favoured by PMI (ref.65)	Little change.
5. Temperature effect on formation of B between different concentrations e.g. 500:1 and 5000:1	Significant change bands assigned to B intensify more quickly at 500:1 than to 5000:1	Little change.

2. VINYL SERIES

Matrix studies of the mono-substituted ethenes ($\text{CH}_2=\text{CH-X}$ where $\text{X} = \text{CH}_3$, Cl, Br, or CN) were mainly restricted to the out-of-plane deformation or wagging vibrations, the assignments of which have been described in many compounds (106-108), since initial studies had revealed that these modes were the most sensitive to annealing and/or changes in deposition conditions. Further studies have involved assignment of vibrational modes between $4000\text{-}400\text{ cm}^{-1}$ for all the members of the series in the matrix phase. The assignments are made both before and after annealing in terms of the presence of both high and low energy forms.

The matrix isolation work carried out on acrylonitrile involved a detailed study of the factors governing the optimum conditions for the production of a matrix spectrum of this compound. These were, method of sample deposition, sample deposition rate, diluent/sample ratio, type of diluent used, contamination effects (atmospheric), window surface reactions and annealing. Many experiments were performed varying these parameters in order to establish what effects if any they had. Acrylonitrile was chosen because like the other members of the series it lacks an axis of internal rotation and therefore has only one conformer which may otherwise have led to complications as a result of the presence of conformer bands.

The methods of sample deposition used were pulsing and slow spray-on. The equipment was constructed to permit the sample to be deposited on the window by either method only by changing tap and needle valve positions hence spectra could be recorded by each method on the same

day using the same sample which allowed for a more definitive comparison of the techniques. Variation of sample deposition rate can only effectively be carried out using the slow spray-on technique whereby the rate is controlled by altering the needle valve setting to produce different spectra of comparable intensity in different times. Diluent/sample ratios ranging from 100:1 to 1000:1 were studied simply by altering the partial pressure of the sample relative to the diluent gas. Two types of diluent were used in this study namely argon and krypton. Atmospheric contamination effects were studied by doping samples with known amounts of air or nitrogen before deposition, whereby the possibility of any surface reactions taking place on the window was studied by first depositing a cushion of argon on the window before sample deposition took place. The effect of annealing was studied by slowly warming the matrix while rapidly scanning a selected region until some change was observed (typically 30-35K) The matrix was then recooled 8K and the spectrum rerecorded.

The results indicated that any band splittings observed in the spectrum recorded were not due to any surface reactions on the window, the type of matrix used or to atmospheric contamination, but to sample aggregation since varying these parameters did not produce noticeable changes. These changes were particularly apparent in the out-of-plane alkene CH_2 deformation or wagging vibrations although other changes were noted and are re-recorded.

Figs. 25 and 26 compare the matrix isolation spectra of acrylonitrile in the region $950\text{-}1000\text{ cm}^{-1}$ by PMI and SSO. The spectrum of the vapour is included for comparison of band shapes. In fig 25 the PMI spectra of samples diluted by 1000:1 in both argon and krypton reveal weakening and disappearance of the strong sharp band

near 975 cm^{-1} and enhancement following annealing of a pattern of bands between 977 and 992 cm^{-1} . This pattern has a well-defined structure in argon with a prominent band at 983 cm^{-1} which becomes progressively more intense on annealing. This band is considerably more intense than other members of the pattern in the krypton matrix.

In fig 26 the SSO spectra of samples of acrylonitrile in argon are seen to have bands centered at 982 and 974 cm^{-1} which weaken and intensify respectively with dilution. The broad band centered at 982 cm^{-1} is very prominent at 100:1; weak at 250:1, only detectable at 500:1 with five-fold scale expansion and undetected at 1000:1. In all cases annealing leads to bands appearing at the same wavenumber values as in PMI but with different intensities. The structure of the annealing-developed band at 1000:1 dilution conforms to the envelope of the unresolved band at 100:1 dilution.

All bands between 960 and 1000 cm^{-1} in acrylonitrile are assigned to trans CH=CH twisting modes in different species. Comparison of PMI and SSO spectra for this mode enables assignments of bands to monomer and polymer species as shown in Table 4. Dilution in argon (similar results have been obtained in krypton) lead to SSO spectra in which the high wavenumber band is absent. Annealing of PMI spectra in argon and krypton removes the low wavenumber band. Hence complete separation (within reasonable detection limits) is achieved. It may be concluded that the low wavenumber feature corresponds to the monomer (favoured by maximum isolation) and the high wavenumber feature corresponds to the polymer (favoured by conditions leading to thermodynamic equilibrium). The various sub-bands of this feature implies more than one polymer species is present, of which that corresponding to the band at 983 cm^{-1} would appear to be the most

Fig.25 Acrylonitrile: pulsed matrix and vapour

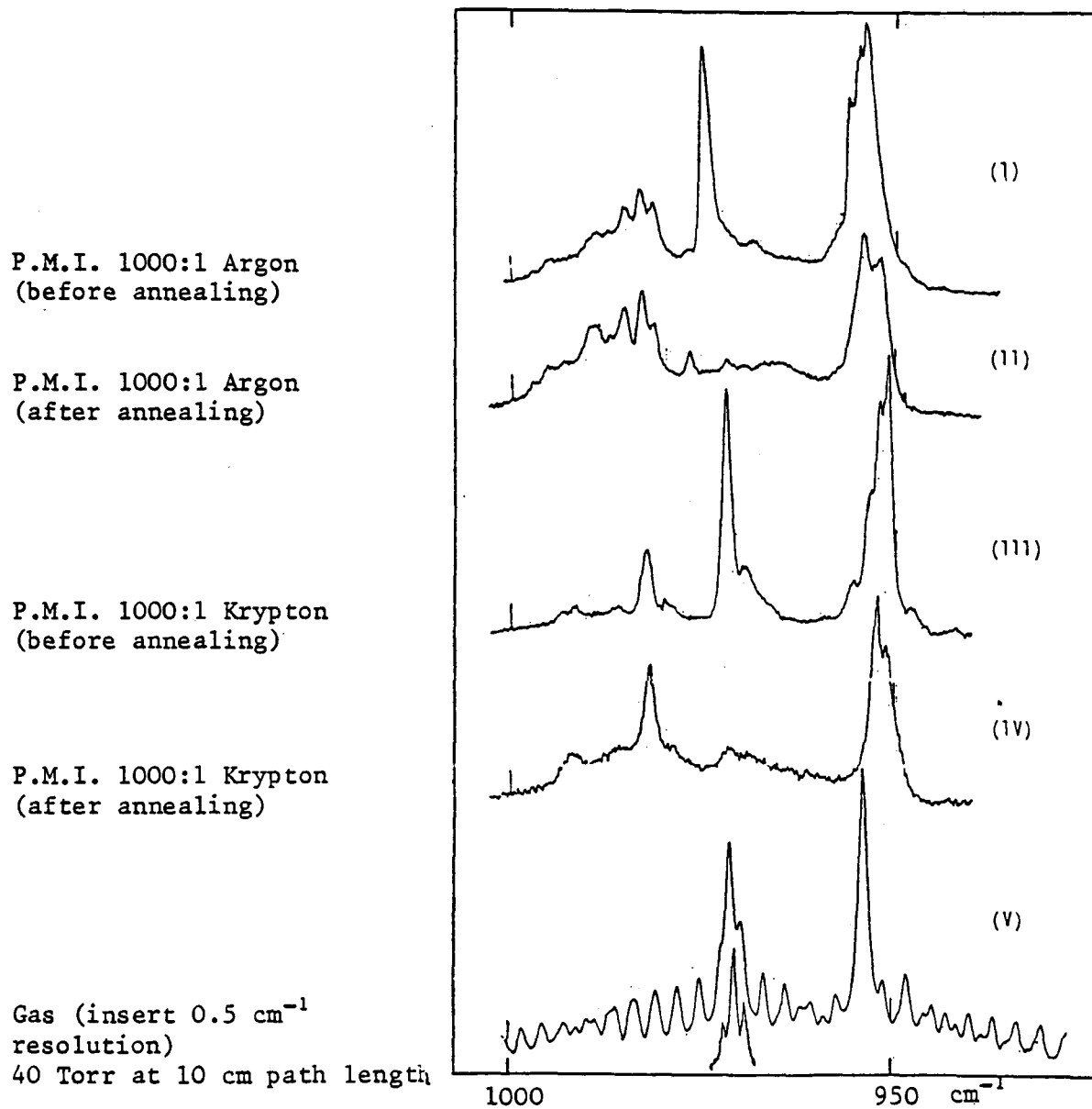


Fig.26 Acrylonitrile: sprayed matrix at several dilutions

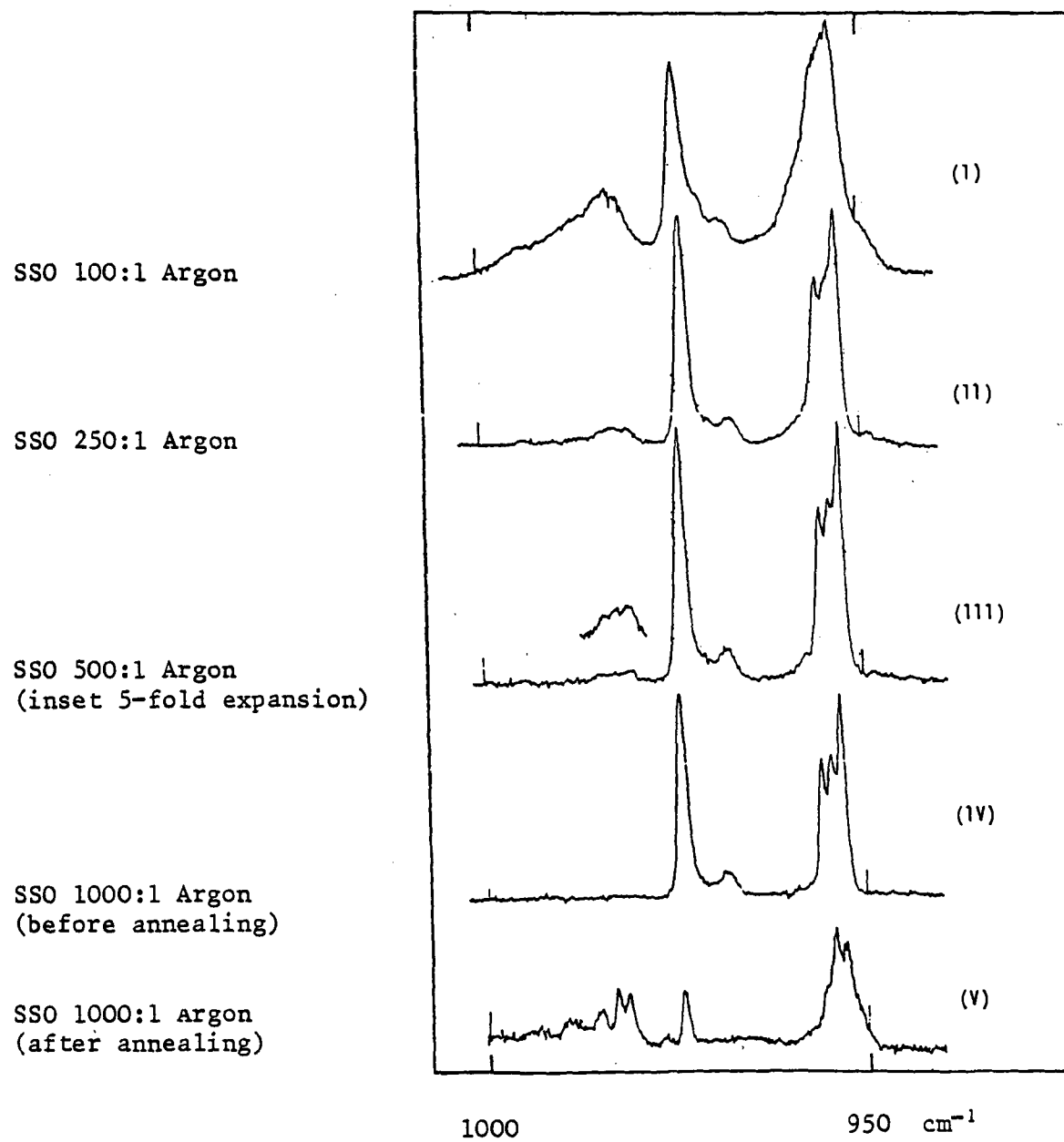


TABLE 4

INFRARED SPECTRA AND ASSIGNMENTS

OF ACRYLONITRILE IN ARGON MATRIX

<u>HIGH ENERGY FORM</u>			<u>LOW ENERGY FORM</u>	
<u>Wavenumber</u> <u>cm-1</u>	<u>Relative</u> <u>Intens</u>	<u>Assignments</u>	<u>Wavenumber</u> <u>cm-1</u>	<u>Relative</u> <u>Intens</u>
		C-H str	3077	m
		CH ₂ sym str	3044	m
			2999	vw
2278	vw		2282	vw
2236	m	C≡N str(H)		
		C≡N str(L)	2234	s
		2xCH=CH twist(L)	1959	vw
1941	vw	2xCH=CH twist(H)		
1910	vw			
1907	m	2xCH ₂ wag	1907	m
1905	vw		1902.5	w
1623	w			
1615	w	C=C str(H)		
		C=C str(L)	1613.5	w
1596	vw		1596	vw
1588	w			
1430	vw			
			1417	m sh
		CH ₂ bend(L)	1414	vs
1412	s	CH ₂ bend(H)		
			1364	w
			1300	vw sh
			1280	w
		CH ₂ rock(L)	1097.5	m
1092	m	CH ₂ rock(H)		
			995.5	w sh
			990	m
			985.5	s
		CH=CH twist(L)	983	s
			981.5	m sh
974.5	vs	CH=CH twist(H)		
968.5	m		972	w
956	vs		955.5	m
954.5	vs		954.5	vs
953	vs	CH ₂ wag	952.5	vs
868	s	C-C str	867.5	w
691.5	s		692	s
683	m			
679	m			

stable particularly in the krypton matrix. Corresponding species-dependent changes are apparent for the CH_2 wagging mode although in this case there is overlap between the polymer and the monomer pattern. The polymer has a doublet near 952 cm^{-1} in argon and krypton. The monomer has bands at similar wavenumber values to those of the polymer but with reversed relative intensities, together with a third band at higher wavenumber. The CH_2 wagging mode therefore has a triplet structure in the monomer form and a doublet structure in the polymer form in both argon and krypton, because of the overlap (all five bands occur within a 4 cm^{-1} interval) experimental information on the characteristics of this splitting is unclear.

The trans CH=CH wagging mode has a weak satellite 6 cm^{-1} to low wavenumbers which is annealing-dependent but not dilution-dependent. It is therefore not assigned to an aggregation effect. Other changes have been noted (Table 4) which are again dilution, pulsing/spraying and annealing dependent. Bands at 1092 and 1097.5 cm^{-1} are both assigned to the CH_2 rock in different species the band 1092 cm^{-1} being assigned to the monomeric form. At high dilution and slow spray-on only the band at lower wavenumber is present however lower dilution or pulsing enhances the higher wavenumber band to the total exclusion of the band at 1092 cm^{-1} . Two bands at 1412 and 1414 cm^{-1} are both assigned to the CH_2 bend in the monomer and polymer respectively. The band at 1412 appears as the main band with a shoulder at higher wavenumber if the sample is sufficiently dilute and is sprayed on, lower dilution, pulsing or annealing leads to the band at 1414 cm^{-1} becoming the prominent feature in this region. The C=C band also shows similar species-dependent changes that are dilution, spray-on and annealing dependent. The C=C stretch occurs at 1615 cm^{-1} in the

monomer and 1613.5 cm^{-1} in the polymer whereas the C=C torsion occurs at 683 cm^{-1} in the monomer and 687 cm^{-1} in the polymer. The C-C stretch shows only a minor change of 0.5 cm^{-1} going from monomer to polymer, that is, 868 cm^{-1} in the monomer to 867.5 cm^{-1} in the polymer, the overtone of the C-C \equiv N bend occurs at 691.5 cm^{-1} in the monomer and 692 cm^{-1} in the polymer. The C \equiv N stretch however shows a more marked shift in the two forms occurring at 2236 cm^{-1} in the monomer and 2234 cm^{-1} in the polymer (Table 4).

Similar studies on vinyl chloride and vinyl bromide, though not so exhaustive, revealed a similar behaviour pattern to that of acrylonitrile. The vinyl region again proved to be the most sensitive to variation of experimental conditions in that high dilution and/or SSO produced spectra of comparable quality to those produced by similar conditions for acrylonitrile. Fig. 27 compares the 1000:1 SSO spectra of vinyl chloride both before and after annealing. The spectra before annealing exhibits two strong bands at 949.5 and 893.5 cm^{-1} corresponding to the twist and wag respectively with a third weaker feature at 940.5 cm^{-1} . The spectra after annealing however, display in addition several weak and only partially resolved bands at both higher and lower frequency on the twist and at higher frequency on the wag the main components of which occur at 958 , 952.5 , 947 , 942.5 , 908.5 , 900.5 , and 896.5 cm^{-1} these bands appear to increase in intensity at the expense of the intensity of the two main bands. Other less dramatic changes are observable elsewhere in the spectrum which are again dilution, annealing and deposition method dependent. The vibrational spectrum of vinyl chloride has been exhaustively studied and the 12 fundamental modes of vibration assigned by many workers. Table 5, therefore presents the assignments for the matrix isolated

Fig.27 Infrared spectra of vinyl chloride 900 - 1000 cm^{-1}

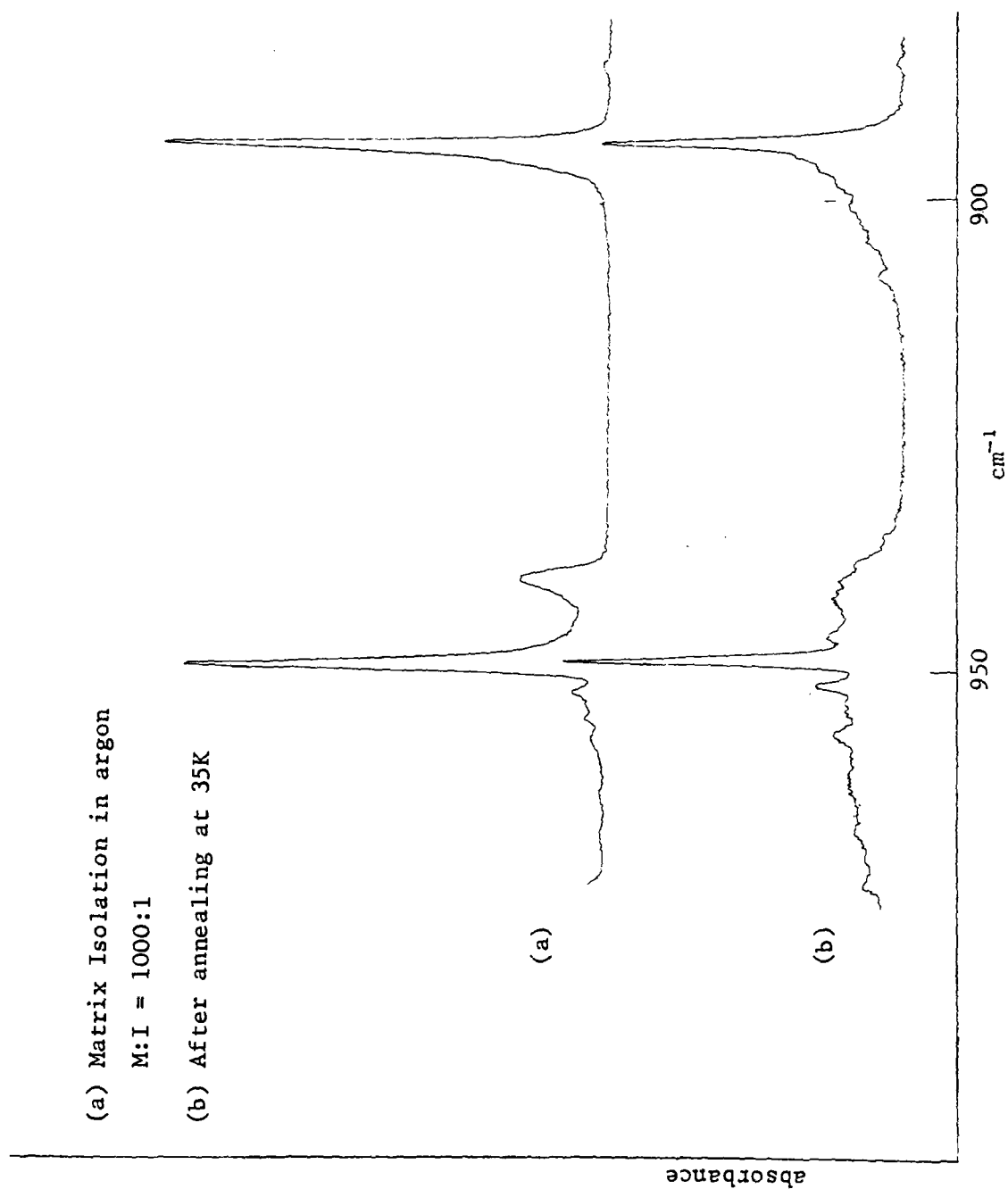


TABLE 5

INFRARED SPECTRA AND ASSIGNMENTS

OF VINYL CHLORIDE IN ARGON MATRIX

<u>HIGH ENERGY FORM</u>			<u>LOW ENERGY FORM</u>	
<u>Wavenumber</u> <u>cm-1</u>	<u>Relative</u> <u>Intens</u>	<u>Assignments</u>	<u>Wavenumber</u> <u>cm-1</u>	<u>Relative</u> <u>Intens</u>
3130	vw		3130	vw
3108	vw	C-H str	3108	vw
3092	vw		3092	vw
1791	vw	2xCH ₂ wag	1791	vw
1609	vs	C=C str	1609	vs
1512	m		1512	m
1460	vw			
1369	s	CH ₂ deform	1369	s
			1292	vw
1284	m		1284	m
1239	vw		1239	vw
1027.5	w		1028	w
1024.5	m	CH ₂ rock	1024.5	m
		CH=CH twist (L)	958	w
		CH=CH twist (L)	952.5	vw
949.5	vs	CH=CH twist (H)	949.5	vw
		CH=CH twist (L)	947	vw
940.5			942.5	w
		CH ₂ wag (L)	908.5	vw
		CH ₂ wag (L)	900.5	vw
		CH ₂ wag (L)	896.5	vw
893.5	s	CH ₂ wag (H)	893.5	s
714	s	C-Cl str	714	s
709	m		709	m
621	w	C=C-Cl twist	621	w

state in terms of high and low energy forms based on these previous assignments (109-110). Bands are therefore assigned to aggregated forms of vinyl chloride although the forms of these various species is not known.

Similar studies were carried out on vinyl bromide Fig.28 compares the 1000:1 SSO spectra before and after annealing for the region 980-850 cm^{-1} . The twist occurs at 948 cm^{-1} and the wag at 898.5 cm^{-1} and as before a third weaker feature is apparent several wavenumbers lower than the twist at 940 cm^{-1} . Annealing the sample reveals a remarkably similar pattern of events to that which occurred for vinyl chloride in that again several weak bands appear as the intensity of the main components decreases at 955.5, 952.5, 945.5, 907.5 and 901.5 cm^{-1} . These bands as with acrylonitrile and vinyl chloride are assigned to aggregated forms of vinyl bromide. The main differences observable in the spectrum of vinyl bromide are also in the out-of-plane region but as before this compound also reveals certain less apparent changes in other regions of the spectrum. Table 6, as for vinyl chloride, therefore presents assignments for bands associated with both the high and low energy form based on previous work (110-111).

A matrix study of propene has previously been carried out by Barnes and Howells (112) and assignments have been made for the 21 fundamentals. A detailed study of the vinyl region between 1000-900 cm^{-1} has again revealed the sensitivity of the out-of-plane modes to sample aggregation. Fig 29 compares the SSO spectrum of propene before and after annealing, the strong band at 998 cm^{-1} before annealing is assigned to the $\text{CH}=\text{CH}$ twist in the monomer form and the band at 992 cm^{-1} assigned to the twist in the polymeric form which increases in intensity on annealing. Similarly the band at 911 cm^{-1} is assigned

Fig.28 Infrared spectra of vinyl bromide 900 - 1000 cm^{-1}

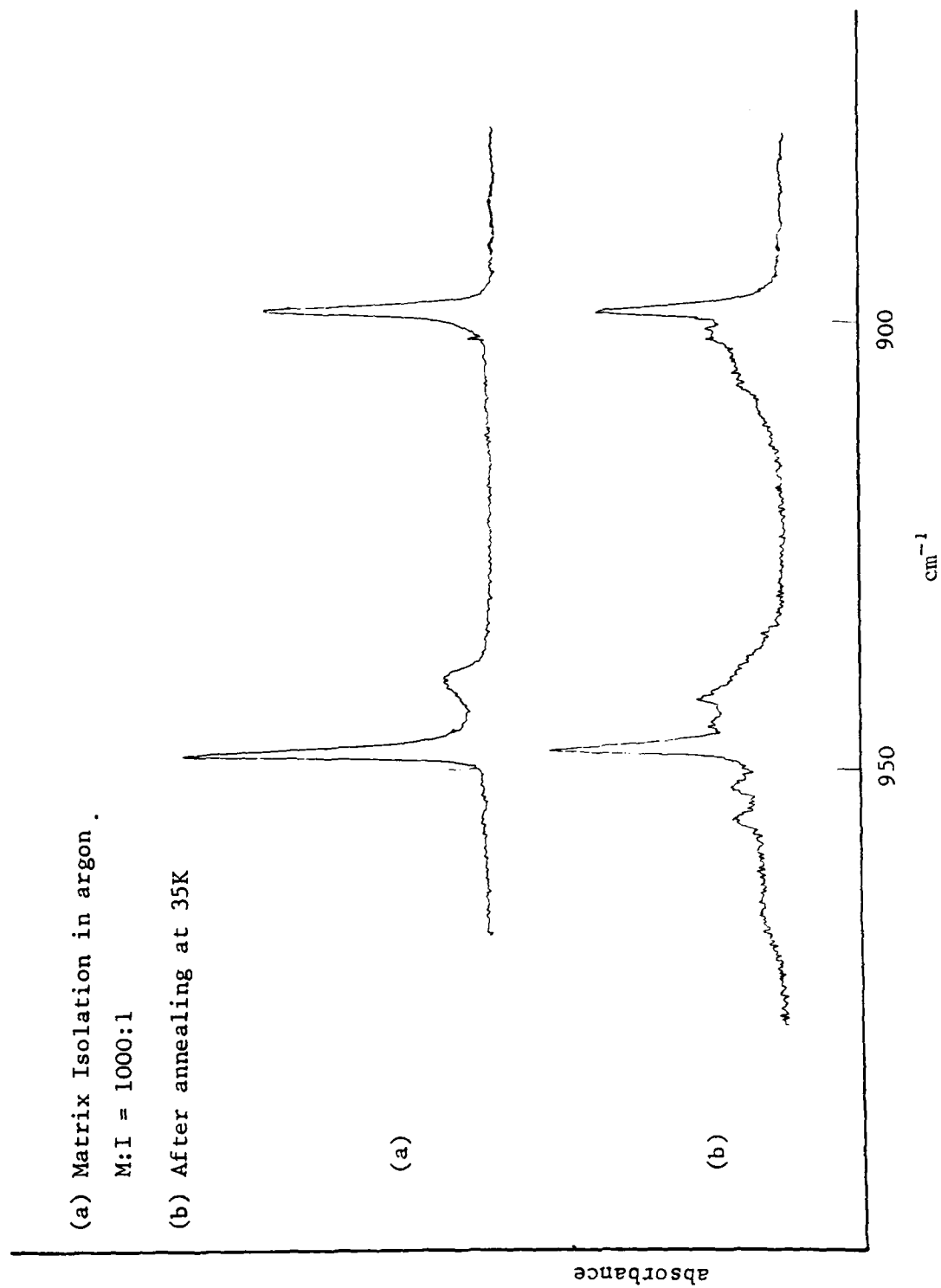


TABLE 6
INFRARED SPECTRA AND ASSIGNMENTS
OF VINYL BROMIDE IN ARGON MATRIX

<u>HIGH ENERGY FORM</u>			<u>LOW ENERGY FORM</u>	
<u>Wavenumber</u> <u>cm-1</u>	<u>Relative</u> <u>Intens</u>	<u>Assignments</u>	<u>Wavenumber</u> <u>cm-1</u>	<u>Relative</u> <u>Intens</u>
3121	vw			
3100	vw	C-H str		
3090	vw		3090	vw
3024	vw			
1800	vw	2xCH ₂ wag		
1599	vs	C=C str	1599	vs
1591	s sh		1591	s sh
1571	vw		1573	vw
1533	vw			
1482	vw			
1380	vw			
1370	m	CH ₂ deformation	1370	m
1348				
1338	vw			
1260	s	CH ₂ rock	1260	s
1257	w sh		1257	m sh
1130	vw		1130	vw
			1010	vw
1003.5	m	CH ₂ rock	1003.5	m
		CH=CH twist (L)	955.5	m
		CH=CH twist (L)	952.5	m
948	vs	CH=CH twist (H)	948	vs
		CH=CH twist (L)	945.5	m
940	m		942.5	m
		CH ₂ wag (L)	907.5	w
		CH ₂ wag (L)	901.5	w
898.5	s	CH ₂ wag (H)	898.5	s
806	vw		806	vw
608	m	C-Cl str	607.5	m
585	w	C=C-Cl twist	586	w
421	vw		421	vw
401	vw		401	vw
380	vw		378	vw
336	w	C=C-Cl rock	336	w

to the CH_2 wag in the monomeric form with the band at 909.5 cm^{-1} assigned to the CH_2 wag in the aggregated form. The third out-of-plane mode at 578 cm^{-1} also shows a remarkable frequency shift of 7 cm^{-1} on annealing appearing at 585 cm^{-1} . A complete assignment of propene both before and after annealing based on the work by Barnes and Howells is shown in Table 7.

These results seem to indicate quite clearly for this class of compounds the additional spectral features observable when samples are either deposited by PMI or are annealed result from some degree of molecular aggregation or association. In the present study the reasons for less polymer in SSO than in PMI are apparent from the spectra. Polymer aggregation is the low energy state and is thermodynamically favoured when the host matrix allows its guest molecules to equilibriate at 30-35K by annealing. PMI produces bursts of energy which are equivalent to the annealing of an SSO spectrum and further annealing provides complete conversion from the high energy state within detectable limits to the low energy polymeric state. Less than 2% of the monomer remains following the annealing of acrylonitrile. Monomer is the high energy state which may only be sustained in a metastable condition in rigid matrix cooled sufficiently quickly and in a sufficiently high dilution. Isolation of monomer with no detectable polymer can only be achieved by careful regard to both these variables. Too rapid spray-on or too high concentration leads to polymer. This work provides an example where attempts to speed up an experiment by PMI will lead to premature annealing which in turn converts the sample in part from a single monomer species to a complex aggregate. The process of annealing which is generally considered to simplify, in this case serves to complicate. Features due to aggregation to polymers may

Fig.29 Infrared spectra of propene 900 - 1000 cm^{-1}

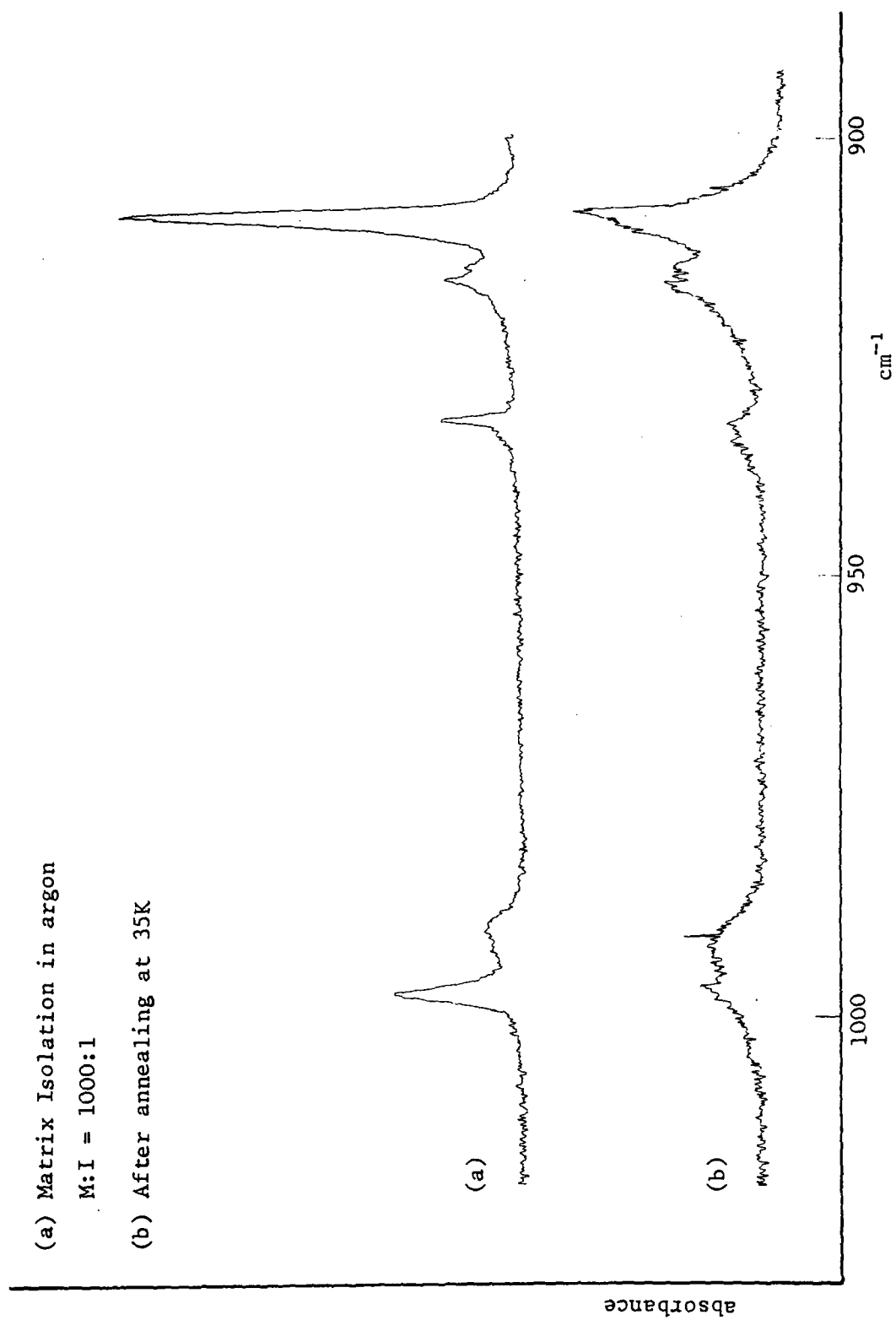


TABLE 7

INFRARED SPECTRA AND ASSIGNMENTS
OF PROPENE IN ARGON MATRIX

<u>HIGH ENERGY FORM</u>			<u>LOW ENERGY FORM</u>	
<u>Wavenumber</u> <u>cm-1</u>	<u>Relative</u> <u>Intens</u>	<u>Assignments</u>	<u>Wavenumber</u> <u>cm-1</u>	<u>Relative</u> <u>Intens</u>
3089	m	CH asym st.	3089	m
3038	w	CH st.	3038	w
2992	vw-sh			
2982	w	CH sym st.		
2947	m	CH asym st.	2947	w
2922	m	CH asym st.	2922	m
2888	w		2888	w
2857	w	CH sym st.	2857	w
2851	w		2851	w
1818.5	w	2xCH ₂ wag		
1648.5	m	C=C st. (M)		
		C=C st. (P)	1646.5	m
1452	s	CH ₂ asym def.	1452	s
1438	m	CH ₂ asym def.	1438	m
1412	vw	CH bend	1412	vw
1372	m	CH ₂ sym def.	1372	m
1353	w		1353	w
1261	w		1261	w
1127	w		1127	w
1089	m		1090	m
1043.5	w	CH ₂ rock	1043	w
998	m	CH=CH twist(M)	998	m
992	w	CH=CH twist (P)	992	m
932.5	w	C-C st.	935	w
916.5	w		918	s
911	vs	CH ₂ wag (M)	911	s
		CH ₂ wag (P)	909.5	vs
		CH ₂ twist (P)	585	w
578	w	CH ₂ twist (M)		

be observed in certain compounds at low temperatures and be non-existent or non-detectable at normal temperatures. Out-of-plane vibrations of vinyl groups appear to be a sensitive probe for this phenomenon in this class of compounds.

3. ALLYL SERIES

The previous results from matrix studies of the vinyl series indicated that the dominant factor leading to band multiplicities was sample aggregation into different polymeric clusters. The distinction between bands as a result of aggregation from those as a result of site effects was simplified by the fact that these compounds lacked an axis of internal rotation and hence displayed no bands due to conformational equilibria. However, all members of this series have axes of internal rotation and hence any band splittings observed for these molecules must be considered not only in terms of site effects and sample aggregation, but also in terms of conformational behaviour.

The compounds studied contained the same substituents as those for the vinyl series and as before it was noted that the out-of-plane deformation region showed the greatest sensitivity to annealing studies and the varying of deposition conditions. Previous studies on allyl chloride and allyl bromide (113) in the gas phase have suggested that the *gauche* conformer is the predominant form. Further studies on allyl chloride using microwave techniques (85) revealed the presence of both the *cis* and *gauche* conformer with the *gauche* conformer being the predominant form whereas for allyl bromide no trace of the *cis* form could be detected (86). A matrix study on allyl chloride revealed bands due to the *cis* form and concluded the relative stabilities of the

gauche and *cis* form appear to be similar in the vapour and condensed phase (84).

The present study of allyl chloride concentrates again primarily on the out-of-plane region and spectra before and after annealing (Fig.30) reveal the following features. In the region $1000-890\text{ cm}^{-1}$ four fundamentals are assigned to the CH=CH twist C-C stretch CH₂ wag and the CH₂ rock at 996, 939, 926.5 and 903 cm^{-1} respectively for the *gauche* conformer. The band at 917.5 cm^{-1} is assigned to the C-C stretch for the *cis* form (84). Annealing the sample leads to a decrease in intensity of these fundamentals and a corresponding increase in intensity of the bands at 989.5, 986.5, 934 and 897.5 cm^{-1} . The bands at 989.5 and 986.5 cm^{-1} are assigned to the twist in the aggregated form with the bands at 937 and 897.5 cm^{-1} assigned to the CH₂ wag and rock in the aggregated form (84).

A matrix study of allyl bromide in the region $1000-900\text{ cm}^{-1}$ before and after annealing (Fig.31) reveals two strong bands at 990 and 926.5 cm^{-1} assigned to the twist and wag in the low energy *gauche* form respectively. Other weaker bands are found at 993.5, 983.5, 975.5, 928.5, and 924.5 cm^{-1} . Comparison of assignments for allyl bromide in the gas phase (95-96) and allyl chloride in the matrix phase (84) along with the present annealing study leads to the shoulders at 988.5 and 928.5 cm^{-1} being assigned to the twist and wag for the *cis* conformer. The third fundamental in this region is the C-C stretch which has been assigned to the band at 933 cm^{-1} for the *gauche* form and 930.5 for the *cis* form. The bands at 993.5, 933, 930.5 and 924.5 are therefore assigned to different forms of aggregated allyl bromide. Annealing the sample leads to a decrease in intensity of all bands associated with monomeric forms of allyl bromide both *cis* and

trans and the appearance of several broad and unresolvable components characteristic of spectra associated with aggregated samples (Fig.31).

A previously conducted matrix study of but-1-ene (112) showed the existence of both the *gauche* and *cis* conformer and concluded that the relative intensities of the CH₂ twisting modes at 631 and 554 cm⁻¹ for the *gauche* and *cis* form respectively, were in the ratio of approximately 3:1. These values were in agreement with the expected relative intensities calculated from the small energy difference between these two forms.

The present work again concentrates primarily on the out-of-plane region between 1000-900 cm⁻¹ and the spectra before annealing (Fig. 32) reveals bands at 999, 992.5, 978, 912, 910 and 907.5 cm⁻¹. Annealing the sample leads to a decrease in intensity of the band at 999 cm⁻¹ and the appearance of a band at 996.5 cm⁻¹ (Fig.32). The band at 999 cm⁻¹ is assigned to the CH=CH twisting mode in the *gauche* form (112) whereas the band at 996.5 cm⁻¹ is assigned to the CH=CH twisting mode in the *cis* form which may be stabilised at low temperatures. Annealing the sample also causes a decrease in intensity of the band at 910 cm⁻¹ and a corresponding increase in intensity in the band at 907.5 cm⁻¹. The bands at 910 and 907.5 cm⁻¹ are therefore assigned to the CH₂ wag for the *gauche* and *cis* form respectively. No other fundamentals appear in this region (112) and therefore the band at 913 cm⁻¹ and the other broad features at 992.5 cm⁻¹ and to high frequency of the wag are probably associated with aggregated but-1-ene since annealing also leads to an increase in intensity of these features. It is clear however that features due to aggregation are not as prominent as for the other members of the series and therefore do not mask bands due to conformers which are separated by only a few

wavenumbers. This observation clearly illustrates the less reactive nature of the methyl group when compared to the substituents on the other members of this series.

The study on allyl cyanide revealed the presence of 8 bands in the vinyl region between 900-1000 cm^{-1} at 909, 924.5, 927.5, 935, 939.5, 942.5, 987.5, and 993 cm^{-1} (Fig. 33). Three fundamentals occur in this region (114) with the twist occurring at 987.5, the CH_2 rock at 939.5 and the wag at 927.5 cm^{-1} . These frequencies compare with 993, 938 and 926 cm^{-1} for the same modes assigned by Harrah et al (114). On annealing the sample, these three strong fundamentals decrease in intensity and the band at 924.5 increases in intensity along with several broad unresolvable features to high frequency of both the twist and wag. Very little information on conformational behaviour is obtainable from this data since the annealed spectra contained very few distinct sharp features. The tendency for this molecule on annealing to give rise to broad bands probably associated with various types of polymeric clusters makes the elucidation of such information very difficult. For other members of this series however the presence of several bands in both the unannealed and annealed spectra has been explained partially in terms of both inter and intramolecular effects, whether the assignment of the several other bands observable in the spectrum of allyl cyanide before annealing can be made in terms of similar modes of vibration in another conformer or as site effect bands (114) is uncertain.

Fig.30 Infrared spectra of allyl chloride 900 - 1000 cm^{-1}

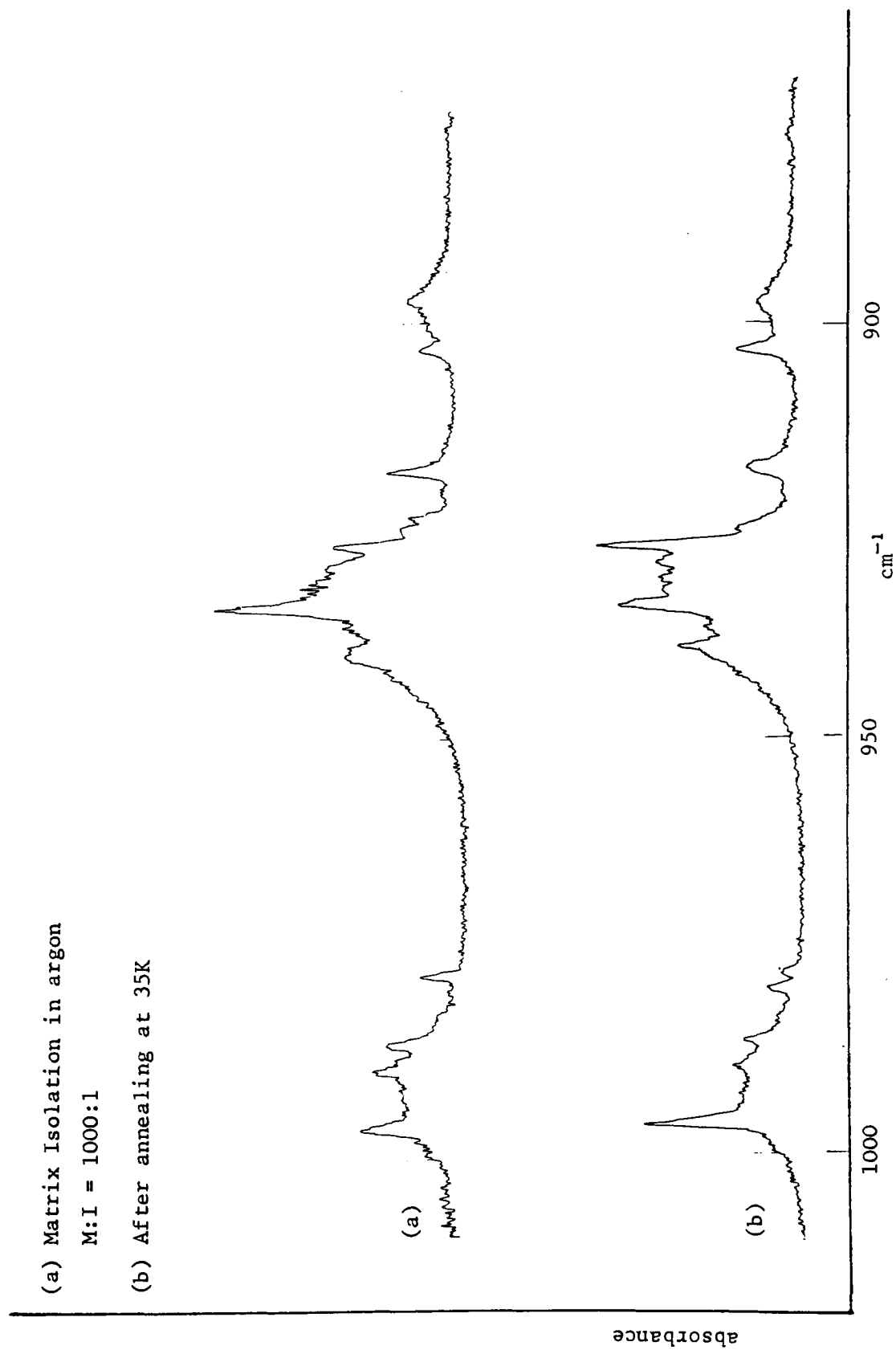


Fig.31 Infrared spectra of allyl bromide 900 - 1000 cm^{-1}

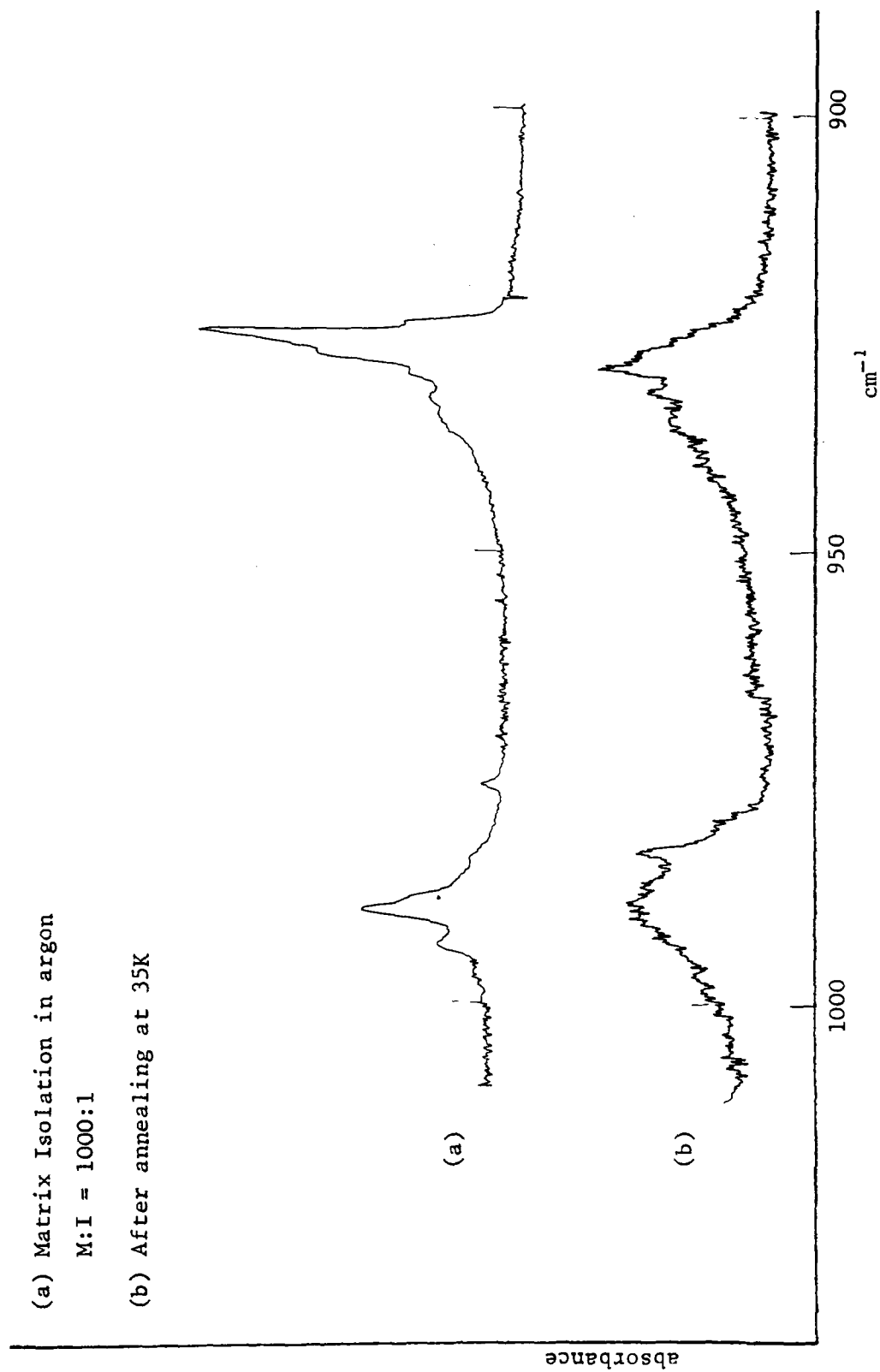


Fig.32 Infrared spectra of but-I-ene 900 - 1000 cm^{-1}

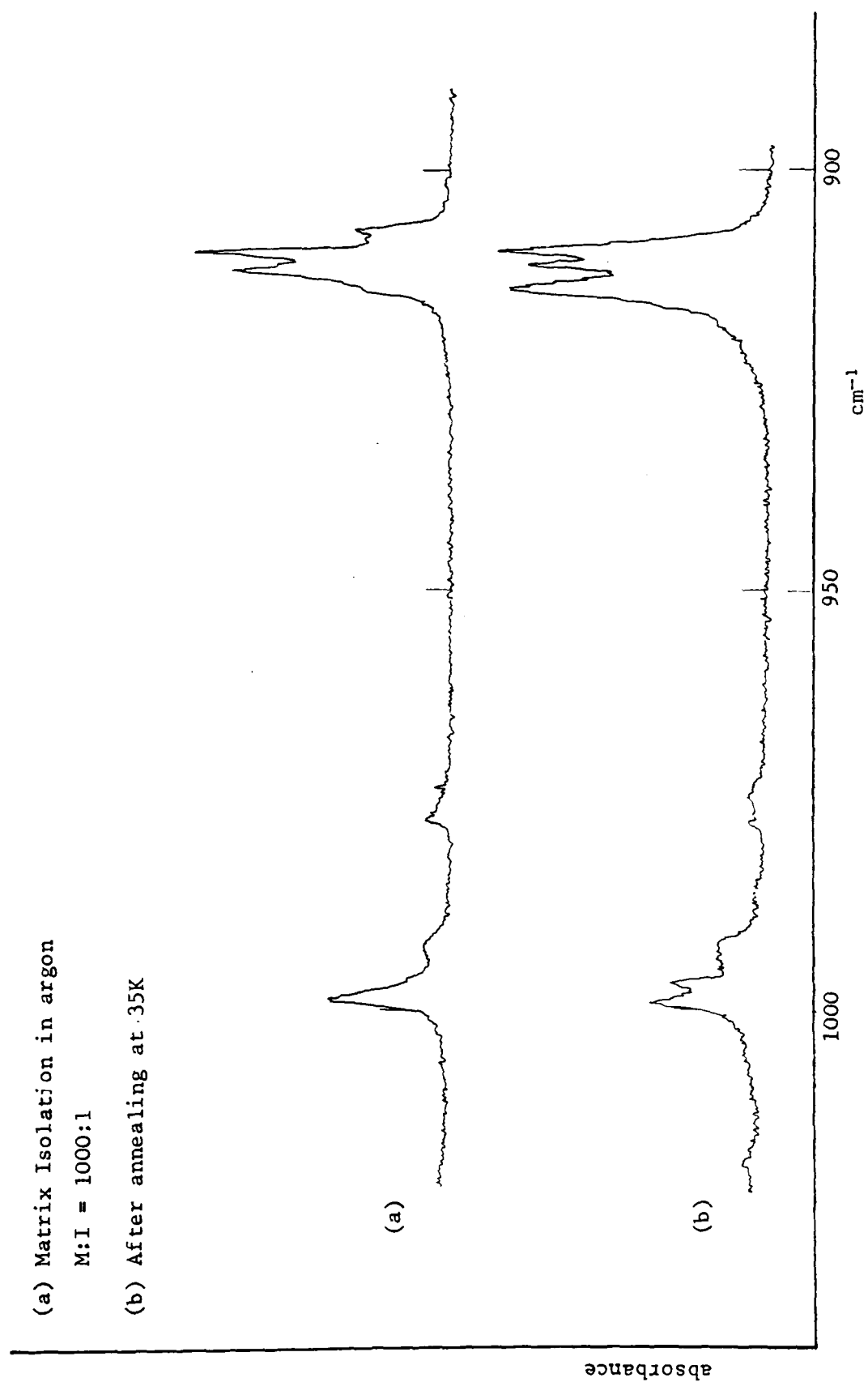
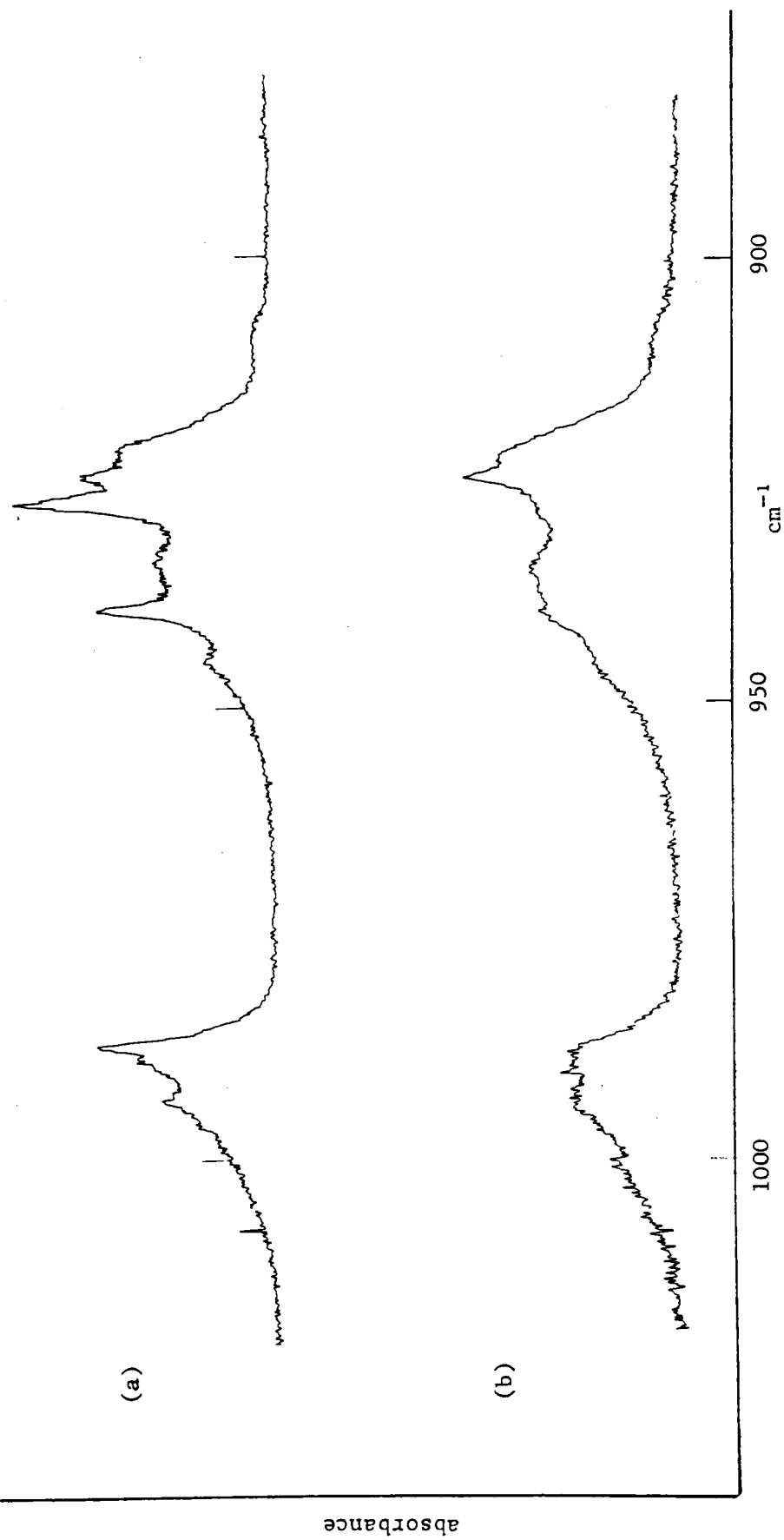


Fig.33 Infrared spectra of allyl cyanide 900 - 1000 cm^{-1}

(a) Matrix Isolation in argon

M:I = 1000:1

(b) After annealing at 35K



4. BUT-1-ENE SERIES

The molecules studied for this particular work also had the same substituents as those for both the vinyl and allyl series. Particular attention was again paid to the region between $1000-900\text{ cm}^{-1}$ but the matrix spectra obtained were not of particularly good quality and little or no structural information could be obtained. The spectra produced consisted of broad unresolved multiplet bands and annealing seemed to produce little or no visible difference to the spectra. The conclusions here must be that the relatively large size and low volatility of these molecules has made their isolation within the inert matrix extremely difficult to accomplish. The bands produced are almost certainly a tangled combination of conformer and aggregate bands. Their large size requires high dilution factors to ensure a relatively high degree of isolation while at the same time necessitating the deposition of large quantities of inert gas resulting in thick and highly scattering matrices. The final result offered little or no improvement over spectra run of these compounds in the liquid phase.

5. CONCLUSIONS

It is apparent that annealing a sample leads to conversion of that sample to the low energy form. However the understanding of the term "low energy form" for this class of compounds encompasses not only aggregation and site effects but also conformational equilibria. Although information may be obtained about conformational behaviour distinction between the various causes of band multiplicities can become very complex and assignment to the various forms therefore even more complex. Table 3 (1-4) indicated normal criteria for

distinguishing between different types of matrix effects, further studies on chloroprene (2-chlorobuta-1,3-diene) however indicated certain similar features to that of acrylonitrile which were not easily distinguished by means of the aforementioned methods. Table 3 Criteria 5 is therefore developed and discussed in detail in the following chapter.

CHAPTER V

MATRIX EFFECTS IN THE INFRARED SPECTRA OF CYANOETHENE (ACRYLONITRILE) AND 2-CHLOROBUTA-1,3-DIENE (CHLOROPRENE)

1. INTRODUCTION

2. MATRIX EFFECTS AND COMPARISON OF INTENSITIES AT DIFFERENT DILUTIONS

3. COMPARISON OF TIME DEPENDENCE OF INTENSITY CHANGES AT DIFFERENT DILUTIONS

4. HIGH AND LOW ENERGY FORMS

(I) ASSIGNMENTS

(II) STRUCTURE

CHAPTER V

MATRIX EFFECTS IN THE INFRARED SPECTRA OF CYANOETHENE (ACRYLONITRILE) AND 2-CHLOROBUTA-1,3-DIENE (CHLOROPRENE)

1. INTRODUCTION

Matrix isolation in conjunction with infrared spectroscopy is a powerful tool for studying both chemical and physical phenomena in molecular systems. The establishment of the effect of temperature on the rate of formation of a low energy form B (Table 3 Criteria 5) between different concentrations in the matrix implies a mechanism which may be monitored kinetically and further enable the distinction between intra and intermolecular interactions.

The potential of matrix isolation for studying kinetic phenomena although recognised early in the development of the technique (115) has had only limited application. Kinetic studies have however been carried out and first order rate constants for the interconversion of *s-cis* and *s-trans* methyl vinyl ketone in a CCl₄ matrix have been reported (116).

The infrared spectra of matrix isolated forms of acrylonitrile and chloroprene are presented. The twisting mode of the vinyl group

in the $970\text{--}990\text{ cm}^{-1}$ region reveals considerable splitting in each compound which is attributable to high and low energy forms. Measurements are reported on rate of change from high to low energy forms compared between 500:1 and 5000:1 dilutions in argon in both compounds at 35K. The results confirm the low energy form is a polymeric aggregate in the case of acrylonitrile but arises from an intramolecular effect in chloroprene. First order rate constants were estimated for acrylonitrile and chloroprene at low and high dilutions. Assignments to high and low energy forms are presented between 400 cm^{-1} and 3500 cm^{-1} in each case and the structure of these forms are discussed.

The chemical and physical properties of chloroprene and acrylonitrile are important and relate to their tendency to readily react to form well known polymers and copolymers. The study of infrared spectra of samples isolated in dilute, low temperature matrices (26) provides information on molecular vibrations and structure for systems which may not be amenable to examination at normal temperatures and phases because of chemical reactivity or physical perturbation of energy levels.

A rigid low temperature matrix can maintain a molecule in an unstable high energy state (A) which may relax to a thermodynamically more stable form on annealing the matrix by heating to a temperature at which the matrix softens and permits reorientation to the low energy state (B). The difference in energy (ΔE) may derive from an energy of interaction within polymeric aggregates, or from a more favourable matrix site or molecular conformation. If the barrier between states is associated with the matrix cage separating adjacent cavities this will

be very large at liquid helium temperatures. On heating the matrix the cage barrier will reduce in height to permit some degree of equilibrium to occur. In the case of barriers associated with internal rotation within the molecule Barnes and Whittle (117) have estimated the range of temperatures and barrier heights at which separate conformers can be isolated. Thus two categories of matrix effect can be distinguished in which the low energy state (B) may be associated either with an intermolecular matrix effect or with an intramolecular matrix effect. Matrix effects appear to be particularly prominent in the region associated with out-of-plane vibrations of the vinyl group. In acrylonitrile (66) matrix effects in this region were described in terms of the existence of monomeric and polymeric or aggregated states resulting from intermolecular changes. In chloroprene (105) similar changes were attributed to conformational or intramolecular changes. The similarity of effects in these compounds suggests rigorous experimental comparison is merited to distinguish categories of low energy forms. Additionally, it is possible to determine small differences in the fundamental modes of vibration between low and high energy states over the region $400\text{--}3500\text{ cm}^{-1}$.

2. MATRIX EFFECTS AND COMPARISON OF INTENSITIES

AT DIFFERENT DILUTIONS.

Intermolecular interactions are reduced by increasing matrix dilution at low temperatures and increased by raising the temperature until mobility of the matrix permits movement between matrix cavities. A study of acrylonitrile restricted to wagging and twisting vibrations of the vinyl group between $950\text{ and }1000\text{ cm}^{-1}$ revealed conditions (66)

under which separation occurred into monomer form (slow spray-on in argon at 1000:1 dilution) and aggregated polymer (annealing of matrix).

The spectrum of chloroprene (105) has closely similar features to that of acrylonitrile in the region $850\text{--}1000\text{ cm}^{-1}$. Two CH_2 wagging modes are observed in the spectrum of chloroprene corresponding to the two terminal CH_2 groups together with the trans $\text{CH}=\text{CH}$ or twisting mode at highest wavenumber value. The twisting mode has the following remarkably similar features to that in acrylonitrile for which values are shown in parenthesis.

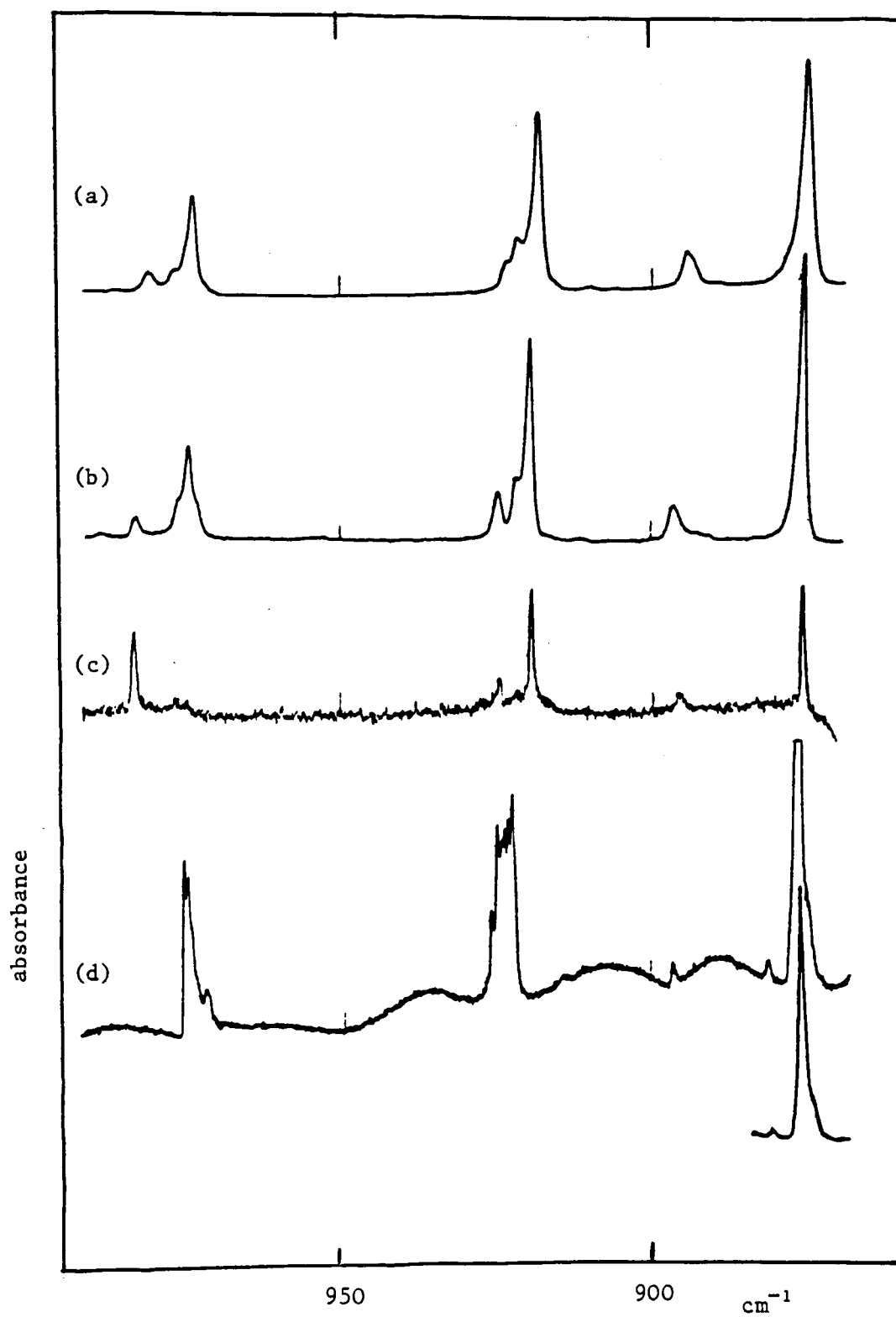
1. A prominent band occurs centered at 975 cm^{-1} in argon (974), 973 cm^{-1} in krypton (972.5) and 975 cm^{-1} in the gas state (971).
2. On annealing the matrix this prominent band disappears in all cases.
3. A weak feature at 983 cm^{-1} in argon (984) and 982 cm^{-1} in krypton (981) intensifies on annealing.

These similarities may suggest the high wavenumber feature in chloroprene is the result of aggregation as shown in the corresponding bands in acrylonitrile. To investigate this possibility careful dilution studies were carried out in argon for 100:1, 1000:1, 5000:1, and 10000:1 over spray on times of 4 hours and 20 hours in each case. These showed identical intensity ratios for the bands at 983 cm^{-1} and 975 cm^{-1} in all cases corresponding to the intensities shown in Fig. 34b.

The persistence of the band at 983 cm^{-1} at various dilutions in

Fig.34 Infrared spectra of chloroprene 850-1000 cm^{-1}

- (a) M:I 1000:1 in Kr
- (b) M:I 1000:1 in Ar (before annealing)
- (c) M:I 1000:1 in Ar (after annealing)
- (d) Gas 10 cm path length and 40 Torr (insert 15 Torr)



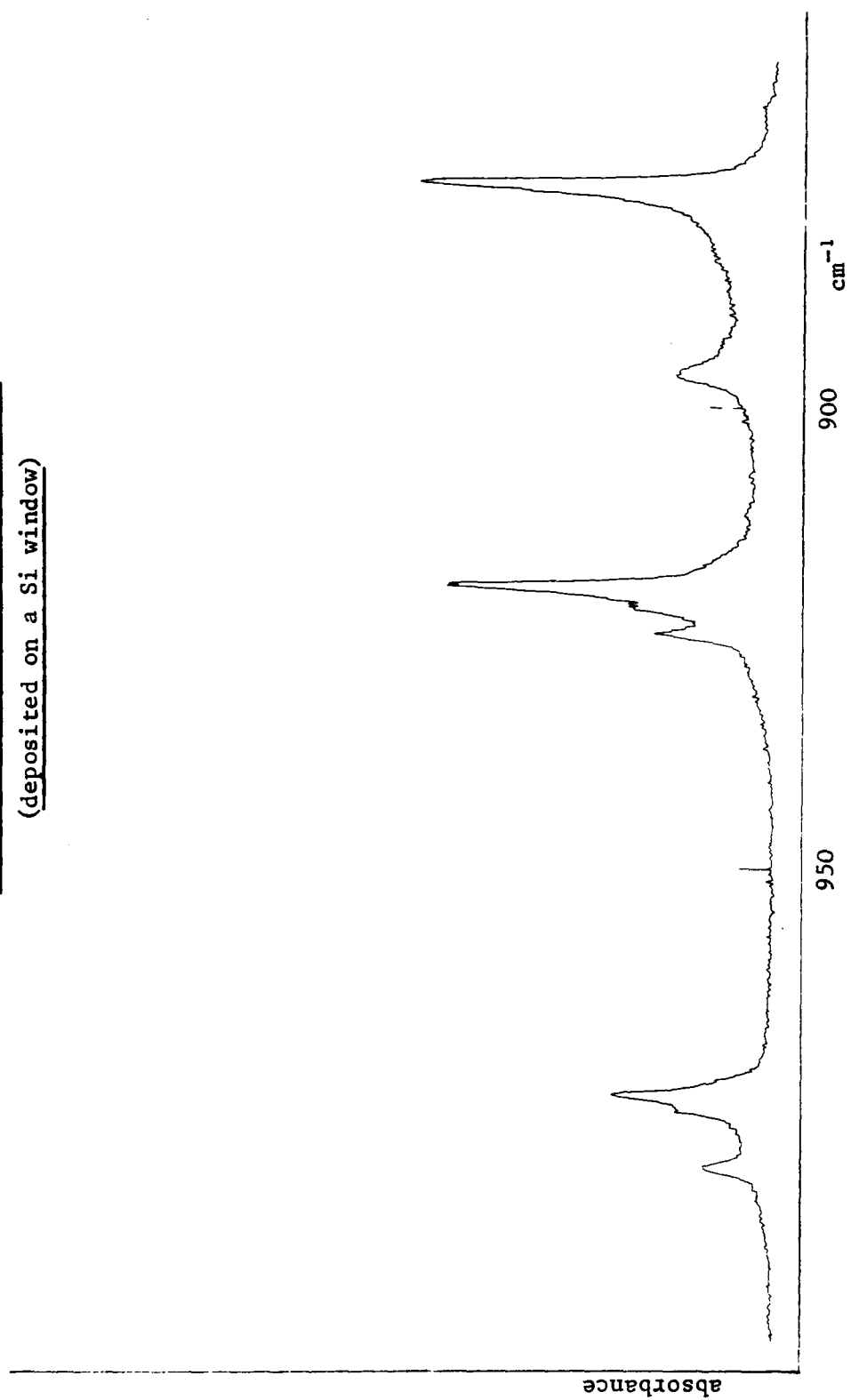
argon may not preclude assignment to aggregated species. A dilution dependence of intensity in a system in which aggregation takes place implies that the law of mass-action is a rate determining step and the amount of aggregation increases with the concentration of the monomer in the mixture with argon in the gas phase. Another possibility in a system in which aggregation occurs is that surface or matrix effects control the thermodynamic or kinetic features of aggregation leading to a persistence of aggregation bands at increasing dilution. To investigate surface effect possibilities comparisons were made of spectra isolated on CsI and Si windows. These experiments yielded identical spectra (Fig. 35). It was concluded the window material had no effect on the species formed in the matrix. To test the possibility of matrix or other non mass-action effects the following experiment was applied to both chloroprene and acrylonitrile.

3. COMPARISON OF TIME DEPENDENCE OF INTENSITY

CHANGES AT DIFFERENT DILUTIONS.

Two dilutions in argon were selected such that the matrix was neither too concentrated to achieve true matrix separation nor too dilute to achieve adequate signal to noise. Comparison of spectra at 500:1 and 5000:1 were chosen and spectra of acrylonitrile (Fig.36) and chloroprene (Fig.37) were recorded between 970 and 990 cm^{-1} . The prominent bands in the region 973-975 cm^{-1} assigned to the twist mode of the vinyl group in each compound are isolated by slow spray on at 8 K. At higher temperatures these bands in both compounds diminish in favour of a high wavenumber band 982-984 cm^{-1} which must correspond to a lower energy state formed by softening or relaxation of the matrix.

Fig.35 Infrared spectrum of chloroprene 900 - 1000 cm^{-1}
Matrix Isolation in argon M:I 1000:1
(deposited on a Si window)



If the rate of change from high to low energy form is greater at 500:1 than at 5000:1 an intermolecular change would be indicated since molecules can come within range of attractive interaction more readily in more concentrated matrices. If the two rates of change are the same at different concentrations this would imply an intramolecular change either within the matrix cavity or within the molecule of a kind which is independent of adjacent molecules in adjacent cavities. Comparisons were achieved by rapidly raising the temperature of the matrix to a value at which appreciable change took place. At 35 K the change from high to low energy form of acrylonitrile took place significantly faster at 500:1 than at 5000:1 (Fig.36). Rate constants were estimated by assuming the proportions of high and low energy forms were equal to the peak absorbances near 975 and 983 cm^{-1} respectively divided by their total. The data revealed a better fit for first order than second order rate expressions. The correlation coefficient for acrylonitrile being 0.988 at both dilutions, corresponding to first order rate constants $k=(3.4\pm0.5)\times10^{-3} \text{ s}^{-1}$ and $k=(2.3\pm0.5)\times10^{-3} \text{ s}^{-1}$ at 500:1 and 5000:1 dilutions respectively (Figs. 38 & 39). In the case of chloroprene the correlation coefficients were 0.955 in each case corresponding to a rate constant $k=(3.5\pm1.5)\times10^{-4} \text{ s}^{-1}$ at each dilution (Figs. 40 & 41). This observation is consistent with the dilution experiment and confirms that the low energy form of chloroprene arises from intramolecular rather than intermolecular interactions.

Fig.36 Acrylonitrile ($970-990\text{ cm}^{-1}$) at 35K and different times (t)

(a) M:I 500:1 in Ar

(b) M:I 5000:1 in Ar

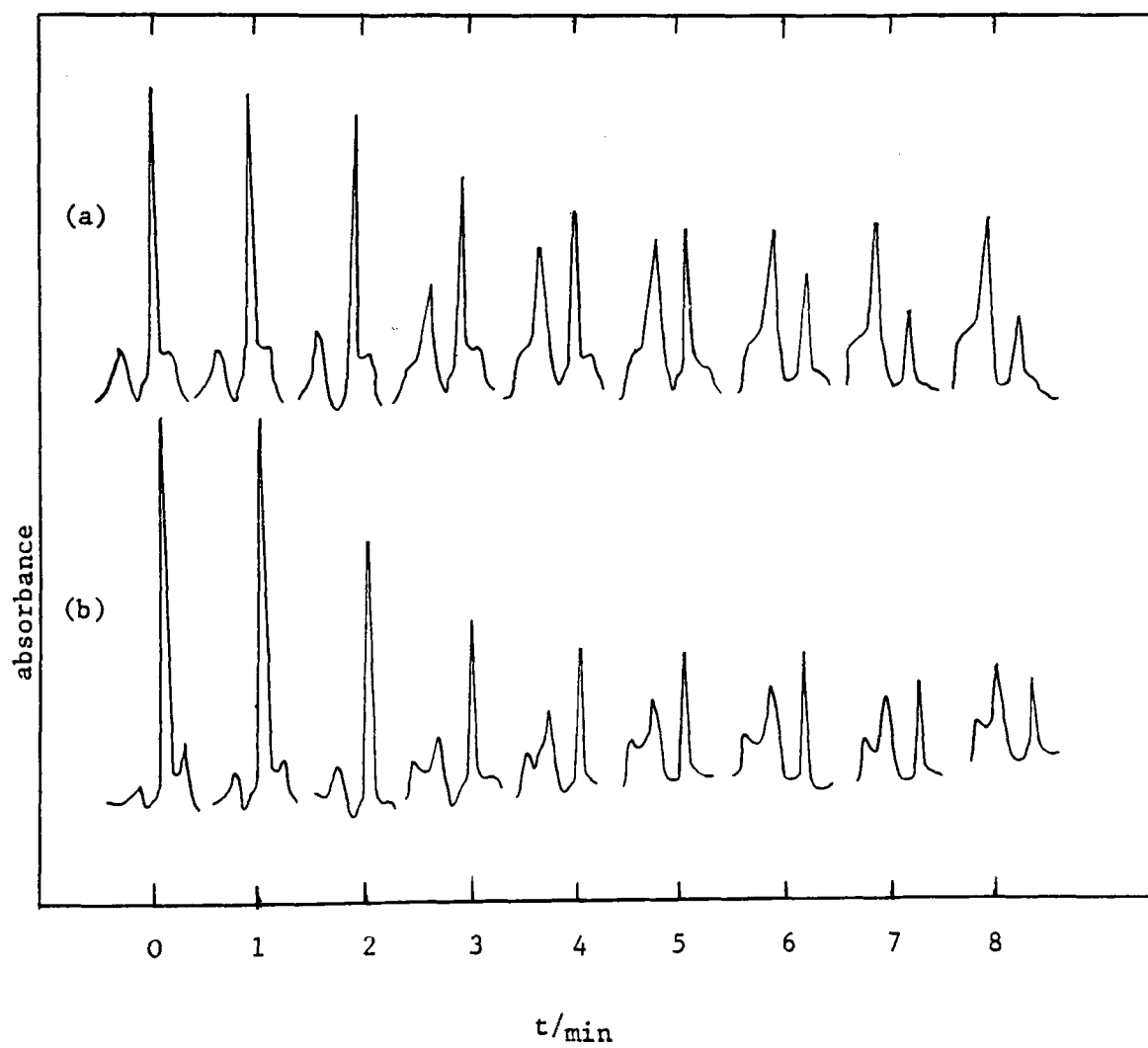


Fig.37 Chloroprene ($970-990\text{ cm}^{-1}$) at 35K and different times (t)

(a) M:I 500:1 in Ar

(b) M:I 5000:1 in Ar

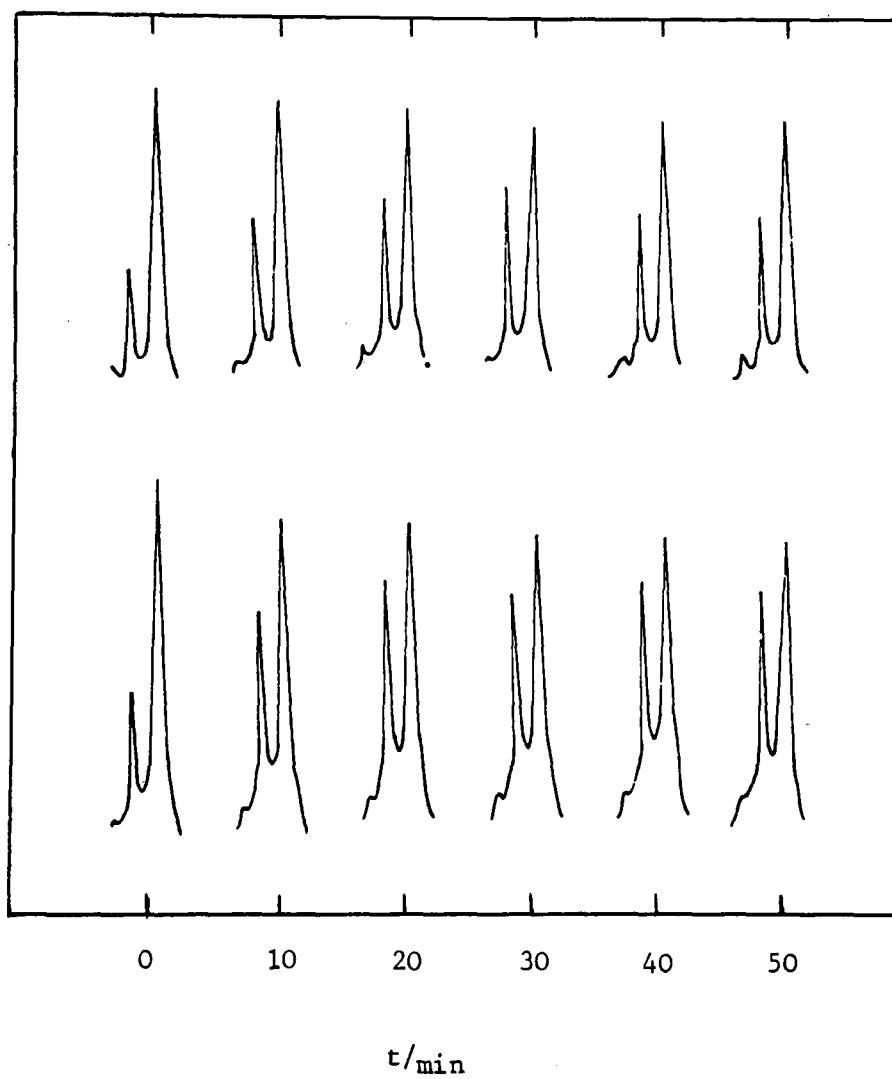


Fig.38 First order rate plot for the conversion of acrylonitrile in argon (M:I 500:1)
from a high energy form (A) to a low energy form (B)

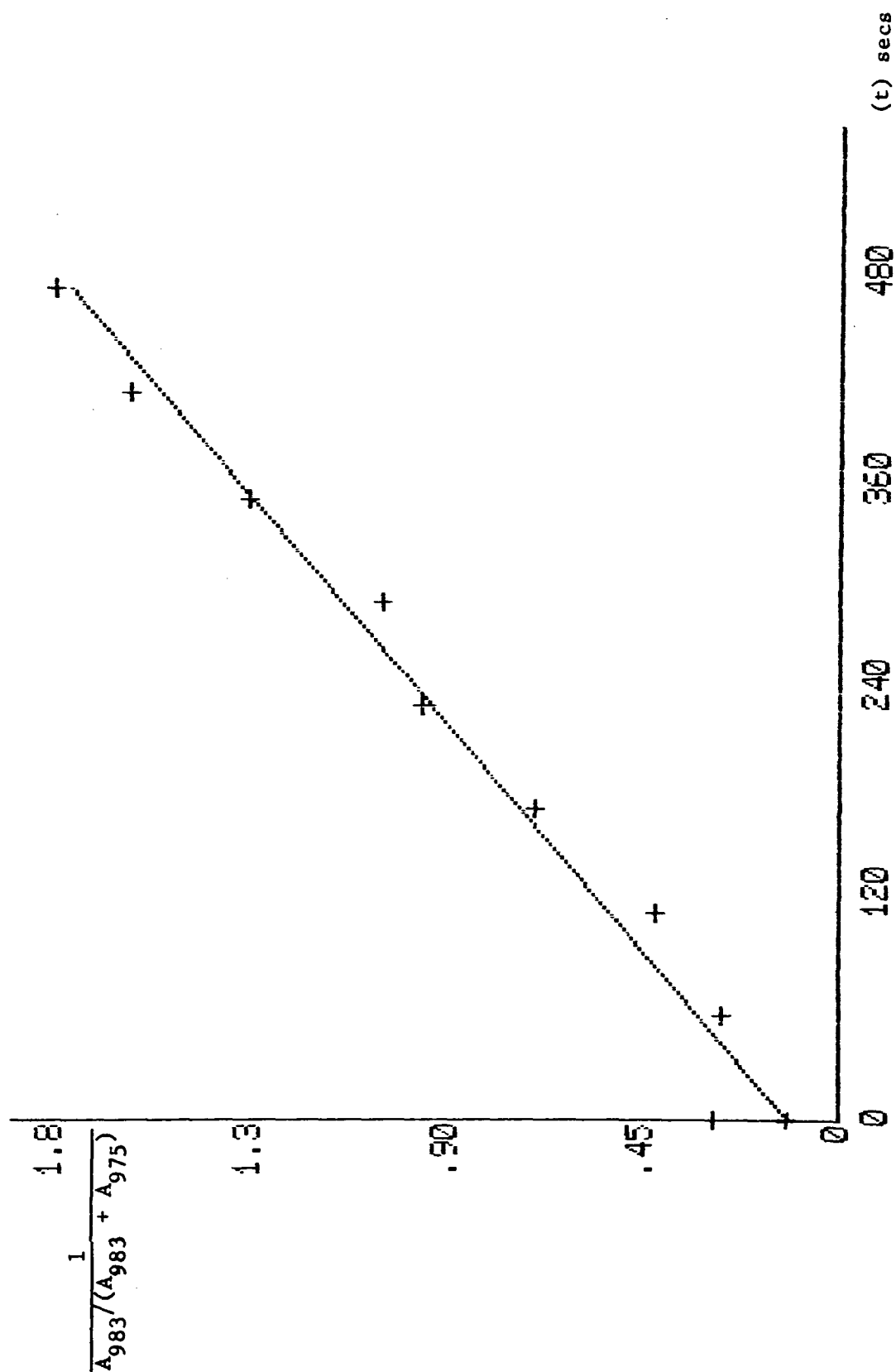


Fig.39 First order rate plot for the conversion of acrylonitrile in argon (M:I 5000:1)
from a high energy form (A) to a low energy form (B)

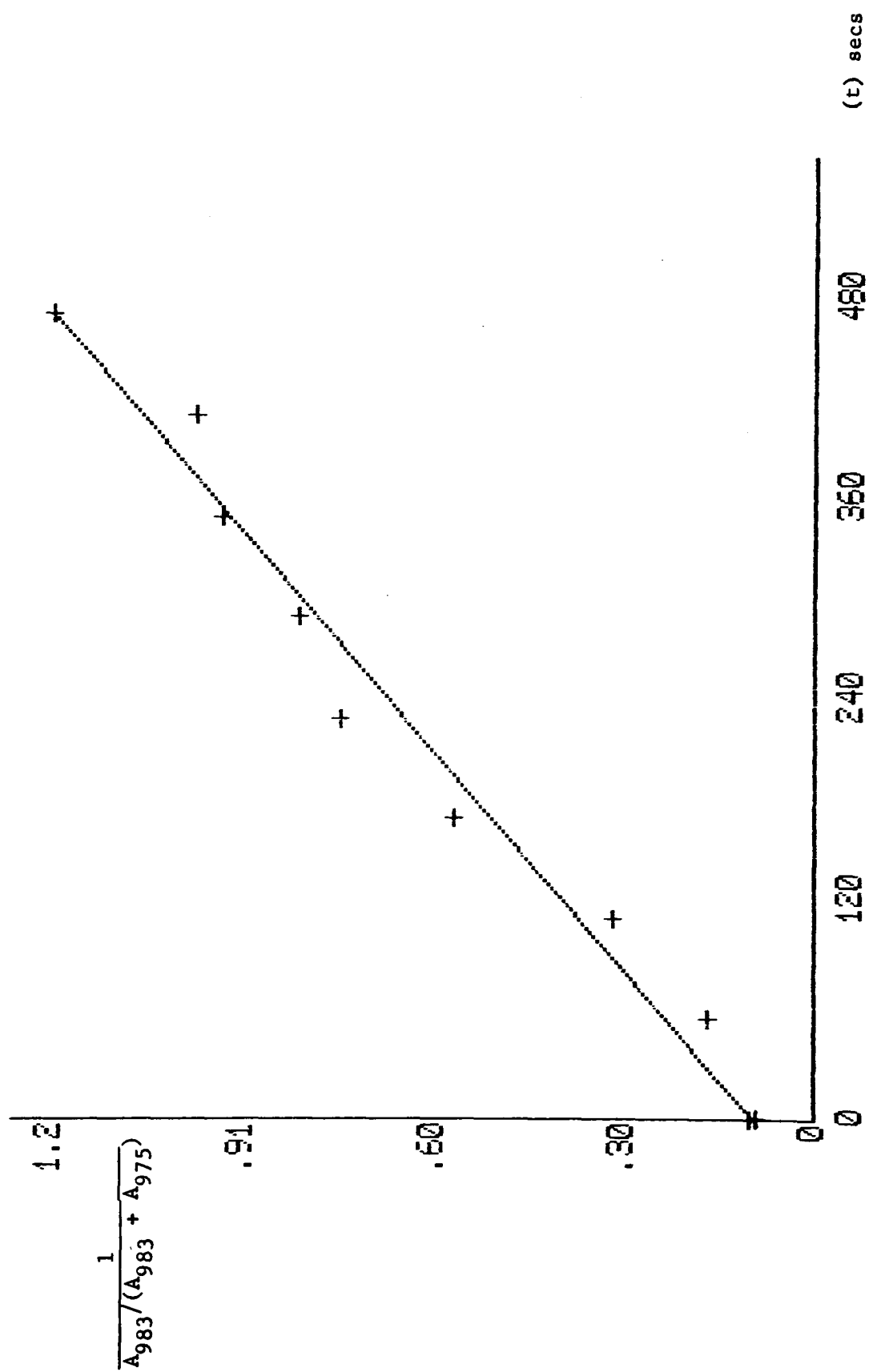


Fig.40 First order rate plot for the conversion of chloroprene in argon (M:I 500:1)
from a high energy form (A) to a low energy form (B)

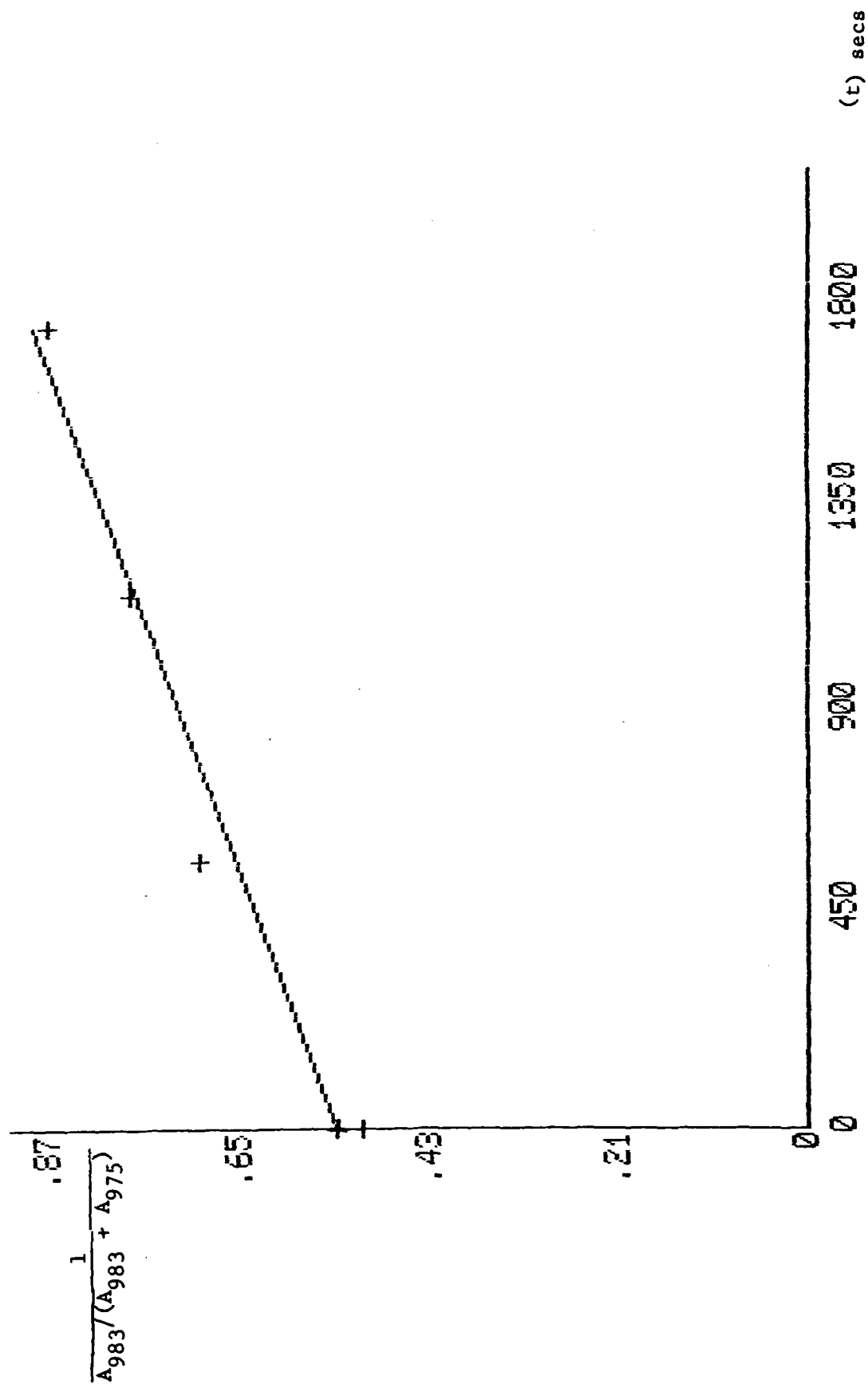
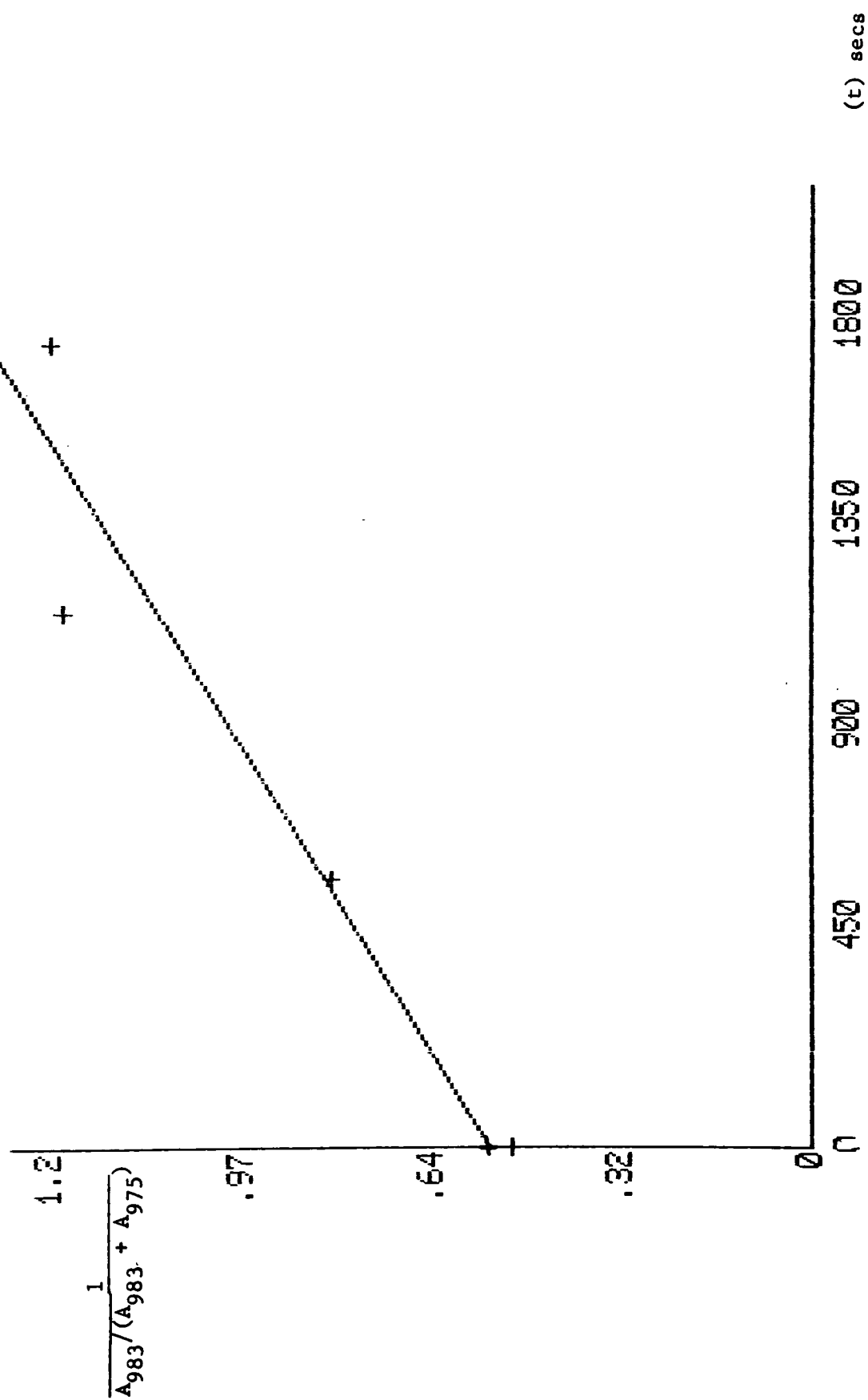


Fig.41 First order rate plot for the conversion of chloroprene in argon (M:I 5000:1)

from a high energy form (A) to a low energy form (B)



4. HIGH AND LOW ENERGY FORMS.

(1) ASSIGNMENTS

An alternative possibility for assignment of the split bands associated with the twisting modes of acrylonitrile and chloroprene would be to a specific effect for that mode such as a Fermi resonance interaction or to an effect localised within a group of the molecule rather than an effect associated with the molecule as a whole. If these changes are correctly attributed to high and low energy forms every other mode will be affected to a greater or lesser extent and it would be remarkable if the twisting mode was unique in achieving sufficient splitting for resolution into separate bands assigned to different states. In order to add weight to the multiple state hypothesis the complete spectra of these states were recorded after maximum separation was achieved using the changes of the twisting mode as a probe to monitor separation.

In the case of acrylonitrile (118-120) assignments have been reported for the solid and vapour states with disagreement only on the relative positions of the twisting and wagging modes. Table 5 reports the assignments of the high energy matrix form (attributed to monomer) and the low energy matrix form (attributed to aggregated polymer). It is noteworthy that the $\text{C}\equiv\text{N}$ and $\text{C}=\text{C}$ stretching modes are shifted by 2 cm^{-1} to lower value in the polymer whilst the CH_2 bending and rocking modes are increased by 2 and 5 cm^{-1} respectively in the polymer form.

In the case of chloroprene (105) assignments have been reported for a range of physical states. In table 8 the high and low matrix isolated states are assigned using the shift of 7.8 cm^{-1} between the

TABLE 8
INFRARED SPECTRA AND ASSIGNMENTS
OF CHLOROPRENE IN ARGON MATRIX

HIGH ENERGY FORM			LOW ENERGY FORM		
Wavenumber	Relative	Assignments	Wavenumber	Relative	
cm-1	Intens		cm-1	Intens	
3122	w	asym =CH ₂ str	3122	w	
3040	w	sym =CH ₂ str	3039	w	
1839.7	vw	2xCH ₂ wag	1839.3	vw	
1754.5	w	2xCH ₂ wag	1754.4	w	
1635.1	s	sym C=C str(H)			
		sym C=C str(L)	1633.9	s	
1591	vw		1591	vw	
1586.5	vs	asym C=C str	1586.5	vs	
1397.3	w	sym CH ₂ sciss	1398.7	w	
1361	m	asym CH ₂ sciss	1361.5	m	
1305					
1291	vw		1292.2	vw	
1267	vw	C-H bend	1267	vw	
1260	vw		1260.8	vw	
1221.9	vs	C-C str(H)			
		C-C str(L)	1220.9	vs	
			1219.5	vs	
1021.9	m	=CH ₂ rock	1022.3	m	
987.8	vw	CH=CH twist(L)	987.8	vw	
			982.2	s	
975.8	m sh				
974.4	s	CH=CH twist(H)			
924.3	vw		924.5	vw	
921.8	w		921.6	w	
919.6	vs	=CH ₂ wag	919.5	vs	
911	vw				
			899.4		
896.4	m	=CH ₂ rock	895.5	m	
			883.8	m	
			880.4	m	
			875.9	vs	
876	vs	=CH ₂ wag			
868	vw				
804.8	vw		804.8	vw	
737.2	w	cis wag	737.9	w	
698.7	w	C-Cl str	699.2	w	
634.6	s	C-Cl str	634.4	s	
630.3	sh				
523.5	w	skeletal bend	523.8	w	
410.7	w	C-Cl bend	413	w	

two twist modes to probe the separation. A shift of 1.2 cm^{-1} is observed between the symmetric C=C stretching modes and of 1.0 cm^{-1} between the two C-C stretching modes. Other small shifts of less than 1.0 cm^{-1} are reported. It is notable that the band centred at 974.4 cm^{-1} in the high energy form has components near 974 and 976 cm^{-1} which respond differently on annealing indicating that the high energy state has some multiplicity.

(11) STRUCTURE

Acrylonitrile may be similar to that of acetonitrile which has been shown by far infrared studies of photochemically produced species to form antiparallel dimers as the low energy state. Statistical calculations (105) for chloroprene in the gas state suggest an equilibria between a low energy *s-trans* conformation and a high energy *s-cis* conformation with a ΔE value of 8.2 KJ mol^{-1} . In the matrix isolated state the high energy form may also correspond to the *s-cis* conformer. The structure of the band centred at 975 cm^{-1} may also imply one or more non-planar forms. These high energy forms can revert to the *s-trans* conformer if the barrier between B and A is reduced by annealing to a level which permits thermodynamic equilibria. This tentative explanation is favoured by the similar behaviour of the isolated species in both argon and krypton matrices.

CHAPTER VI

A SPECTROSCOPIC STUDY OF HEAD TO HEAD MODEL COMPOUNDS FOR HEAD TO HEAD PVC AND PVBr

1. INTRODUCTION

2. MODEL COMPOUNDS FOR HEAD TO HEAD PVC

3. MODEL COMPOUNDS FOR HEAD TO HEAD PVBr

4. CONCLUSIONS

CHAPTER VI

A SPECTROSCOPIC STUDY OF HEAD TO HEAD MODEL

COMPOUNDS FOR PVC AND PVBr

1. INTRODUCTION

Infrared and Raman spectroscopy are good probes for studying the configurational and conformational structure of the PVC and PVBr chains. The C-Cl/C-Br stretching region is particularly sensitive for detailed analysis of these polymers. By comparison with related compounds of known structure bands in the infrared (121-123) and Raman (124) have been assigned to four conformational forms of syndiotactic PVC and three conformational forms of isotactic PVC.

There is now however considerable interest in the possible presence of occasional head to head (H-H) units in the normal head to tail (H-T) structure of poly (vinyl chloride) as such units may be the precursors of branches (125) which influence the macroscopic properties of the polymer. It is also known that the polymer with the pure head to head structure, made by the chlorination of 1,4-polybutadiene, is of lower thermal stability than the conventional polymer (126). Hence, head to head units may act as initiation points in the degradation of the polymer and it is important to be able to characterise them in order to gain a fuller understanding of the factors included in the degradation process.

Unfortunately only one method, a suspect chemical technique (127) is available for the characterisation of head to head units. The evaluation of potentially promising spectroscopic approaches by the examination of pure head to head PVC is open to question; for example, the vibrational frequencies of isolated H-H units in a predominantly H-T polymer may not coincide with those of the pure H-H polymer.

The results of limited studies on degraded poly (vinyl bromide) show that the conjugated polyene sequences formed are longer than those in PVC degraded under comparable conditions (128). In that there is strong evidence that cross linking reactions limit the length of the conjugated polyene sequences in PVC (129), with the effect occurring more readily with the more ordered low temperature polymers, cross linking may be controlled by steric factors. The bulky nature of the bromine atoms in poly (vinyl bromide) will predispose towards bent structures, but little information is available. A spectroscopic approach for studying the normal head to tail forms of PVC was the synthesis and analysis by infrared spectroscopy, in various phases, of model compounds of comparatively low molecular weight (130). This study indicated that a similar approach may be possible on the head to head forms.

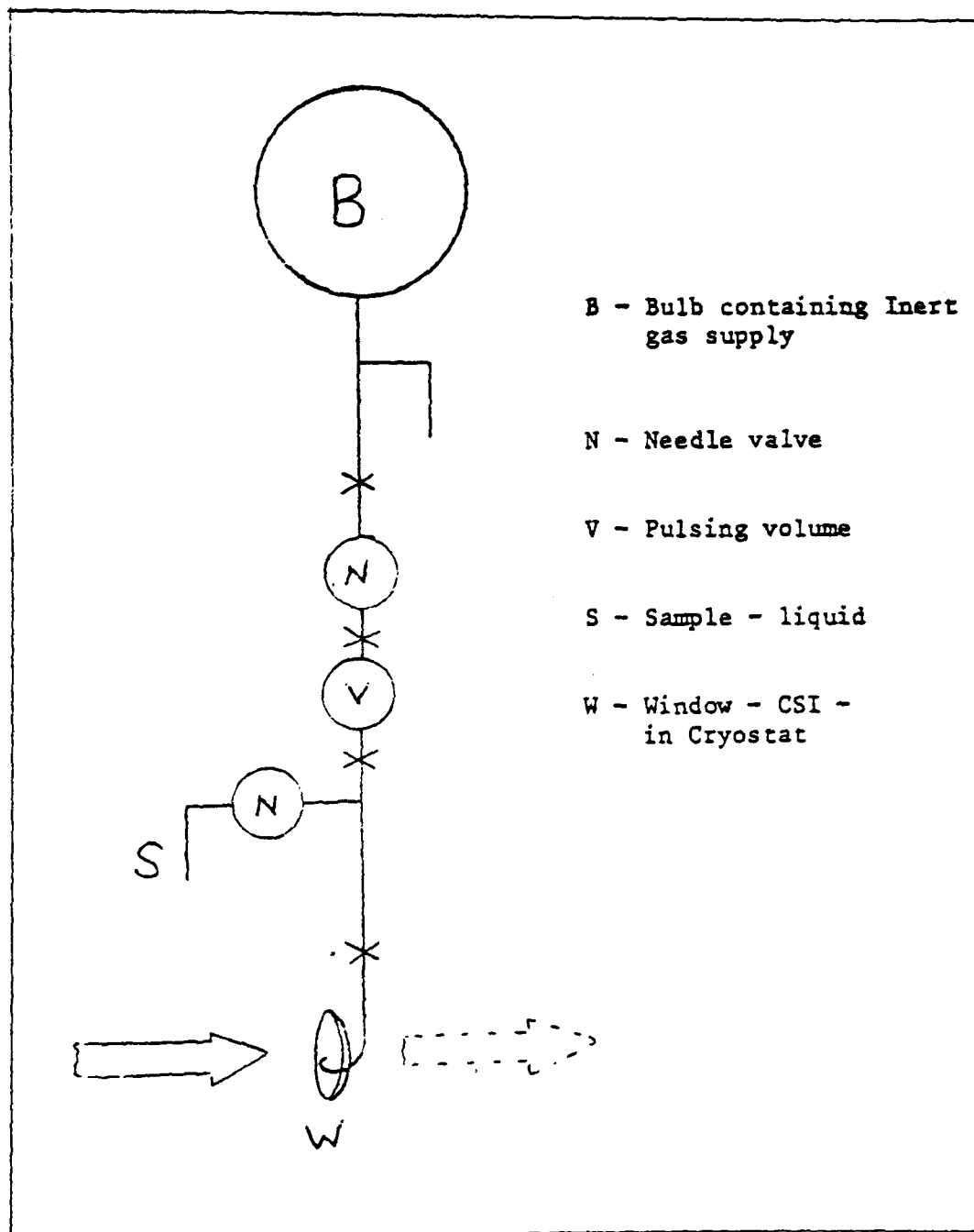
Various model compounds for head to head PVC and PVBr were prepared, meso-2,3-dichlorohexane meso and d,l-3,4-dichlorohexane and meso-4,5-dichlorooctane, together with their bromoanalogues. The meso derivatives act as model compounds for isotactic head to head PVC and PVBr, and the d,l derivatives acting as model compounds for syndiotactic head to head PVC and PVBr.

The measurement of the infrared spectra in the matrix phase of these samples proved unsatisfactory using the conventional system due

to their low volatilities. The technique requires the sample to be in the gas phase before condensation and hence sample preparation and spectral quality are severely affected by the inability to get sufficient amounts of the sample into the gas phase. The conventional system failed to produce any usable spectra and computer enhancement (Perkin-Elmer Data Station) proved only marginally helpful. Spectra of higher quality could only be produced by adapting the present system (Fig.42). This was achieved by allowing the two separate components (inert gas and sample) to mix just prior to deposition on the window, hence, mixing takes place at far lower partial pressures than before and as a result samples of quite high concentration can be deposited using this technique. The ratios of sample to matrix gas can be effectively altered by the two needle valves which govern the flow rate of the two gases respectively.

Even with the improved experimental system the spectra produced were still of inferior quality. Little or no obvious differences existed between the spectra before and after annealing on all the compounds studied. The reasons for this may be twofold. Firstly the spectra recorded after annealing were of such poor quality that any inferences deduced from changes in relative intensities of different bands would be open to question. Secondly bands produced were far broader than those produced by studies on saturated hydrocarbons of lower molecular weight (130) possibly as a direct result of the increase in the number of possible conformers and/or the greater complexity and size of the molecules in terms of site effects and numbers of vibrational modes. The ability therefore to obtain good information about conformational isomerism within this class of

Fig.42 Modified sample deposition system for
compounds of low volatility



compounds by matrix isolation seems doubtful. In this respect comparisons between infrared for both liquid and matrix isolation and liquid Raman frequencies has been carried out in order to obtain the best vibrational assignments of the structural units associated with the head to head forms. Tables of frequencies for all the compounds studied are therefore presented.

Previous infrared studies on other model compounds for PVC has tended to concentrate primarily on the C-Cl stretching region. This region is considered to be particularly sensitive to any conformational or structural change, and as such provides an excellent probe for studying such phenomenon within the PVC and PVBr chain. This observation therefore, constitutes the basis of this work in that correlation of the characteristic frequencies of the C-Cl and C-Br stretching regions of vicinally substituted model compounds may indicate the degree to which these units may be present in the normal PVC chain. Various workers (121,122, 131-133) have studied the C-Cl stretching region of PVC ($700\text{-}600\text{ cm}^{-1}$) and the locations and number of bands reported varies from author to author depending on the polymer source or resolving power of the spectrometer used. Rubcic and Zerbi (123) state however that the two C-Cl stretching $k=0$ phonon bands of PVC occur approximately at 640 and 604 cm^{-1} .

2. MODEL COMPOUNDS FOR HEAD TO HEAD PVC

Meso-3,4-dichlorohexane (Fig.43, Table 9) shows a strong band at 640 cm^{-1} in the liquid phase and at 653.5 cm^{-1} in the matrix phase with a corresponding weak band at 655 cm^{-1} in the liquid Raman. These values are in agreement with those values obtained by Horhold et al (134-135) for the *trans* conformer indicating this to be the predominant form in

Fig.43 Spectra of meso-3,4-dichlorohexane

(a) liquid infrared

(b) liquid Raman

(c) matrix isolation infrared

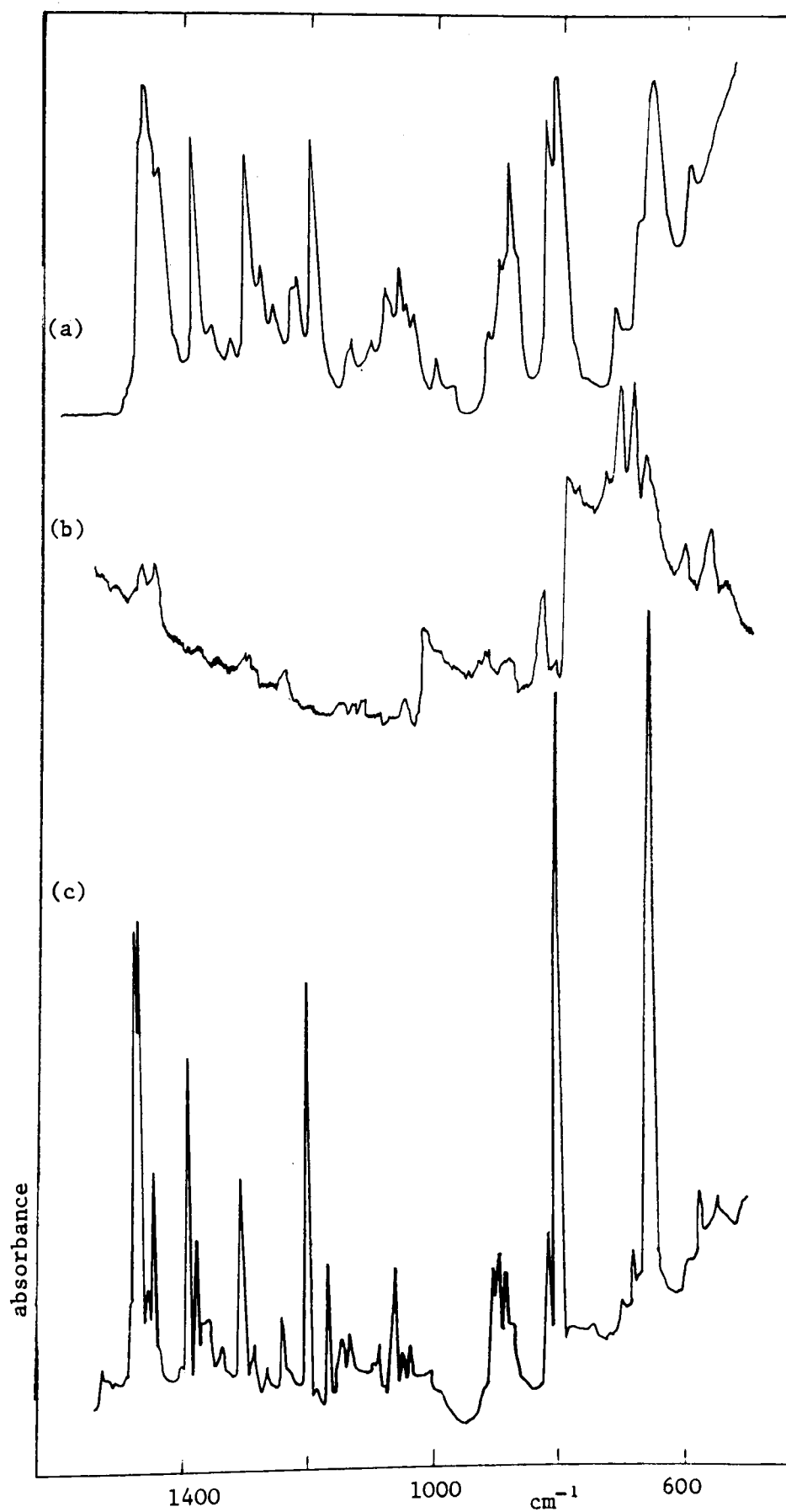


TABLE 9

MESO-3,4-DICHLOROHEXANE

<u>MATRIX</u>		<u>LIQUID</u>		<u>LIQUID RAMAN</u>	
<u>Wavenumber</u> <u>cm-1</u>	<u>Relative</u> <u>Intens</u>	<u>Wavenumber</u> <u>cm-1</u>	<u>Relative</u> <u>Intens</u>	<u>Wavenumber</u> <u>cm-1</u>	<u>Relative</u> <u>Intens</u>
2988	vs			2980	m-sh
2981.5	vs				
2951.5	s	2961	vs	2955	m-sh
2925	m	2927	vs	2935	s
2890	s	2875	s	2880	m
2850.5	w	2845	m	2851	w
1466	s				
1458	s	1455	vs	1460	w
1446	w				
1439	m	1435	s	1440	w
1383.5	m	1380	s		
1369	m			1370	vw
1361	vw	1358	vw		
1352	vw				
1333	vw	1330	vw		
1302	m	1297	s	1290	vw
1293	vw-sh				
1281	vw	1277	w		
1259.5	vw	1258	vw		
1238	w	1230	vw	1226	vw
1194	s	1190	s		
1162	w				
1143	vw				
1131	vw	1132	vw	1140	vw
1084	vw	1080	w		
1058	w	1055	m		
1047.5	vw	1043	w	1040	vw
1036.5	vw	1033	w		
		999	vw		
		973	vw		
		913	w		
904	w-sh			903	vw
901	w				
893	w	896	m		
887.5	w	885	m-sh		
882	w				
872	w-sh	875	s	867	vw
816.5	w	811	vs	816	m
812	vw-sh				
800	vs			795	w
796	vs	796	vs	718	vw
719	vw	708	w	700	m
703	vw				

TABLE 9 CONTINUED

<u>MATRIX</u>		<u>LIQUID</u>		<u>LIQUID RAMAN</u>	
<u>Wavenumber</u> <u>cm-1</u>	<u>Relative</u> <u>Intens</u>	<u>Wavenumber</u> <u>cm-1</u>	<u>Relative</u> <u>Intens</u>	<u>Wavenumber</u> <u>cm-1</u>	<u>Relative</u> <u>Intens</u>
681.5	w	668	m	676	m
653.5	vs	640	vs	655	w
596.5	vw				
575.5	w	583	m	592	vw
548	w			551	w
				523	vw
				440	w
				424	vw
				405	vw
				386	m
				367	vw
				331	m
				296	m
				285	m
				142	vs

Fig.44 Spectra of dl-3,4-dichlorohexane

(a) liquid infrared

(b) liquid Raman

(c) matrix isolation infrared

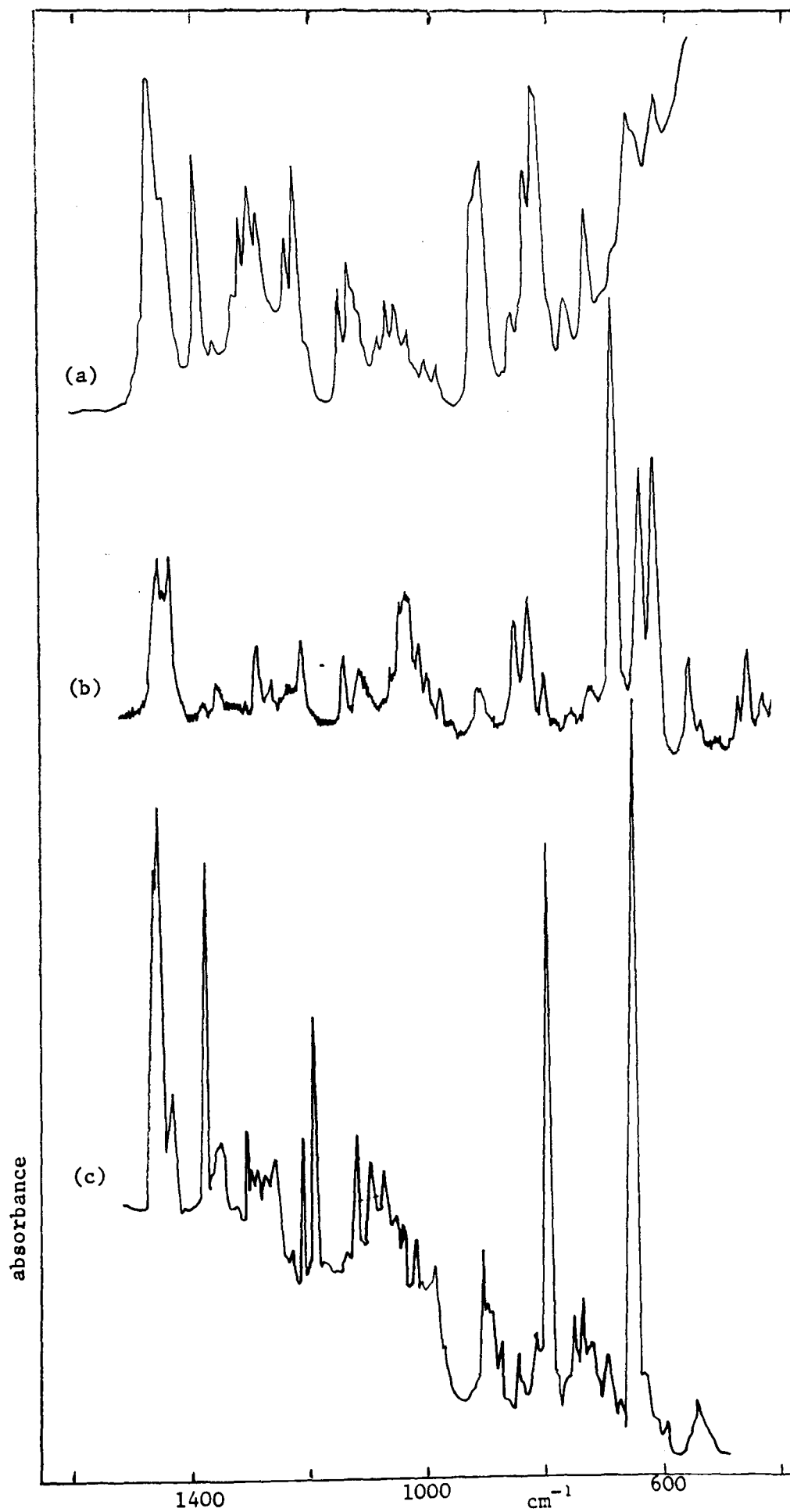


TABLE 10

d,1-3,4-DICHLOROHEXANE

<u>MATRIX</u>		<u>LIQUID</u>		<u>LIQUID RAMAN</u>	
<u>Wavenumber</u> <u>cm-1</u>	<u>Relative</u> <u>Intens</u>	<u>Wavenumber</u> <u>cm-1</u>	<u>Relative</u> <u>Intens</u>	<u>Wavenumber</u> <u>cm-1</u>	<u>Relative</u> <u>Intens</u>
2984	vs				
2949	s	2961	vs	2965	m-sh
2937	m				
2920.5	m	2928	vs	2930	s
2890	s	2873	vs	2875	m
2858.5	w				
2851	w	2842	m	2850	vw
		2735	vw	2737	vw
1465.5	s				
1460	s	1457	vs	1455	m
1437	w	1432	s	1440	m
1383	s				
1380	s	1380	s	1380	vw
1359	vw			1360	vw
1353	vw	1352	vw		
1327	vw	1322	w		
1310	w	1308	m		
1302	vw				
1293	vw	1290	s	1295	w
1282.5	vw				
1267	vw	1272	m	1267	vw
1260.5	vw				
1234	vw	1239	m	1235	vw
1217	m	1211	s	1215	m
1195.5	m	1192	w-sh		
1147.5	vw	1139	w	1140	m
1126	m	1121	w	1120	m
1103	vw	1104	vw-sh		
1098.5	vw				
		1072	vw		
1057.5	vw	1058	w	1065	m
1048	vw	1042	w	1035	s
1027.5	vw	1021	vw		
1000	vw	1010	vw	1010	m
994.5	vw	994	vw	1000	w
975	vw	971	vw	977	w
913	m	909	s-sh		
905	vw	900	s-sh		
897.5	vw	893	s		

TABLE 10 CONTINUED

<u>MATRIX</u>		<u>LIQUID</u>		<u>LIQUID RAMAN</u>	
<u>Wavenumber</u> <u>cm-1</u>	<u>Relative</u> <u>Intens</u>	<u>Wavenumber</u> <u>cm-1</u>	<u>Relative</u> <u>Intens</u>	<u>Wavenumber</u> <u>cm-1</u>	<u>Relative</u> <u>Intens</u>
881.5	vw				
852	vw	858	vw	849	s
845	vw	842	w		
823.5	vw	818	s	847	s
804	vs	800	vs	798	m
796	m-sh				
757	vw	750	w	750	vw
743.5	vw				
728	vw	712	m	720	vw
700.5	vw				
680	vw	685	vw	675	vs
655	vs	668	vw		
637	vw-sh	638	vs	625	vs
				602	vs
598	vw	591	vs		
548	vw			545	m
				525	vw
				460	w
				445	m
				415	w
				390	s
				373	vs
				335	m-sh
				320	vs
				273	m
				210	vw
				175	m

Fig.45 Spectra of meso-2,3-dichlorohexane

(a) liquid infrared

(b) liquid Raman

(c) matrix isolation infrared

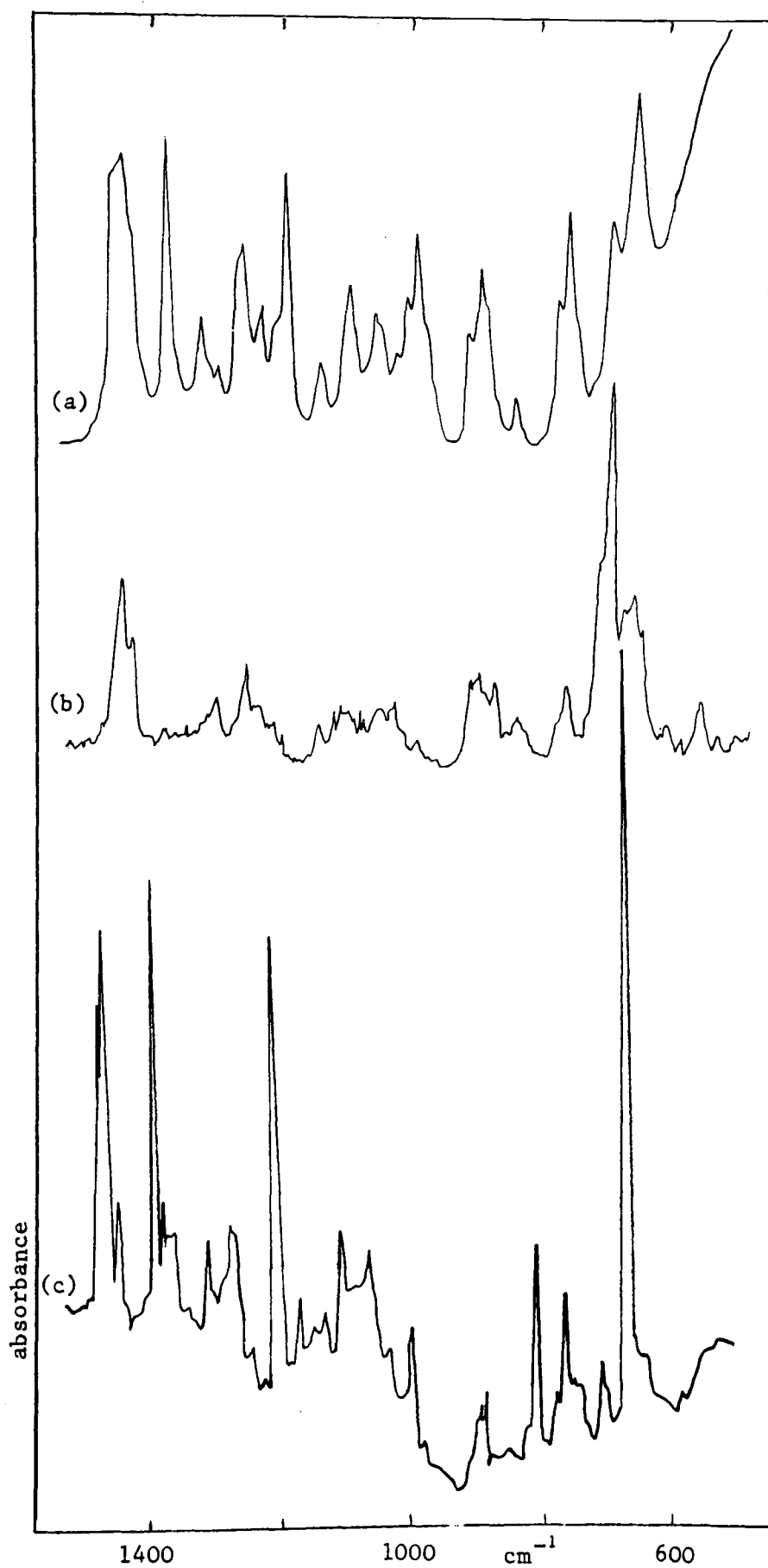


TABLE 11
MESO-2,3-DICHLOROHEXANE

<u>MATRIX</u>		<u>LIQUID</u>		<u>LIQUID RAMAN</u>	
<u>Wavenumber</u> <u>cm-1</u>	<u>Relative</u> <u>Intens</u>	<u>Wavenumber</u> <u>cm-1</u>	<u>Relative</u> <u>Intens</u>	<u>Wavenumber</u> <u>cm-1</u>	<u>Relative</u> <u>Intens</u>
		2955	vs		
2923	m	2927	vs	2935	s
2889	s	2868	s	2870	m
2853	w	2840	m-sh	2870	m
		2725	vw	2735	vw
1469	s	1465	s-sh		
1461	s	1458	s-sh	1455	m-sh
1452	m-sh	1449	s	1440	w
1435	w	1435	m-sh		
1380	s	1378	s	1385	vw
1369	w				
1360.5	vw				
1352	vw				
		1325	w		
1302.5	w	1300	vw	1305	w
1266.5	w	1270	w-sh		
1260.5	w	1260	m	1260	m
1238	vw	1232	w	1240	w-sh
1217	vw	1213	w-sh		
1195	s	1192	s		
1162.5	vw				
1141.5	vw	1140	w	1145	w
1126	vw				
1100.5	w	1092	m	1105	w
1058	w	1052	w	1052	w
1028	vw	1020	vw	1025	w
994	w	989	m	990	vw
987	vw				
905	vw	910	w	910	m
892.5	vw				
887.5	w	889	m	895	m
881.5	w	878	w-sh	870	m
		835	vw	832	w
801	m				
796.5	m	793	w		
770	vw	767	w	760	m
756.5	w	750	s		
744	vw				
700.5	w	710	vw	707	s-sh
				690	vs
		680	s	670	s-sh
				650	s

TABLE 11 CONTINUED

<u>MATRIX</u>		<u>LIQUID</u>		<u>LIQUID RAMAN</u>	
<u>Wavenumber</u> <u>cm-1</u>	<u>Relative</u> <u>Intens</u>	<u>Wavenumber</u> <u>cm-1</u>	<u>Relative</u> <u>Intens</u>	<u>Wavenumber</u> <u>cm-1</u>	<u>Relative</u> <u>Intens</u>
658	vs	642	vs	640	s-sh
				600	vw
578	vw			545	w
				460	w
				420	s
				390	w
				340	m
				315	w
				280	s
				210	w

Fig.46 Spectra of meso-4,5-dichlorohexane

(a) liquid infrared

(b) liquid Raman

(c) matrix isolation infrared

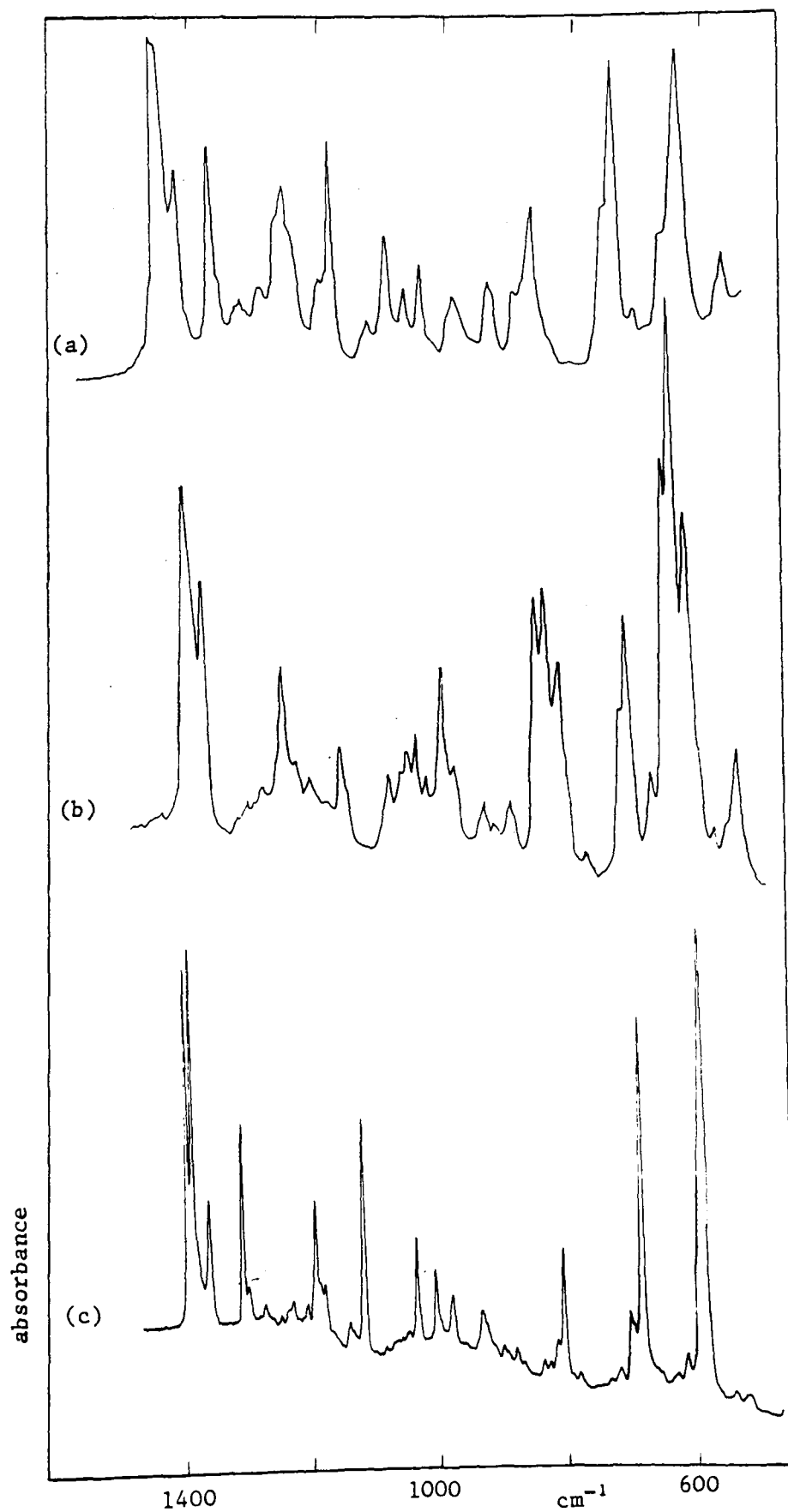


TABLE 12
MESO-4,5-DICHLOROCTANE

<u>MATRIX</u>		<u>LIQUID</u>		<u>LIQUID RAMAN</u>	
<u>Wavenumber</u> <u>cm-1</u>	<u>Relative</u> <u>Intens</u>	<u>Wavenumber</u> <u>cm-1</u>	<u>Relative</u> <u>Intens</u>	<u>Wavenumber</u> <u>cm-1</u>	<u>Relative</u> <u>Intens</u>
2970	vs				
		2953	vs	2955	m-sh
2944	s	2925	vs	2935	vs
2918	m	2910	s-sh	2910	s-sh
2884	s	2868	vs	2865	s
2852	w	2840	m-sh	2840	vw-sh
		2727	vw	2730	vw
1461	s	1463	s		
1460		1457	s-sh	1451	s
1435	w	1430	m	1435	s
1383	m	1380	m	1370	vw
1374	vw-sh				
1310	vw				
1307	vw	1300	vw	1305	m
1283	vw	1277	vw	1287	w
1268	w	1265	m	1265	vw
1255	vw-sh				
1216	vw	1210	w-sh	1215	w
1192	m	1189	m		
				1140	w
1110	w	1104	w	1110	w
1080	w	1075	vw	1080	vw
1053	w	1050	w	1052	m
				1037	w
1008	w	1000	vw		
				990	w
974	vw			975	vw
955	vw	942	w	945	w
910	vw	905	w-sh	905	s
900	vw				
888	vw-sh			887	s
877	w	874	m	867	s
853	vw				
				830	vw
807	vw				
790	vw				
772	w-sh	765	m-sh	775	m-sh
752	s	746	s	760	s
		717	vw	725	w
700	vw			698	vs
685	vw	671	w	671	vs
656	s	642	s		
				625	vw
608	vw			605	vw

TABLE 12 CONTINUED

<u>MATRIX</u>		<u>LIQUID</u>		<u>LIQUID RAMAN</u>	
<u>Wavenumber</u>	<u>Relative</u>	<u>Wavenumber</u>	<u>Relative</u>	<u>Wavenumber</u>	<u>Relative</u>
<u>cm-1</u>	<u>Intens</u>	<u>cm-1</u>	<u>Intens</u>	<u>cm-1</u>	<u>Intens</u>
588	vw	577	w	587	m
535	vw				
522	vw			520	vw
				488	w
472	vw				
				450	vw
				402	w
				397	s
				333	m-sh
				290	vs
				251	w
				217	vw

both the liquid and matrix phases. The d,l analogue of meso-3,4-dichlorohexane (Fig.44, Table 10) gave rise to two strong bands in this region in both the liquid infrared and liquid Raman spectrum at 638 and 591 cm^{-1} and 625 and 602 cm^{-1} respectively. The matrix spectrum however, had only one strong band in this region at 655 cm^{-1} . The two bands associated with the liquid spectra are assigned to the *trans* and *gauche* conformers with the higher frequency band assigned to the *trans* conformer. The presence of only one strong band at 655 cm^{-1} in the matrix phase indicates the presence of only the *trans* conformer which like the meso derivative appears to be the low energy stable form at cryogenic temperatures. As stated previously the matrix spectra were of relatively poor quality and as such annealing studies carried out contributed no extra information on any conformational equilibria.

The study carried out on meso-2,3-dichlorohexane (Fig.45, Table 11) again revealed two strong bands in the liquid phase at 680 and 642 cm^{-1} with one strong band in the matrix phase at 658 cm^{-1} , while the Raman spectrum consisted of two main bands in this region at 690, 650 cm^{-1} . The presence of two bands in the liquid and Raman phases and only one in the matrix phase indicates a similar behaviour to that observed for d,l-3,4-dichlorohexane in that both the *trans* and *gauche* conformers may be present at room temperature while only the lower energy conformer is present at 8 K. The spectra obtained for meso-4,5-dichlorooctane (Fig.46, Table 12.) revealed only one strong band in the liquid phase, occurring at 642 cm^{-1} , and one strong band at 656 cm^{-1} in the matrix. This indicates a similar behaviour pattern to that observed for meso-3,4-dichlorohexane in that there is only one predominant conformer at both room and matrix temperature.

3. MODEL COMPOUNDS FOR HEAD TO HEAD PVB

Studies carried out on the dibromohexanes and octanes yielded similar spectra to those obtained for the dichlorohexanes and octanes. Again frequencies associated with the C-X group are considered to be the most sensitive probes for structural information and as such the C-Br stretching region between $670\text{--}520\text{ cm}^{-1}$ is studied in detail.

The matrix infrared spectra of meso-3,4-dibromohexane have three bands in this region at 670, 655 and 562 cm^{-1} while the Raman spectra have three bands at 665, 645 and 530 cm^{-1} , with no information for the liquid i.r. (Fig.47, Table 13). The band at 562 cm^{-1} in the matrix is assigned to the C-Br stretch for the *trans* conformer whereas the band at 530 cm^{-1} in the Raman is assigned to the C-Br stretch for the *gauche* conformer. The bands at 645 and 665 cm^{-1} are therefore assigned to the *trans* conformer. These results indicate the presence of both conformers at room temperature but with the predominant conformer being *trans* in the matrix phase. A very weak band appears at 537 cm^{-1} in the matrix and is assigned to the *gauche* conformer. These results, as for the chloro derivatives, indicate the low energy conformer is the *trans* form which agrees with those results obtained by Heublein et al (136).

The matrix infrared spectra of meso-4,5-dibromooctane (Fig.48, Table 14.) shows two bands in the C-Br stretching region at 564 and 558 cm^{-1} with three weaker bands at 655, 628 and 591 cm^{-1} . The Raman spectrum has two strong bands at 645 and 620 cm^{-1} with a weaker band at 592 cm^{-1} and an even weaker feature at 527 cm^{-1} . Correlation with the data obtained for meso-3,4-dibromohexane suggests that both bands at 564 and 558 cm^{-1} are assigned to the *trans* form, possibly in

Fig.47 Spectra of meso-3,4-dibromohexane

(a) liquid infrared

(b) liquid Raman

(c) matrix isolation infrared

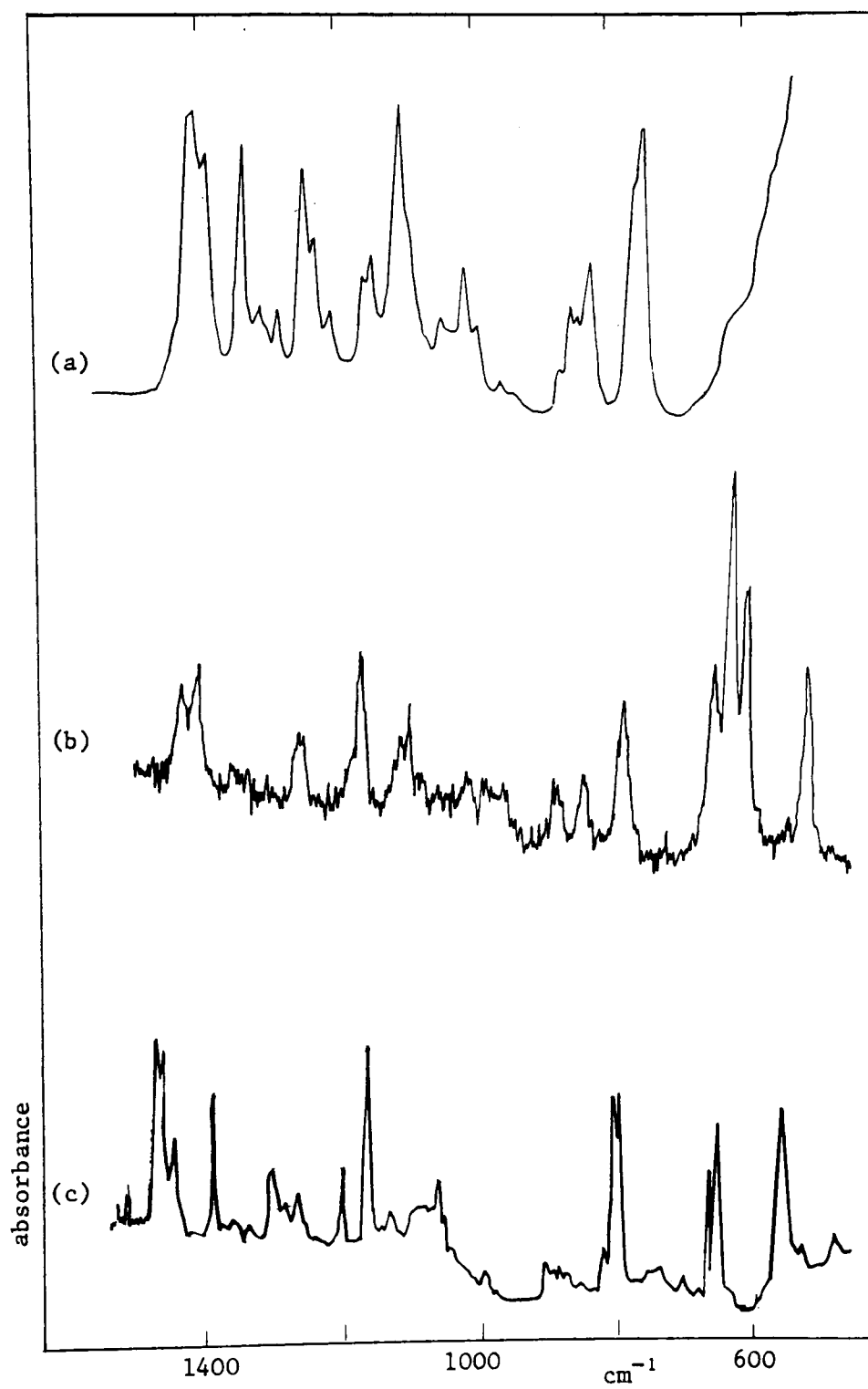


TABLE 13

MESO-3,4-DIBROMOHEXANE

<u>MATRIX</u>		<u>LIQUID</u>		<u>LIQUID RAMAN</u>	
<u>Wavenumber</u> <u>cm-1</u>	<u>Relative</u> <u>Intens</u>	<u>Wavenumber</u> <u>cm-1</u>	<u>Relative</u> <u>Intens</u>	<u>Wavenumber</u> <u>cm-1</u>	<u>Relative</u> <u>Intens</u>
2982	vs				
2958	m	2960	vs	2965	m
2940	m				
2920	m	2925	vs	2930	vs
2905	m				
2897	m				
		2872	s	2875	m
2855	m	2843	m	2850	vw
		2730	vw	2735	vw
1470	s				
1461	s-sh	1465	s-sh	1460	m
1444	m	1432	s	1435	m
1377	s	1380	s		
1360	vw	1351	w		
1338	vw	1325	w		
1282	vw	1289	s	1285	w
1270	vw	1272	m		
		1248	w		
1202	w	1202	w-sh	1200	m
		1188	w		
1165	s	1150	vs	1140	w
1132	vw			1125	m
1061	w	1084	vw		
1043	vw	1050	m	1040	vw
		1030	w-sh		
				1010	vw
995	vw	995	vw	980	vw
		972	vw		
908	vw	908	vw	900	vw
888	vw	891	w		
		881	w		
		862	m	860	w
823	vw				
810	s				
800	s	800	s-sh	805	m
		788	vs		
708	vw				
684	vw			665	s
670	s			645	vs
655	s				
562	s			530	s
537	vw				
489	vw				

TABLE 13 CONTINUED

<u>MATRIX</u>		<u>LIQUID</u>		<u>LIQUID RAMAN</u>	
<u>Wavenumber</u> <u>cm-1</u>	<u>Relative</u> <u>Intens</u>	<u>Wavenumber</u> <u>cm-1</u>	<u>Relative</u> <u>Intens</u>	<u>Wavenumber</u> <u>cm-1</u>	<u>Relative</u> <u>Intens</u>
				420	m
				385	vw
				355	w
				310	m
				205	s
				185	vs

Fig.48 Spectra of meso-4,5-dibromooctane

(a) liquid infrared

(b) liquid Raman

(c) matrix isolation infrared

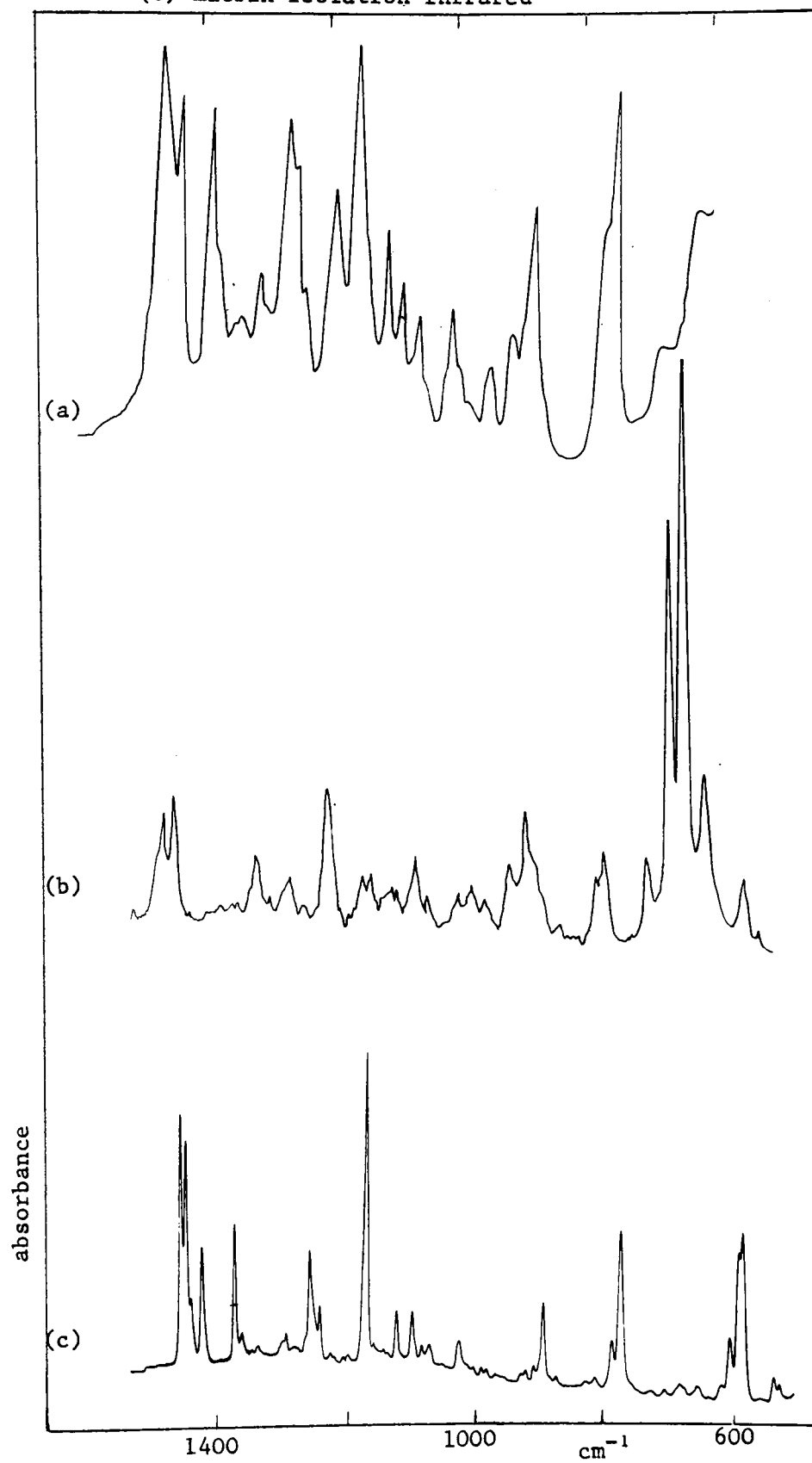


TABLE 14

MESO-4,5-DIBROMOOCTANE

<u>MATRIX</u>		<u>LIQUID</u>		<u>LIQUID RAMAN</u>	
<u>Wavenumber</u> <u>cm-1</u>	<u>Relative</u> <u>Intens</u>	<u>Wavenumber</u> <u>cm-1</u>	<u>Relative</u> <u>Intens</u>	<u>Wavenumber</u> <u>cm-1</u>	<u>Relative</u> <u>Intens</u>
2975	vs				
2944	s	2950	vs-sh	2955	m-sh
2921	m	2922	vs	2930	s
				2910	s
2883	s				
2852	w	2862	vs	2862	s
		2837	s	2840	vw
2742	vw	2722	vw	2730	vw
1469	s				
1460					
1452	w-sh	1456	vs	1450	m
1434	m	1420	m-sh	1430	m
1383	m	1378	s		
1371	vw	1365	m-sh		
1347	vw	1340	vw		
		1328	vw		
1302	vw	1298	w	1300	w
1265	m	1260	s		
1249	w	1243	m	1250	vw
1232	vw	1227	w		
1190	vw	1181	m	1185	m
1158	vs	1150	vs		
1140	vw	1130	m-sh	1130	vw
1123	vw			1120	vw
1103	w	1098	m		
1079	w	1074	w	1080	vw
1063	vw				
1052	vw	1047	w	1050	w
1005	w	995	w		
980	vw			980	vw
970	vw				
960	vw			955	vw
		931	w	940	vw
908	vw-sh				
900	vw	900	w	900	w
888	vw				
872	w	868	m	872	m
850	vw				
790	vw				
763	w	758	m-sh	760	w
750	m	742	s	749	w
680	vw			680	w
655	vw			645	vs

TABLE 14

<u>MATRIX</u>		<u>LIQUID</u>		<u>LIQUID RAMAN</u>	
<u>Wavenumber</u>	<u>Relative</u>	<u>Wavenumber</u>	<u>Relative</u>	<u>Wavenumber</u>	<u>Relative</u>
<u>cm-1</u>	<u>Intens</u>	<u>cm-1</u>	<u>Intens</u>	<u>cm-1</u>	<u>Intens</u>
628	vw			620	vs
591	vw			592	m
578	w				
564	m				
558	m				
509	vw			527	w
500	vw				
455	vw			455	w
				277	m
				260	m
				180	vs

Fig.49 Spectra of meso-2,3-dibromohexane

(a) liquid infrared

(b) liquid Raman

(c) matrix isolation infrared

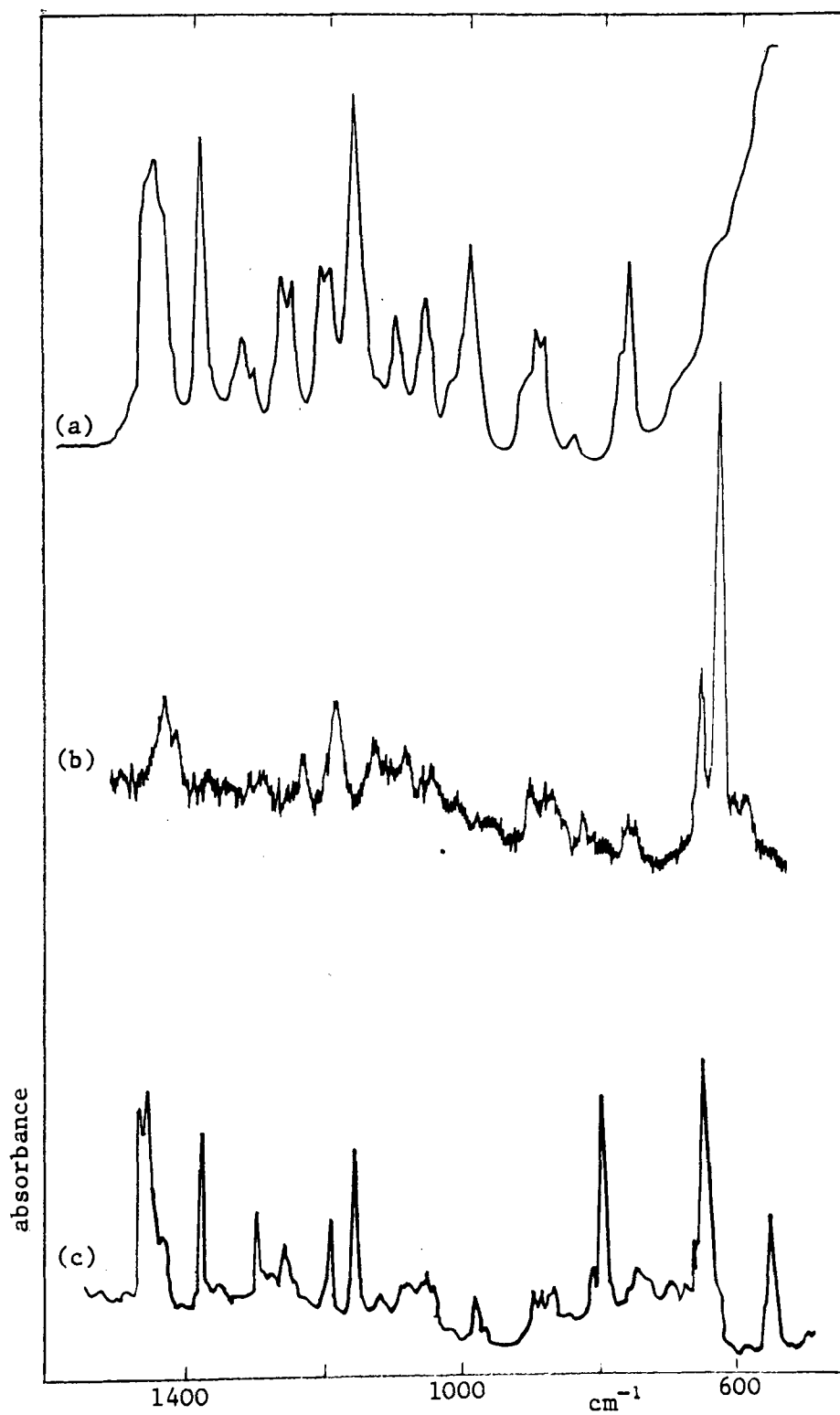


TABLE 15

MESO-2,3-DIBROMOHEXANE

<u>MATRIX</u>		<u>LIQUID</u>		<u>LIQUID RAMAN</u>	
<u>Wavenumber</u> <u>cm-1</u>	<u>Relative</u> <u>Intens</u>	<u>Wavenumber</u> <u>cm-1</u>	<u>Relative</u> <u>Intens</u>	<u>Wavenumber</u> <u>cm-1</u>	<u>Relative</u> <u>Intens</u>
2981	vs	2955	vs	2960	m-sh
2950	s	2922	vs	2930	vs
2920	m	2910	s-sh	2910	m
2891	m	2863	s	2865	m
2850	w	2835	m-sh	2840	vw
2745	vw	2723		2735	vw
1472	s-sh				
1463	s	1458	s-sh	1450	m
1442	w	1430	s-sh	1430	w-sh
1385	s	1378	s	1385	vw
1360	vw				
1307	m	1315	w	1305	vw
1287	vw	1296	vw		
1268	w	1260	m		
1252	vw	1242	m	1245	w
1200	m	1200	m	1197	m
		1188	m		
1162	s	1153	vs		
1130	vw	1135	vs	1140	w
1100	vw-sh	1090	m	1090	w
1060	vw	1058	w-sh	1055	vw
1040	vw	1046	m		
		1037	w-sh		
		1011	vw-sh		
990	vw	990	w-sh		
975	vw-sh	980	m		
		968	m-sh		
908	vw			907	w
898	vw	895	w		
885	vw-sh				
878	vw	880	m	877	w
		870	m		
820	vw	825	vw	827	vw
806	s				
756	vw	756	m-sh	760	vw
		743	m		
708	vw				
682	vw				
657	vs			655	m
				630	vs
598	vw				
				580	w
561	m				

TABLE 15 CONTINUED

<u>MATRIX</u>		<u>LIQUID</u>		<u>LIQUID RAMAN</u>	
<u>Wavenumber</u>	<u>Relative</u>	<u>Wavenumber</u>	<u>Relative</u>	<u>Wavenumber</u>	<u>Relative</u>
<u>cm-1</u>	<u>Intens</u>	<u>cm-1</u>	<u>Intens</u>	<u>cm-1</u>	<u>Intens</u>
				402	vw
				505	vw
				362	vw
				300	vw
				215	vw-sh
				185	s

different sites, whereas the weak band at 509 cm^{-1} is assigned to the *gauche* conformer. The band at 655 cm^{-1} in the Raman spectra is assigned to the *trans* conformer and the band at 592 cm^{-1} assigned to the *gauche* form. The ratio of these two bands gives some indication of the percentage of the two forms present in the liquid phase.

Finally for meso-2,3-dibromohexane (Fig.49, Table 15) the Raman spectrum contains three bands in this region, occurring at 655, 630 and 580 cm^{-1} . The strongest band at 630 cm^{-1} is assigned to the *trans* conformer with the much weaker band at 580 assigned to the *gauche* conformer the strongest band in the infrared matrix occurs at 561 cm^{-1} and is therefore assigned to the *trans* conformer.

4. CONCLUSIONS

These results suggest that at room temperature for both the chloro and bromo meso compounds the predominant conformer is *trans* whereas for the d,l derivatives there is a greater contribution from the other species. These results are in agreement with those obtained by calculations using semiempirical potential functions and those obtained by nmr (136-137). This analysis has only considered the main bands found in the C-Cl and C-Br stretching regions corresponding to the two main conformers found in the liquid state. These conformers result from rotation about the two carbon atoms containing the halogen substituents. Several other weaker bands may be distinguished (Tables 9-15) corresponding to the other conformers as a result of rotation about the other axes. The results reported here indicate that matrix studies of these relatively large molecules may not produce sufficiently good information for a conclusive study of conformational behaviour within this class of compounds without further development of

the deposition system outlined here. Further studies to elucidate conformational information for these compounds may be more effectively obtained by variable temperature infrared studies.

REFERENCES

1. H.E.Hallam, "Vibrational Spectroscopy of Trapped Species" (Wiley Interscience 1973).
2. G.N.Lewis, D.Lipkin, J.Amer. Chem. Soc., 64, 2801 (1942).
3. I.Norman, G.Porter, Nature, 174, 508 (1954).
4. E.Whittle, D.A.Dows, G.C.Pimentel, J.Chem. Phys., 22, 1943 (1954).
5. E.D.Becker, G.C.Pimentel, J.Chem. Phys. 25, 244 (1956).
6. G.C.Pimentel, Pure Appl. Chem., 4, 61 (1962).
7. G.C.Pimentel, S.W.Charles, Pure Appl. Chem., 7, 111 (1963).
8. M.E.Jacox, D.E.Milligan, Appl. Optics, 3, 873 (1964).
9. F.J.Adrian, E.L.Cochran, V.A.Bowers, "Free Radicals in Inorganic Chemistry", Adv. Chem. Ser., 36, 50 (1962).
10. H.E.Hallam, Molecular Spectroscopy, Proc. 4th. Inst. Petroleum Hydrocarbon Research Conf. Inst. London, 329 (1968).
11. A.J.Barnes, H.E.Hallam, Quart. Rev., 23, 392 (1969).

12. A.J.Downs, S.C.Peake, "Molecular Spectroscopy", The Chemical Society, Ch.1., 9 (1973).
13. B.M.Chadwick, "Molecular Spectroscopy", The Chemical Society, Ch.4., 3 (1975).
14. B.M.Chadwick, "Molecular Spectroscopy", The Chemical Society, 6, (1979).
15. J.S.Ogden, J.J.Turner, Chem. in Britain, 7, 186 (1970).
16. J.W.Hastie, R.H.Hauge, J.L.Margrave, "Spectroscopy in Inorganic Chemistry" Eds. C.N.R.Rao, J.R.Ferraro, Vol.1. 57, (Academic Press New York 1970).
17. D.E.Milligan, M.E.Jacox, Adv. High Temp. Chem., 4, 1 (1971).
18. H.E.Hallam, Ann. Reports (A), 67, 117 (1970).
19. T.S.Hermann, S.R.Harvey, Appl. Spectroscopy, 23, 435 (1969).
20. T.S.Hermann, S.R.Harvey, C.N.Hants, Appl. Spectroscopy, 23, 451 (1969).
21. T.S.Hermann, Appl. Spectroscopy, 23, 473 (1969).
22. M.J.Linevsky, J.Chem. Phys., 34, 587 (1961).
23. A.Snelson, K.S.Pitzer, J.Chem. Phys., 67, 882 (1963).
24. C.M.King, E.R.Nixon, J.Chem. Phys., 48, 1185 (1968).
25. M.M.Rochkind, Spectrochim. Acta., 27A, 547 (1971).

26. A.J.Barnes, W.J.Orville-Thomas, A.Muller, R.Gaufres,
(Eds.), "Matrix Isolation Spectroscopy", (D.Reidel
Publishing Co. Dordrecht Holland, 1981).
27. A.J.Barnes, H.E.Hallam, Trans. Faraday Soc., 66, 1932 (1970).
28. P.Huber-Walchi, H.H.Gunthard, Chem. Phys. Lett., 30, 347 (1975).
29. M.T.Bowers, W.H.Flygare, J.Chem.Phys., 44, 1389(1966).
30. J.M.Verstegen, H.Golding, S.Kimel, B.Katz, J.Chem.
Phys., 44, 3216 (1966).
31. B.Katz, A.Ron, O.Schnepp, J.Chem. Phys., 46, 1926(1967).
32. A.J.Barnes, H.E.Hallam, G.F.Scrimshaw, Trans Faraday
Soc., 65, 3150, (1969).
33. W.G.Von Holle, D.W.Robinson, J.Chem. Phys., 53, 3768 (1970).
34. J.B.Davies, H.E.Hallam, Trans. Faraday Soc., 67, 3176 (1971).
35. A.J.Barnes, H.E.Hallam, Trans. Faraday Soc., 66, 920 (1970).
36. M.Van Thiel, E.D.Becker, G.C.Pimentel, J.Chem. Phys.,
27, 486 (1957).
37. M.T.Bowers, G.I.Kerley, W.H.Flygare, J.Chem. Phys.,
45, 3399 (1966).
38. L.J.Schoen, D.E.Mann, C.Knobler, D.White, J.Chem.
Phys., 37, 1146 (1962).

39. H.F.Shurvell, K.B.Harvey, Can. Spectroscopy, 14, 32
500 (1969).
40. D.W.Robinson, J.Chem. Phys., 39, 3430 (1963).
41. E.Catalano,D.E.Milligan, J.Chem. Phys., 30,45 (1959).
42. J.A.Glasel, J.Chem. Phys., 33, 252 (1960).
43. R.L.Redington, D.E.Milligan, J.Chem. Phys., 37, 2162, (1962).
44. D.E.Milligan, R.M.Hexeter, K.Dressler, J.Chem. Phys.,
34, 1009 (1961).
45. A.Cabana, G.Savitsky, D.F.Horning, J.Chem. Phys., 39,
2942 (1963).
46. A.Cabana, A.Anderson, R.Savoile, J.Chem. Phys., 42,
1122 (1965).
47. F.H.Fayer, G.E.Ewing, J.Chem. Phys., 46, 1994 (1967).
48. F.H.Fayer, G.E.Ewing, J.Chem. Phys., 48, 781 (1968).
49. A.J.Barnes, "Vibrational Spectroscopy of Trapped Species",
Ed., H.E.Hallam, Chap.4., 136, (WileyInterscience 1973).
50. J.E.Lennard-Jones, Proc. Roy. Soc., A106, 463 (1924).
51. D.W.Robinson, J.Chem. Phys., 39, 3430 (1963).
52. K.B.Harvey, H.F.Shurrell, J.Mol.Spec., 25, 120 (1968).
53. B.R.Cairns, G.C.Pimentel, J.Chem. Phys., 43, 3432(1965).

54. M.E.Jacox, D.E.Milligan, Spectrochim. Acta., 17, 1196 (1961).
55. D.E.Mann, N.Acquista, D.White, J.Chem. Phys., 44, 3453 (1966).
56. H.Friedmann, J.Kimel, J.Chem. Phys., 43, 3925 (1965).
57. A.J.Barnes, H.E.Hallam, G.F.Scrimshaw, Trans. Faraday Soc., 65, 3159 (1969).
58. G.C.Pimentel, A.M.Bass, H.P.Broida, "Formation and Trapping of Free Radicals", Chap.4., (Academic Press, New York 1960).
59. S.N.Foner, E.L.Cochran, V.A.Bower, C.K.Jen, J.Chem. Phys., 32, 96 (1960).
60. A.J.Barnes, H.E.Hallam, G.F.Scrimshaw, Trans. Faraday Soc., 65, 3172 (1969).
61. S.W.Charles, F.C.Cullen, N.L.Owen, J.C.S. Chem. Comm., 1063 (1976).
62. M.Kriemann, D.Barnett, J.Chem. Phys., 43, 364 (1965).
63. M.M.Rochkind, Analyt. Chem., 39, 567 (1967).
64. M.M.Rochkind, Analyt. Chem., 40, 762 (1968).
65. R.N.Perutz, J.J.Turner, Trans. Faraday Soc., 69, 452 (1973).
66. W.O.George, E.N.Lewis, D.A.Williams, W.F.Maddams, Appl. Spectroscopy, 36, (5) 592 (1982).
67. A.R.H.Cole Tables of Wavenumbers for the Calibration of Infrared Spectrometers, (Pergamon, Oxford 1977).

68. F.A.Mauer, A.M.Bass, H.P.Broida, (Eds.), "Formation and Trapping of Free Radicals", Chap.5, Academic Press, New York (1960).
69. C.L.Angell, D.Mc.Leod, Inst. News, 18, 20 (1967).
70. J.M.Geist, P.K.Lashmet, Adv. Cryogenic Eng., 5, 324 (1960).
71. J.M.Geist, P.K.Lashmet, Adv. Cryogenic Eng., 6, 73 (1961).
72. D.White, D.E.Mann, Rev. Sci. Instr., 34, 1370 (1963).
73. J.W.L.Kohler, Sci.Amer., 212, 119 (1965).
74. D.R.Hepburn, H.R.Hudson, Chem. and Ind., 664, (1974).
75. S.O.Lawesson, E.H.Larsen, H.J.Jakobsen, Arkiv. Kemi., 23, 453 (1965).
76. A.J.Barnes, J.B.Davies, H.E.Hallam, G.F.Scrimshaw, G.C.Hayward, R.C.Milward, Chem. Comm., 1969, 1089.
77. M.T.Bowers, W.H.Flygare, J.Chem. Phys., 44, 1389 (1966).
78. G.Herzberg, "Infrared and Raman Spectra of Polyatomic Molecules" (Van Nostrand Reinhold, New York, U.S.A. 1945).
79. J.M.Hollas, "High Resolution Spectroscopy" (Butterworths London 1982).
80. A.R.H.Cole, H.W.Thompson, Proc. Roy. Soc., A200, 10 (1949).

81. G.A.Savariraj, J.P.Gosselin, Am. Soc. Sci. Bruxelles, 79,
163 (1965).
82. M.DeHempentinne, G.Germain-Lefevre, R.Van Riet, D.Lenaerts,
Bull. Classe Sci. Acad. Roy. Belg., 46, 310 (1960).
83. H.W.Thompson, P.Torkington, J.Chem. Soc., 303 (1944).
84. A.J.Barnes, S.Holroyd, W.O.George, J.E.Goodfield, W.F.Maddams,
Spectrochim. Acta., 38A, 1245 (1982).
85. E.Hirota, J.Mol. Spectroscopy, 35, 9 (1970).
86. Y.Niide, M.Takano, T.Satoh, J.Mol. Spectroscopy, 63, 108 (1976).
87. S.Kondo, E.Hirota, Y.Morino, J.Mol. Spectroscopy, 28, 471 (1968).
88. A.A.Bothner-By, C.Naar-Colin, J.Amer. Chem. Soc., 83, 231 (1961).
89. L.Kahovek, K.W.F.Kohlransch, Z.Physik. Chem., B46, 165 (1940).
90. P.B.Woller, E.W.Garbisch, J.Org. Chem., 37, 4281 (1972).
91. K.V.L.N.Sastry, V.M.Rao, S.C.Dass, Can. J.Phys., 46, 959 (1968).
92. B.Silvi, C.Sourisseau, J.Chim. Phys., 73, 101 (1976).
93. J.B.Moffat, J.Mol. Spectroscopy, 35, 211 (1976).
94. D.A.C.Compton, J.Mol. Struct., 87, 65 (1982).
95. R.D.McLachlan, R.A.Nyquist, Spectrochim. Acta., 24A, 103 (1968).
96. C.Sourisseau, B.Pasquier, J.Mol. Struct., 12, 1 (1972).

97. D.Van Lerberghe, I.J.Wright, J.L.Duncan, J.Mol. Phys., 42, 251 (1972).
98. D.Van Lerberghe, A.Fayt, J.Mol. Phys., 31, 1875 (1976).
99. J.Harper, A.R.Morrison, J.L.Duncan, Chem. Phys. Lett., 83, 32 (1981).
100. D.R.Cowieson, A.J.Barnes, W.J.Orville-Thomas, J.Raman Spectroscopy, 10, 224 (1981).
101. P.Herbin, G.Blanquet, J.Walrand, C.P.Courtoy, J.Mol. Spectroscopy, 93, 389 (1982).
102. Y.Verbist-Scieur, C.P.Courtoy, A.Fayt, D.Van Lerberghe, J.Mol. Phys., 33, 351 (1977).
103. Y.Verbist-Scieur, C.P.Courtoy, A.Fayt, J.Mol. Spectroscopy, 85, 480 (1981).
104. E.Knozinger, D.Leutloff, J.Chem. Phys., 74, 4812 (1981).
105. D.A.C.Compton, W.O.George, J.E.Goodfield, W.F.Maddams, Spectrochim. Acta., 37A, 147 (1981).
106. W.J.Potts, R.A.Nyquist, Spectrochim. Acta., 15, 679 (1959).
107. J.R.Cowles, W.O.George, W.G.Fateley, JCS. Perkin Trans. II, 396 (1975).
108. J.R.Scherer, W.J.Potts, J.Chem. Phys., 30, 1527 (1959).
109. M.Z.El-Sabban, B.J.Zwolinski, J.Mol. Spectroscopy, 27, 1 (1968).

110. C.W.Gullikson, J.R.Nielsen, J.Mol. Spectroscopy, 1, 158 (1957).
111. J.Charette, M.De Hempentinne, Bull. Class. Sci. Acad.
roy. Belg., 38, 934 (1952).
112. A.J.Barnes, J.D.R.Howells, J.Chem. Soc., Faraday
Trans. II, 69, 532 (1973).
113. K.Radcliffe, J.L.Wood, Trans. Faraday Soc., 62, 2038 (1966).
114. G.H.Griffith, L.A.Harrah, J.W.Clark, J.R.Durig, J.Mol.Struct.,
4, 255 (1969).
115. G.C.Pimentel J.Amer. Chem Soc., 80, 62 (1958).
116. R.Pong, T.D.Goldfarb, A.Krantz, J.Phys Chem., 82, 9 (1978).
117. A.J.Barnes, G.C.Whittle, Molecular Spectroscopy of Dense
Phases Proceedings of the 12th European Congress on Molecular
Spectroscopy, Elsevier Publishing Co., Amsterdam, 1976.
118. I.Kanesaka, K.Miyawaki, K.Kawai, Spectrochim. Acta.,
32A, 195 (1976).
119. M.F.Farona, G.R.Tompkins, Spectrochim. Acta., 24A,
788 (1968).
120. M.F.Farona, J.G.Grasselli, Inorg. Chem., 6, 1675 (1967).
121. S.Krimm, U.G.Folt, J.J.Shipman, A.R.Berens, Polym.
Lett. 2, 1009 (1964).
122. H.U.Pohl, D.O.Hummel, Makromol. Chem. 113, 203 (1968).

123. A.Rubcic, G.Zerbi, *Macromolecules* 7, 754 (1974).
124. M.E.R.Robinson, D.I.Bower, W.F.Maddams, *Spectrochim. Acta.*
34A, 683 (1978).
125. A.Rigo, G.Palma, G.Talamini, *Makromol. Chem.* 153, 219 (1972).
126. S.Grawley, I.McNeill, *J.Polym. Sci., Polym. Chem. Ed.*
16, 2593 (1978).
127. A.Shimizu, T.Ohtsu, *Kogyo Kagaku Zasshi*, 67, 966, (1978).
128. D.Braun, M.Thallmaier, *Macromol. Chem.*, 99, 59 (1966).
129. D.L.Gerrard, W.F.Maddams, *Macromolecules*, 10, 1221 (1977).
130. J.Goodfield, Ph.D. Thesis (1980).
131. M.Tasumi, T.Shimanouchi, *Spectrochim Acta* 17, 731 (1961).
132. T.Shimanouchi, M.Tasumi, Y.Abe, *Makromol. Chem.*, 86,
43 (1965).
133. C.G.Opaskar, S.Krimm, *J.Polym.Sci., Part A-2*, 7, 57 (1969).
134. H.H.Horhold, R.Kumstedt, P.Hindersin, H.Dawczynski, G.drefahl,
Die Makromolekulare Chemie, 122, 145 (1969).
135. H.H.Horhold, D.Gunther, P.Hindersin, *Z.Chem.*, 8, (8) 300 (1968).
136. G.Heublein, R.Kuhmstedt, H.Dawczynski, P.Kadura,
Tetrahedron, 26, 32 (1970).
137. G.Heublein, R.Kuhmstedt, H.Dawczynski, *Z.Chem.*, 10, 32 (1970).

APPENDIX

Contributions to Scientific Meetings

ASPECTS OF INFRARED SPECTROSCOPY - PRINCIPLES AND APPLICATION

INFRARED AND RAMAN DISCUSSION GROUP - THE POLYTECHNIC OF WALES

TUESDAY APRIL 12 - FRIDAY APRIL 15 1983

Tues. April 12

LECTURE PROGRAMME

- 9.15 - 9.30 Welcome Address - W O George
- 9.30 - 9.45 T L Threlfall (May & Baker, Dagenham)
The infrared spectra of thioureas and ureas
- 9.50 - 10.05 N Lewis (The Polytechnic of Wales)
Matrix Isolation Studies of Substituted Olefins
- 10.10 - 10.25 D A Williams (The Polytechnic of Wales)
Complexes between olefins and HCl in low temperature matrices and in the gas phase
- 10.30 - 10.45 Coffee
- 10.45 - 11.00 P S Davison (Scientific Documentation Centre, Dunfermline)
Spectroscopic Data and Information Services: Review of Services available and Future Problems
- 11.05 - 11.20 G Parnham (Technicon Instruments, Basingstoke)
Correlation Transform NIR Spectroscopy
- 11.25 - 11.40 G Maes (University of Leuven, Belgium)
Some Hydrogen Bonding Studies

Wed. April 13

- 9.30 - 9.45 T E Jenkins (University of St Andrews, Scotland)
Raman/Brillouin Spectroscopy of a low temperature phase transition in Diamantane
- 9.50 - 10.05 W Kiefer (University of Bayreuth)
New Techniques in Raman Spectroscopy
- 10.10 - 10.25 N Librovich (Academy of Sciences, USSR)
ATR investigations of acids and bases solutions
- 10.30 - 10.45 Coffee
- 10.45 - 11.00 B van der Veken (University of Antwerp, Belgium)
Conformational Applications of gas phase asymmetric top infrared profile simulation
- 11.05 - 11.20 Magdalena Szostak (University of Wroclaw, Poland)
Infrared dichroism as a possible tool for detection of nonlinear electrooptic properties of molecular crystals. Metanitroaniline case
- 11.25 - 11.40 L M Proniewicz (Jagellonian University, Cracow, Poland)
FT-IR Spectroscopy of compounds with eucryptite/LiAlSiO₄/Structures

INFRARED AND RAMAN DISCUSSION GROUP PROGRAMME

Wed. April 13

- 2.00 - 3.00 I M Mills (University of Reading)
Principles and Practice of Fourier Transform Infrared Spectroscopy
- 3.15 - 3.30 Coffee
- 3.30 - 4.30 W G Fateley (Kansas State University)
Analytical Applications of FT-IR Spectroscopy

Thurs April 14

- 9.30 - 10.30 J J Turner (University of Nottingham)
Why Matrix Isolate?
- 10.45 - 11.00 Coffee
- 11.00 - 12.00 J H van der Maas (University of Utrecht)
Organic Correlations and New Teaching Methods

<u>DAY</u>	<u>DATE</u>	<u>TIME</u>	<u>EVENT</u>	<u>ROOM</u>
Mon	14 Feb	5.00 pm	STRUCTURE AND PROFITABILITY IN POLYMER AND PETROCHEMICALS Royal Society of Chemistry <i>Mr W F Maddams</i> <i>B P Ltd, Sunbury</i>	G219
Thurs	17 Feb	1.00 pm	MAKING PIG MANURE SMELL LESS OBJECTIONABLE - OPERATION OF A NOVEL TYPE OF ANAEROBIC DIGESTER Departmental Research Colloquium <i>Mr J R S Floyd</i>	G219
Thurs	24 Feb	6.30 pm	RECENT DEVELOPMENTS IN SILICONE TECHNOLOGY Society of Chemical Industry <i>Dr C A Pearce</i> <i>Dow Corning Ltd</i>	G219
Wed	2 Mar	2.30 pm	MODERN METHODS OF PROCESS CONTROL IN THE CHEMICAL INDUSTRY SCI/RSC Symposium with Process Technology Group	G219
Thurs	10 Mar	1.00 pm	BIOLOGICAL MEMBRANES AND N M R - A STUDY OF THE COMPLEMENT SYSTEM Departmental Research Colloquium <i>Mr Alun Davies</i>	G219
Thurs	24 Mar	1.00 pm	INFORMATION FROM INFRARED STUDIES NEAR (REAL) ZERO TEMPERATURES Departmental Research Colloquium <i>Mr Neil Lewis</i>	G219
Tues- Fri	12 - 15 April		ASPECTS OF INFRARED SPECTROSCOPY - PRINCIPLES AND APPLICATION Joint Meeting with the Infrared and Raman Discussion Group	
Thurs	12 May	1.00 pm	PROBLEMS OF TRACE ELEMENT DETERMINATION IN COAL Departmental Research Colloquium <i>Mr Alan Abraham</i> <i>National Coal Board</i>	G219
Thurs	26 May	1.00 pm	HOW DO PSYCHROPHILIC BACTERIA ADAPT THEIR MEMBRANE FLUIDITY AT LOW TEMPERATURES? <i>Dr N J Russell</i> <i>Dept of Biochemistry</i> <i>University College, Cardiff</i>	G219
Thurs	9 June	1.00 pm	DIETARY FAT AND CORONARY HEART DISEASE - RESULTS OF A CASE/CONTROL STUDY Departmental Research Colloquium <i>Dr S E Olpin</i>	G219

For further information please contact:

The Secretary
Department of Science
The Polytechnic of Wales
Pontypridd
Mid Glamorgan CF37 1DL
Tel: Pontypridd (0443) 405131
Ext.2681